The role of liquid water in recent surface processes on Mars

Susan J. Conway, David Stillman

The role of liquid water in recent surface processes on Mars

Susan J. Conway[1*]

David E. Stillman[2]

1. CNRS UMR 6112 Laboratoire de Planétologie et Géodynamique, Université de Nantes, France.

2. Dept. of Space Studies, Southwest Research Institute, 1050 Walnut St. #300, Boulder, CO 80302, USA

Abstract

We provide an up-to-date review on the different landscapes and landforms that have been attributed to the action of liquid water in the Amazonian epoch on Mars and the current state-of-the-art regarding their interpretation. This chapter accompanies Chapter DUNDAS (pages xxx-xxx) where the counterarguments are presented. The Amazonian epoch is thought to be dominated by hyper-arid climate conditions hostile to surface liquid water, and our review reveals that this steady-state is likely to be punctuated by episodic appearances of liquid water at the surface. The proposed sources of liquid water are varied: groundwater, thawing of surface-ice, deliquescence, ground-ice or glaciers, with triggers as variable as microclimates, climate-shifts, geothermal anomalies and impact cratering.

Our review covers recently active surface processes in the form of Slope Streaks, dark dune flows and Recurring Slope Lineae, all hypothesised at one point or another to be seeps of liquid water. We then cover landscapes and landforms which are proposed to be a result freeze-thaw cycles in the recent past, including gullies, lobate forms on hillslopes, pingo-like mounds, low-centred polygons, patterned ground and ice-loss landscapes. We present evidence that liquid water has been produced at the base of glacial landforms during the Amazonian, resulting in sinuous ridges (eskers) and enhanced crater-wall erosion. Liquid water brought up-from depth is thought to have produced mud-volcanos and other features related to sedimentary volcanism in the Amazonian and small fluvial channels amongst other features are thought to be related to melting induced by periodic impact events.

We end by summarising the importance of the search evidence of liquid water on Mars and by proposing solutions to the current impasses where progress is hindered due to limitations in data or our understanding.

1 Present-day and recent surface conditions on Mars

Of the planets of the Solar System Mars and Earth are the only two inner planets whose surfaces are thought to have hosted abundant liquid water early in their history (4.5-3.5 Ga). Liquid water is key for supporting life and seeking it out is a key tenet of astrobiology (Abrevaya et al. 2016). Hence, when searching for signs of extra-terrestrial life, space agencies have made Mars one of their principal targets. Mars is a rocky planet located outside Earth's orbit at a solar distance between 1.38 AU and 1.67 AU and has 1/3 the radius of the Earth (the mean martian radius is 3389.5 km). It orbits the sun in 687 earth days (~2 Earth years) and has a very similar day-length to the Earth (24hrs 37min). Its present-day axial tilt is close to the Earth's (25.19° compared to 23.44° on the Earth), giving rise to similar temporal and spatial patterns of insolation over a martian year. The eccentricity of the martian orbit is greater than the Earth (0.0935 compared to 0.0167), and the precession of its aphelion/perihelion through the seasons leads to greater seasonal amplitudes and asymmetries than experienced on Earth. For example, with the current position of perihelion, the southern winters are colder and shorter, compared to the southern winters which are warmer and longer. Mars lost its internally generated magnetic field approximately 3.6 Ga (Lillis et al. 2008; Milbury et al. 2012) that probably led to the loss of the majority of its atmosphere (Jakosky & Phillips 2001). Surface geomorphology and sedimentary composition both point to declining activity of liquid water on Mars' surface over the last 3.5 Ga, which is strongly linked to the loss of Mars' atmosphere (Jakosky & Phillips 2001). Mars' present-day atmospheric pressure ranges from 5-12 mbar (e.g., Hess et al. 1980; Ordonez-Etxeberria et al. 2019) and its main constituent gas is CO_2.

The low atmospheric pressure combined with the greater solar distance, mean that surface temperatures on Mars are on average much lower than on Earth (global mean is ~210K or -60°C) and the diurnal variation of temperature much greater. The lowest surface temperature is buffered around the condensation temperature of CO_2 at around 150K, while peak summer temperatures on and directly above favourable surface materials and orientations can exceed 300K (e.g., Stillman et al. 2014). The pressure and temperature conditions on present-day Mars mean that water should only be stable in solid or gaseous state. Atmospheric humidity on Mars is measured in precipitable microns, i.e. if the whole atmospheric column was condensed, only microns of water would result. Humidity typically ranges up to hundreds of precipitable microns (Smith 2002), which is enough to generate, thin, yet visible surface frosts (Svitek & Murray 1990). These general ranges of atmospheric pressure, humidity and temperature are below the triple point for liquid water, making this phase unlikely to occur in bulk.

However, there is theoretical and indirect evidence to support the possibility of thin films of water or brines developing within the martian soil at the present-day (e.g., Boxe et al. 2012; Jouglet et al. 2007; Milliken et al. 2007; Kereszturi & Rivera-Valentin 2012; Möhlmann 2008) or in the recent past (Sizemore et al. 2015)(. Pores within a regolith where water ice is also present can form microenvironments where the sublimation of the water ice can lead to increased humidity conditions (beyond those of the atmosphere). Under such conditions even at temperatures below the frost point transient liquid water films can form at the regolith or ice grain contacts and surfaces. Since data sent by the Phoenix mission (Hecht et al. 2009) perchlorate salts are now thought to be widespread on Mars (Navarro-González et al. 2010; Glavin et al. 2013a) and depress the freezing point and evaporation rate of water on Mars favouring the formation of thin water films. Atmospheric humidity can increase to levels and beyond near the surface within the diurnal cycle (e.g., Maltagliati et al. 2011) and where the soil is in diffusive exchange with the atmosphere this could promote the formation of thin films of brine/water by deliquescence (Pál & Kereszturi 2017; Cull et al. 2014). Additionally, even before a water saturated

atmosphere is reached, perchlorate salts can adsorb water from the atmosphere via deliquesce and can form brines, which then have remarkable metastable properties (e.g., Gough et al. 2011; Nuding et al. 2015; Toner et al. 2014b; Primm 2018; Primm et al. 2019; Primm et al. 2018)(e.g., Gough et al., 2011; Nudging et al., 2014; Toner et al., 2014; Primm et al., 2018; Primm and Stillman, 2019). Whether or not such films constitute habitable environments has not reached consensus, but their water activity tends to be too low to support life (Martín-Torres et al. 2015; Jones & Lineweaver 2012).

Some researchers have theorised that bulk transient liquid water could exist in the recent martian climate, either brought-up from underground aquifers (e.g., Gaidos 2001; Goldspiel & Squyres 2011; Malin & Edgett 2000; Stillman et al. 2016) or melted from ice under extremely rare favourable combinations of temperature, and humidity conditions (e.g., Chevrier & Rivera-Valentin 2012; Grimm et al. 2014; Hecht 2002; Kossacki & Markiewicz 2010). Melting from surficial ice is particularly difficult as there is a kinetic barrier to melting even if conditions are conducive: because latent heat is consumed by sublimation at the surface of the ice which prevents the temperature from rising sufficiently to allow melting to occur (Mellon & Phillips 2001).

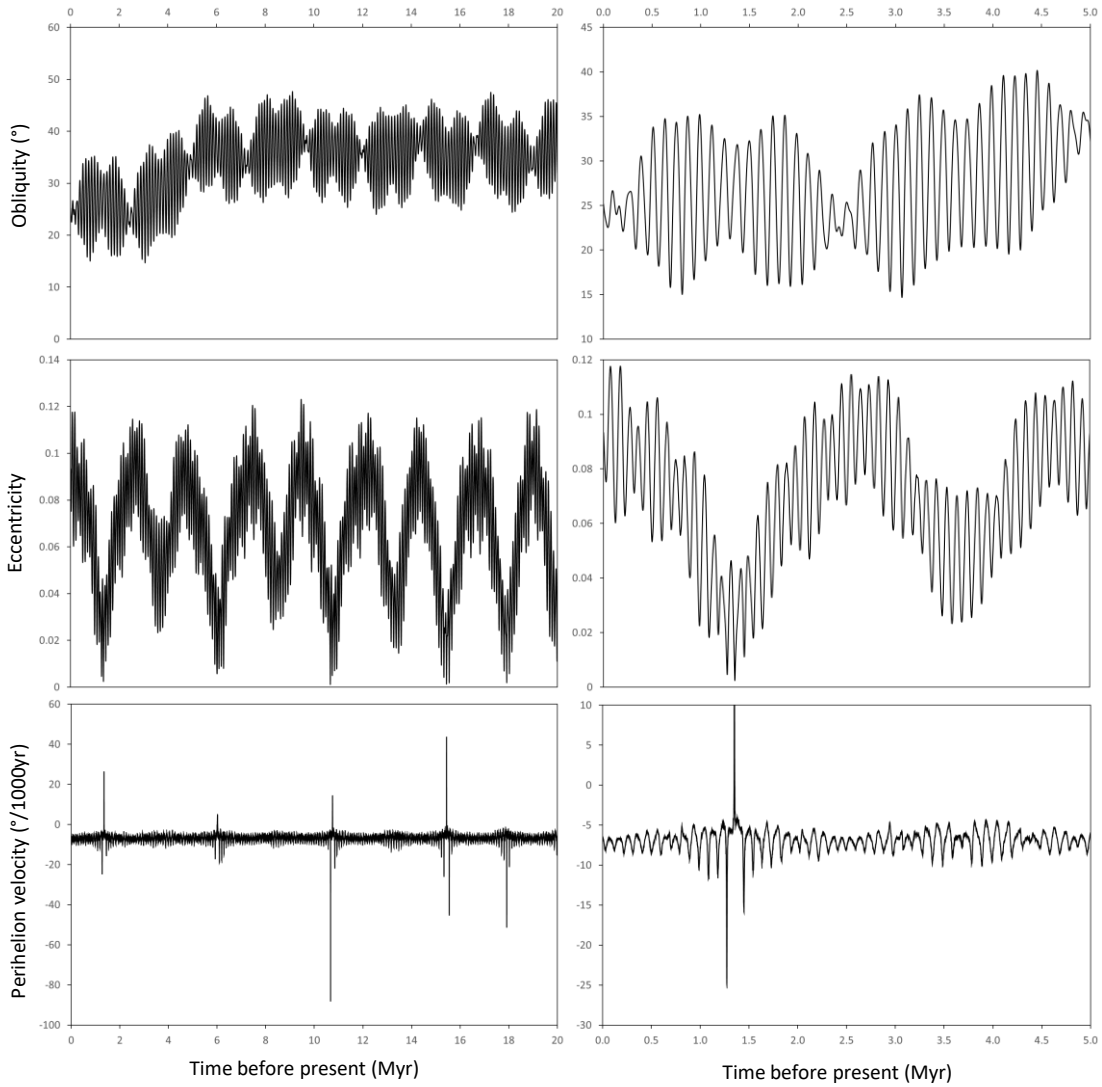

Figure 1: Secular changes in Mars orbital parameters for the last 20 Myr and 5 Myr as calculated by Lascar et al. (2004) *with initial conditions of Yoder et al.* (2003) *downloaded from: http://vo.imcce.fr/insola/earth/online/mars/La2003-04/index.html*

Many researchers have hypothesised that Mars' climate was substantially different in the recent past and may have been more conducive than at the present-day to the emergence and stability of liquid water (e.g., Costard et al. 2002; Richardson & Mischna 2005). This is because Mars' orbital parameters (Fig. 1) are much more variable than those of Earth and we already know that Earth's climate undergoes glacial-interglacial cycles as a result of periodic changes in orbital obliquity, eccentricity and the solar longitude L_s of perihelion – so called Milankovitch cycles – which change the amount and distribution of incoming solar radiation. Hence, the larger variations experienced by Mars should have more impact on the climate system than on Earth. Having a lower mass (i.e. moment of inertia) than the Earth and without a large Moon to stabilise the planet, Mars' axial tilt (obliquity) has varied between 15° and 40° in the last 5 Ma (compared to ±1.3° around the present value for Earth) with a period of 120 ka. Mars' eccentricity varies between 0 and 0.12 (compared to 0 to 0.068 for Earth) over 95 ka and L_s of perihelion takes ~51 ka years to return to its starting season (Fig. 1) (Ward 1992; Ward 1979; Ward 1974). Global Climate Models (GCMs) have been used to try and predict the influence that these orbital changes should have on Mars' climate. Despite these large variations in incoming radiation, the low atmospheric pressure on Mars means that reaching the triple point of water is still challenging (Richardson & Mischna 2005). Using current values for atmospheric pressure with obliquity at 35° Richardson and Mischna (2005) predict at most 100 days per year of transient liquid water (i.e. the time above the triple point) located at the base of Hellas Basin. It is hypothesised that at very high obliquities (>35°) sufficiently intense incoming solar radiation, at certain latitudes and times of year, means that ground ice could melt if it is protected from the low atmospheric pressure by an overburden slowing heat-loss by sublimation and impeding gas diffusion (e.g., Williams et al. 2009). At such obliquities, the two water ice polar caps are sublimated away due to the increased insolation at the poles. This significantly increases the atmospheric water vapour concentration (Mellon & Jakosky 1995) and leads to a massive redistribution of water ice by cold trapping in the mid latitude region that is the coldest. It is also the region that experiences the most intense increases in solar radiation, so it is at the mid-latitudes where the most intense surface-atmosphere exchange of water is thought to occur. Conversely, at obliquities <17°, the atmospheric water vapour concentration decreases by more than an order of magnitude from the current value (Mellon & Jakosky 1995) and prevents migration of any atmospheric water vapour. The recent discovery of large volumes of CO_2 ice sequestered in the south polar cap (Bierson et al. 2016; Manning et al. 2019; Phillips et al. 2011), opens up the possibility for a slightly higher atmospheric pressure (Buhler et al. 2019; Manning et al. 2006) than assumed by previous modelling studies, which would allow liquid water to be stable for a few more degrees above freezing before it boils.

These conditions – that of a hyper-arid cold desert – have thought to have reigned on Mars during the whole Amazonian period (since ~3 Ga) even if uncertainties in the orbital solutions do not allow us to predict the orbital parameters further than several tens of millions of years in a reliable way.

2 Present-day reservoirs of water on Mars

Even if surface conditions allow for the presence of liquid water, there must be a source of water (ice or vapour) for liquid water to be produced. Precipitation in the form of rain is generally accepted to be highly unlikely during the Amazonian (since ~3 Ga). There are three potential reservoirs for water:

seasonally deposited ices/frosts from vapour in the atmosphere, surface ice reservoirs, or underground aquifers. Here, surface ice reservoirs are defined as those ices which can be reasonably considered to have exchanged with the atmosphere under Amazonian climate conditions. We discuss each of these sources in turn below and their likelihood for generating liquid water.

2.1 Seasonal ices and frosts

The most visible manifestation of Mars' seasonal cycle is the waxing and waning of the seasonal polar caps, which were noted even in early telescopic observations (Herschel 1784). The seasonal polar caps comprise atmospherically deposited seasonal ices that brighten the surface. The majority of the ice is comprised of CO_2 and as a result the deposition of the seasonal ices causes a substantial fluctuation in the atmospheric pressure (Haberle et al. 2017). A minor component of water ice is included in these ices (Appéré et al. 2011; Brown et al. 2012; Brown et al. 2010). The ices are thought to originate as directly condensed frosts or fall as snow (e.g., Giuranna et al. 2008; Hayne et al. 2014), with direct observation being hindered by the polar hood (low lighting combined with a hazy atmosphere). The continuous seasonal polar caps, comprised of CO_2 and a minor component of H_2O, extend to 50-55° in both hemispheres (e.g., Piqueux et al. 2015) and are thought to reach a thickness of metres near the poles (e.g., Karatekin et al. 2006; Smith et al. 2001). Discontinuous deposits of ices are found down to latitudes of 30° in both hemispheres (Dundas et al. 2019b; Vincendon et al. 2010a; Vincendon et al. 2010b), where water ice is found to lower latitudes than CO_2 ice. Discontinuous CO_2 extends to 35°S on steep pole-facing slopes in the southern hemisphere (Vincendon et al. 2010a), but its extent has not yet been measured in the northern hemisphere. Sublimation of the seasonal ices drives peaks in atmospheric water vapour to around tens of precipitable microns (Pankine et al. 2010; Pankine & Tamppari 2019). Water ice frost forms an annulus around the retreating seasonal ices and as it sublimates is cold-trapped onto the retreating CO_2 ice before sublimating again later. Exchange of water vapour between hemispheres is strongest during the solstices (Haberle et al. 2017).

In general, water frosts and ices deposited seasonally are deemed to be unlikely sources of liquid water at the present-day and in the recent past, due to the very small quantities and the kinetic barrier to melting discussed in Section 1.

2.2 Surface Ice reservoirs

Surface ice reservoirs are our most accessible evidence that Mars has abundant water, and these can be split into:

- The polar caps (~10^6 km^3 each) (Plaut et al. 2007; Selvans et al. 2010)
- Mid-latitude glaciers (~10^5 km^3) (Levy et al. 2014)
- Ground ice (~10^4 km^3) (Conway & Balme 2014; Kreslavsky & Head 2002; Mustard et al. 2001)

Radar data have confirmed that the polar caps are almost exclusively water ice (Plaut et al. 2007; Selvans et al. 2010). The polar caps are the most voluminous reservoir of water on Mars and form upstanding broadly domal landforms with up to three kilometres of relief (Plaut et al. 2007; Selvans et al. 2010). The internal structure of the two caps is broadly similar, comprising layers of ice with variable dust-contents, visible in surface exposure at internal scarps and at depth via radar sounding (e.g., Becerra et al. 2017; Blasius et al. 1982; Fishbaugh & Hvidberg 2006; Plaut et al. 2007; Selvans et al. 2010) and thus are generally accepted to form via atmospheric deposition of water ice. Both caps are dissected by spiral troughs which are thought to form during cap accumulation through a balance between sublimation and

accumulation (Bramson et al. 2019; Smith et al. 2013; Smith & Holt 2010) and they are more marked in the northern cap than in the southern cap. However, in the detail the two caps are quite different, likely as a result of the huge difference in altitude between the two hemispheres (base at -5000 m in the north and +1000 m in the south), which has a profound effect on atmospheric circulation (e.g., Haberle et al. 2017). The northern polar cap has a younger surface age than the southern cap (a few thousand compared to ~10 Ma; Herkenhoff & Plaut 2000; Landis et al. 2016), and its bulk is estimated to have formed in the last few millions of years (Jakosky et al. 1995; Laskar et al. 2002; Levrard et al. 2007) even though its surface may be being continuously renewed (Herkenhoff & Plaut 2000; Landis et al. 2016). It is thought to comprise a lower unit of ice-rich sands and an upper unit of polar layered deposits. It is broadly centred on the pole and is surrounded by outliers which formed separately (Bapst et al. 2018; Brothers & Holt 2016; Brown et al. 2008; Conway et al. 2012). Hovius et al. (2008) suggested that some re-entrants into the cap represented channels carved by water released by volcanic heating, but later work showed these features were more consistent with wind erosion (Brothers et al. 2013). In contrast, the southern polar cap is located off-centre with respect to the southern pole and only a very small proportion of the cap has exposed water ice at the surface in summer (Hansen et al. 2005), compared to the complete exposure expressed by the northern cap.

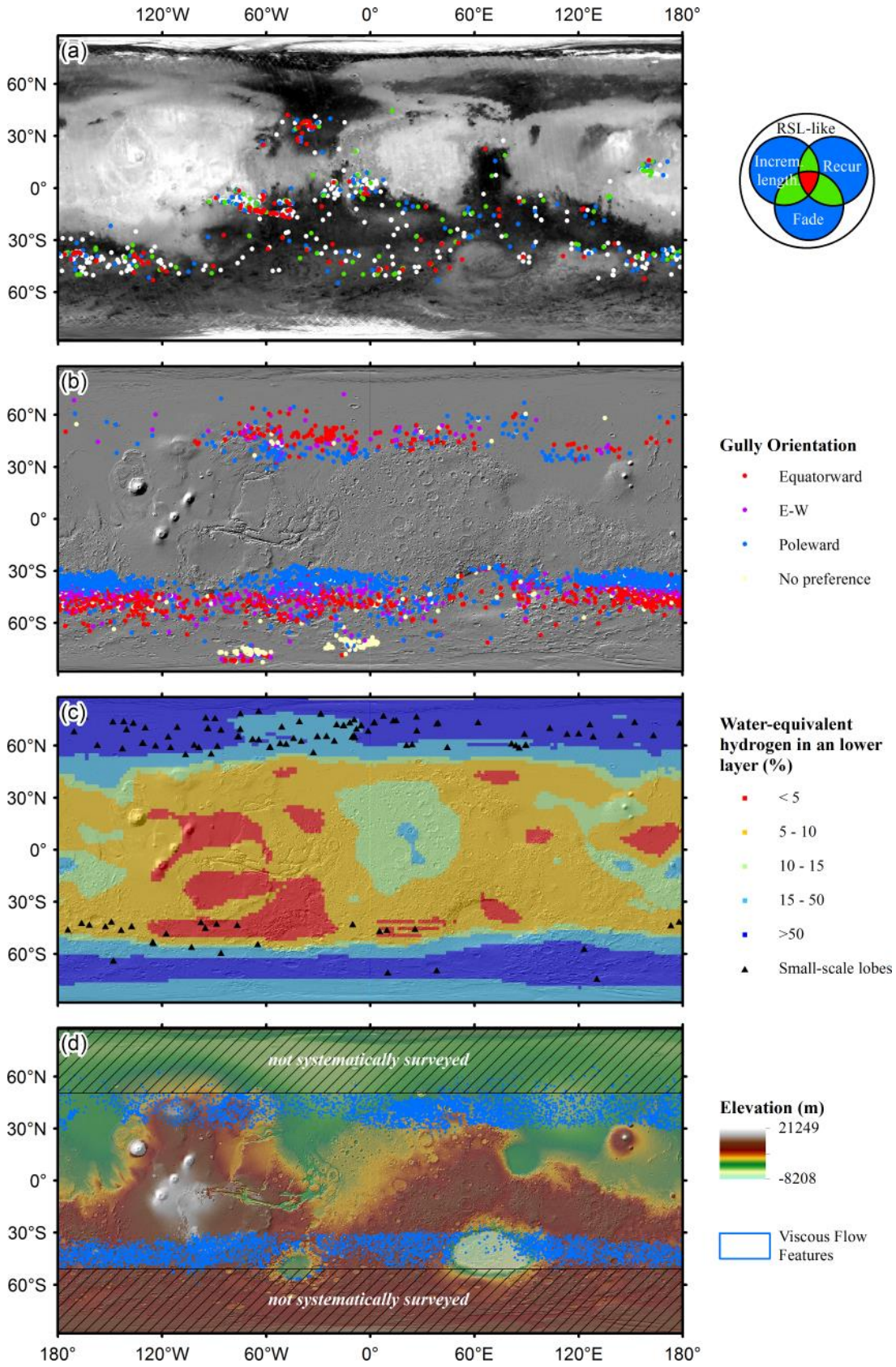
120°W
60°W
0°
60°E
120°E
180°
(a)
(b)
(c)
(d)
60°N
30°N
0°
30°S
60°S
RSL-like
Increm. length
Recur
Fade
Gully Orientation
Equatorward
E-W
Poleward
No preference
Water-equivalent hydrogen in an lower layer (%)
< 5
5 - 10
10 - 15
15 - 50
>50
Small-scale lobes
not systematically surveyed
not systematically surveyed
Elevation (m)
21249
-8208
Viscous Flow Features

185

Figure 2: Global distribution of relevant landforms in the quest for evidence of liquid water on Mars. (a) Mars Odyssey Thermal Emission Spectrometer global albedo map overlain by the global distribution of Recurring Slope Lineae (RSL), where the legend to the right shows how many RSL attributes are displayed at each site, a confirmed RSL site being in red having evidence of incremental lengthening, recurrence and fading. (b) Mars Orbiter Laser Altimeter (MOLA) derived shaded relief map overlain with the locations of gullies as published by Harrison et al. (2015)*. (c) Semi-transparent MOLA-derived shaded relief map with water equivalent hydrogen data from Pathare et al.* (2018) *overlain with locations of small-scale lobes from Johnsson et al.* (2018)*. (d) Semi-transparent MOLA-derived shaded relief map with colour-keyed MOLA-elevation overlain by the locations of glacial forms, or VFF as mapped by Levy et al.* (2014)*.*

The bright part of the cap is instead CO_2 ice. The deep structure of the polar cap has been harder to decode than for the northern cap because there are significantly fewer internal radar reflections. The cap is believed to have a series of packets of polar layered deposits with significant zones where CO_2 is thought to be sequestered (Bierson et al. 2016; Manning et al. 2019; Phillips et al. 2011). Much of the cap is covered by dust and hence has a lower albedo than exposed ice (Herkenhoff 2001). The surface of the exposed cap is covered by a metres-thick layer of CO_2 ice which is currently retreating at metres per year (Buhler et al. 2017; Byrne 2003; Thomas et al. 2009). There are numerous outliers of the southern cap and these might represent a more extensive cap in the past (Sori et al. 2019; Westbrook 2009). Ancient units that surround the south polar cap (e.g., Fastook et al. 2012; Scott & Tanaka 1987; Head & Pratt 2001) are thought to represent water production at the base of the cap, which will be discussed in more detail in Section 3.5 in the context of a recent report of sub-glacial lakes found via radar sounding under the southern polar cap (Orosei et al. 2018; Lauro et al. 2020).

The mid-latitude glaciers are common and widespread across areas with topographic relief in the mid-latitudes (30-60°; Fig. 2d) and have been classified by morphology and context into several groups including: viscous flow features (VFF), Concentric Crater Fill (CCF), Lobate Debris Aprons (LDA), Lineated Valley Fill (LVF) and Glacier-Like Forms (GLF). The glacial origin of all these features has now been generally accepted with the most convincing evidence coming from orbital sounding radar (Holt et al. 2008; Petersen et al. 2018; Plaut et al. 2009) and further conformed by their overall shape/form and surface textures (e.g., Baker & Carter 2019a; Baker & Carter 2019b; Head et al. 2010; Karlsson et al. 2015; Levy et al. 2009c; Mangold 2003; Parsons et al. 2011). These glaciers are thought to comprise almost pure ice with a metres- to decametres-thick debris cover derived from the headwall and englacial materials. The present-day systems are believed to be out of equilibrium with the current climate and show extensive evidence for retreat and downwasting (Brough et al. 2016). Superposition relationships (Hepburn et al. 2019) and estimations of age derived from crater-size frequency distributions on their surfaces suggest that they formed during several "glacial maxima" over the last tens to hundreds of millions of years (Baker et al. 2010; Berman et al. 2015; Hartmann & Werner 2010; Morgan et al. 2009). Each individual feature is likely to represent a series of ice-accumulation events (Fastook & Head 2014; Weitz et al. 2018). As a general rule, martian glaciers are thought to be cold-based, i.e. no melting occurs near the base as is common in terrestrial glaciers, and they move via viscous deformation of the ice, rather than sliding over their bed (e.g., Parsons et al. 2011), which is consistent with their form. Possible exceptions to this general rule will be discussed in Section 3.5.

Ground ice is extensive on Mars and is spatially associated with surface deposits that tend to drape the topography, variously termed "mantling units", "mantle", latitude dependant mantle", "pasted on terrain", "dust-ice mantle" amongst other terms. The main line of evidence for ground ice comes from

the neutron spectrometer on Mars Odyssey (Boynton et al. 2002; Feldman et al. 2011; Feldman et al. 2008; Feldman et al. 2007; Feldman et al. 2004; Maurice et al. 2011; Pathare et al. 2018; Wilson et al. 2018), where the content of ice in the top metre of the regolith is estimated to be 50-80% at latitudes >50°N/S (Fig. 2c). These predictions were shown to be locally valid by the Phoenix lander, which found ice at depths of a few centimetres both in the form of pore-filling ice and excess ice (Mellon et al. 2009). Surface temperature data from Mars Climate Sounder and Thermal Emission Imaging System indicate that ice occurs within centimetres to tens of centimetres of the surface at latitudes down to 35°N/45°S (Piqueux et al. 2019). In addition, high ice-contents from the neutron data correlation spatially with the observations of polygonally patterned ground (e.g., Levy et al. 2010b; Mangold 2005), which is generally accepted to be a result of thermal contraction of ice-cemented ground (Mellon 1997). Phoenix landed amongst such polygons and excavated and detected ground ice with a mean depth of 4.6 cm (Mellon et al. 2009). Additionally, Phoenix also detected segregated ice above the ground ice table. New impacts that reveal ice in their ejecta generally confirm this distribution (Byrne et al. 2009; Dundas et al. 2020; Dundas et al. 2014), and even extend to lower latitudes (~40°) where the ice is predicted to be deeper than can be detected by the neutron spectrometer. At these latitudes, the surface mantling units become dissected, exposing layering and exhibiting pitting (Milliken et al. 2003; Schon et al. 2009b). These discontinuous mantles are found preferentially on pole-facing slopes at lower latitudes (e.g., Christensen 2003). This latitude marks the boundary where the topography at scales of hundreds of metres becomes measurably smoother where these mantles are present (Kreslavsky & Head 2002; Kreslavsky & Head 2000).

Ground ice is thought to be responsive to climate change and in diffusive equilibrium with the current climate (Aharonson & Schorghofer 2006; Mellon & Jakosky 1993; Schorghofer & Aharonson 2005). The relationship between the near-surface ground ice detected by the neutron and thermal orbital data and the surface mantling units (with their ice content) is ambiguous. In some cases such surface mantling units can be locally decametres thick and have evidence for massive ice, from geomorphic and radar evidence (Bramson et al. 2015; Conway & Balme 2014; Dundas et al. 2018; Stuurman et al. 2016). Such enrichments cannot come about from atmospheric diffusion into the regolith because of self-blocking, even if this can be bypassed by contraction cracking (Fisher 2005) only tens of centimetres depths can be reached (see Section 3.4.5). The alternative is that these mantles represent units laid down under past high-obliquity climate conditions when snow/frost could be directly accumulated at the surface (Head et al. 2003; Madeleine et al. 2014; Madeleine et al. 2009) and protected from later sublimation by the accumulation of a sublimation lag of atmospherically derived dust centimetres in thickness. However, a universal composition of nearly pure ice for these units is not supported by the geomorphic evidence, which rather suggests development of the ground ice within a regolith matrix, i.e. excess ice (e.g., Levy et al. 2010b; Pathare et al. 2018; Soare et al. 2015). We discuss the development of excess ice further in the context of ice-loss landforms in Section 3.4.5.

Ground ice is generally considered to be an improbable, but still viable source for liquid water in the present and recent-past, as the soil above protects it from sublimation, removing some of the constraint of the kinetic barrier to melting.

2.3 Subsurface water reservoirs

Numerous authors have hypothesised the presence of aquifers on Mars (e.g., Abotalib & Heggy 2019; De Toffoli et al. 2019; Gaidos 2001; Goldspiel & Squyres 2011; Salese et al. 2019), initially as a way to explain the fate of the large quantity of liquid water that is thought to have existed on Mars early in its history,

as evidenced by the existence of the extensive valley networks (e.g., Craddock & Howard 2002; Hynek & Phillips 2003; Kereszturi & Petrik 2020; Luo et al. 2017; Penido et al. 2013; Williams & Phillips 2001; Hynek et al. 2010), the clay deposits found in Noachian terrains (e.g., Carter et al. 2015; Ehlmann et al. 2011b; Loizeau et al. 2007; Lowe et al. 2020; Lowe et al. 2020; Milliken & Bish 2010; Poulet et al. 2005), the outflow channels dated to the Hesperian or later (Andrews-Hanna & Phillips 2007; Komar 1979; Leask et al. 2007; Marra et al. 2014; Max & Clifford 2001; Montgomery & Gillespie 2005; Vijayan & Sinha 2017; Wilson 2004) and the hypothesised northern ocean (e.g., Baker et al. 1991; Carr & Head 2019; Clifford & Parker 2001; Palumbo & Head 2019). Mars is thought to possess a deep cryosphere (Carr 1996; Clifford et al. 2010; Grimm et al. 2017; Lasue et al. 2019), where this cryosphere is impinged on by the geothermal heat flux, liquid water is thought to exist. Tectonic and surface temperature fluctuations perturbing the pressure state of this aquifer are thought to be responsible for the hundred-kilometre scale outflow channels which occurred in the Hesperian (Baker 1979; Carr 1979; Coleman 2005; Harrison & Grimm 2008; Marra et al. 2014). Smaller, yet similar perturbations have been proposed to explain gullies and RSL (Abotalib & Heggy 2019; Gaidos 2001), bringing up water from kilometres in depth. Shallower surface aquifers, including perched aquifers, have also been proposed (Goldspiel & Squyres 2011; Marquez et al. 2005), but these are within reach of the orbital ground penetrating radars, such as the European Space Agency's MARSIS and NASA's ShaRAD, which have found no evidence for such bodies of water (Nunes et al. 2010). The non-detection of shallow aquifers by orbital radar is not definitive proof of their absence because the penetration of these radars into the martian crust is much lower than initially anticipated (Stillman & Grimm 2011) and they are limited to detecting interfaces that aquifers may in fact not present (Farrell et al. 2009; Nunes et al. 2010).

Circulation of groundwater in the past has been hypothesised from in situ observation of post-digenetic alteration products, such as veins and nodules (e.g., Chan et al. 2004; L'Haridon et al. 2018; Stack et al. 2014) found within the sedimentary rocks deposited in impact craters and evidence from meteorite studies (Bridges et al. 2001; Gillet et al. 2002; Schwenzer et al. 2016), evidence for sedimentary volcanism (e.g., Brož et al. 2019; Gallagher et al. 2018; Oehler & Allen 2010; Okubo 2016; Skinner & Mazzini 2009; Wheatley et al. 2019), and orbital detection of hydrothermal alteration products (e.g., Bishop et al. 2004; Ehlmann et al. 2011a; Viviano et al. 2013). Hence, present-day impingement of these hypothesised aquifers on the surface is hard to rule out and often relies on arguments based around Occam's razor – the simplest hypothesis is the most likely – as proving/disproving the presence of aquifers relies on knowledge of the subsurface that we do not have. So, unlike the other reservoirs of water discussed above, the presence of deep or shallow aquifers (and the cryosphere) remains purely hypothetical and would require significant progress in our understanding of Mars to prove or disprove. Nevertheless liquid water sourced from aquifers is generally perceived to be unlikely to cause present-day or recent (last few millions of years) surface modifications, because of arguments based on structural and topographic context that will be discussed in Section 3.3 (e.g., Treiman 2003). It is generally considered as a viable source of liquid water in the early Amazonian (Baker & Milton 1974; Rodriguez et al. 2015; Dohm et al. 2001).

3 What is the evidence for recent liquid water on Mars?

As detailed above, our knowledge of the current surface temperature, pressure and humidity conditions on Mars and our expectations derived from Global Climate Models of the recent past, and lack of knowledge regarding the deep subsurface of Mars means that researchers believe that the production of surface liquid water is unlikely. Hence, evidence presented in favour of near-surface liquid water on Mars

is, almost without exception, highly scrutinised. Despite this many surface features have been ascribed to the action of surface liquid water often in tight analogy with equivalent landforms found on Earth.

Below each of the major landscape elements that have been used to argue for recent surface water on Mars are described, the evidence supporting its generation by liquid water summarised and the current assessment of the likelihood of the liquid water hypothesis described. The topics are addressed in a rough chronological order starting at the present-day and working towards the past.

3.1 Slope Streaks and dark dune flows

Three broad types of low albedo downslope-oriented "streaks" resembling a downslope flow have been observed to form at the present-day on Mars: Recurring Slope Lineae, Slope Streaks and dark dune flows. All three have been linked to liquid water occurrence at the present-day on Mars. Recurring Slope Lineae are detailed in the next section.

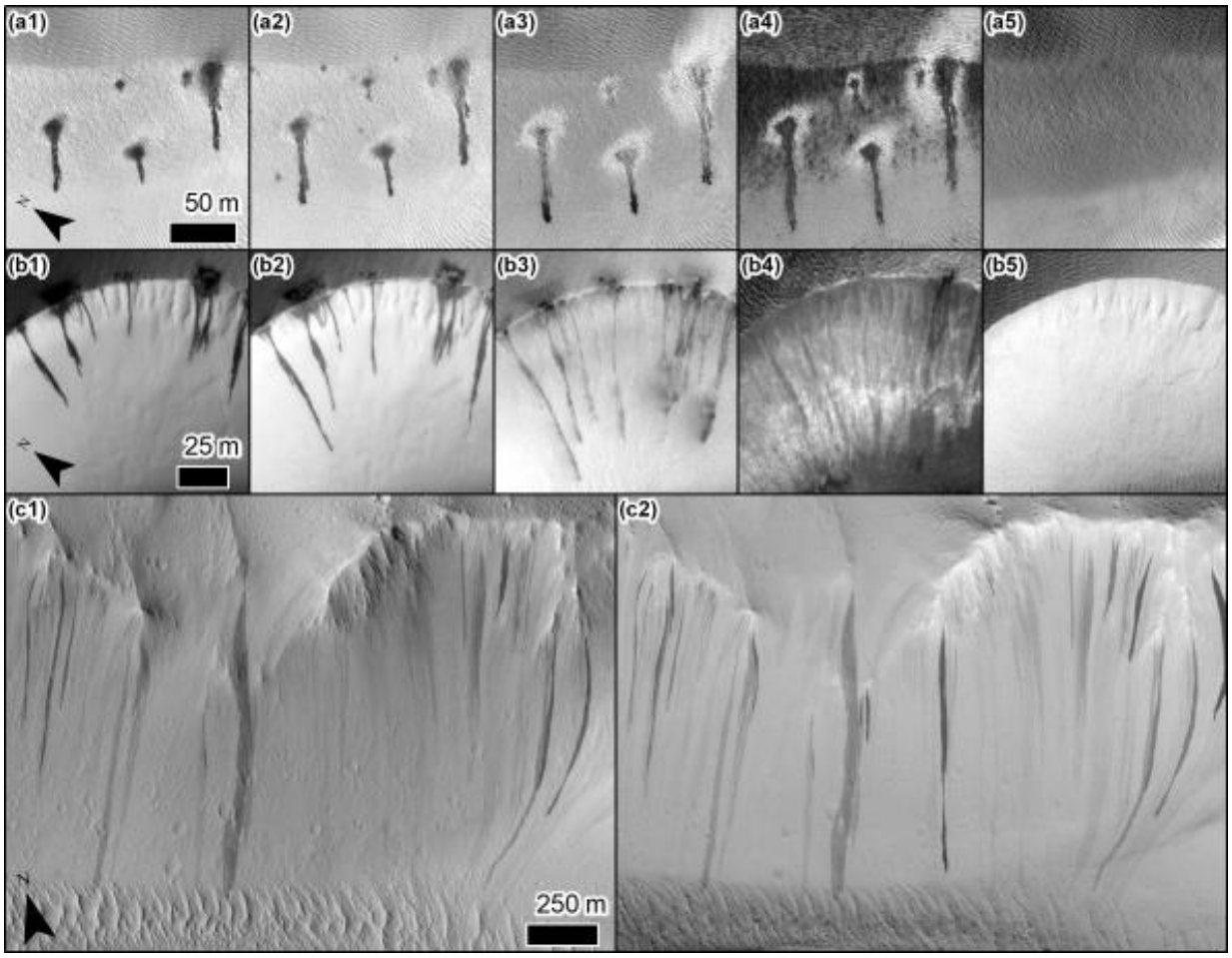

Figure 3: Examples of dark dune flows and slope streaks on Mars. Each letter represents a location while each number represents a different time of year. Please note each panel has been individually contrast-stretched to enhance visibility. Panels a1-5 show the evolution of a dark flows emanating from dark spots on the slip face of a linear dune in Richardson Crater (72.0°S, 179.4°E) in the southern hemisphere from MY27 Ls 210-340°. Note the development of the bright halo, the darker albedo at the tip of the flow and the lack of any morphological signature once the frost is removed. Panels b1-5 show the evolution of a

dark flows located on the slip face of a barchan dune at a site informally named "buzzel" (84.0°N, 233.2°E) in the circum-polar erg in the norther hemisphere in MY 29 from Ls 029-087°. Again, note the lack of morphological signature once activity is over. Panels c1-2 show the appearance of new slope streaks on a slope located in the mid-latitude region of Mars (31.1°N, 226.0°E) in MY 31. HiRISE images: a1 PSP_003175_1080 Ls=210.6°, a2 PSP_003386_1080 Ls=220.7°, a3 PSP_003742_1080 Ls=238.1°, a4 PSP_003953_1080 Ls=248.5°, a5 PSP_005931_1080 Ls=340.4°, b1 PSP_007193_2640 Ls=28.8°, b2 PSP_007404_2640 Ls=36.3, b3 PSP_007905_2640 Ls=53.7°, b4 PSP_008248_2640 Ls=65.5°, b5 PSP_008867_2640 Ls=86.6°, c1 ESP_027092_2115 Ls=107° and c2 ESP_031971_2115 Ls=323°. Credit NASA/JPL/UofA.

Slope Streaks (Fig. 3c) can be metres to kilometres in total length and they originate on steep slopes (e.g., Sullivan et al. 2001) in the equatorial regions of Mars. They often originate at a point, fan out to reach a maximum width, then terminate in a series of digitate lobes (e.g., Schorghofer et al. 2007) yet their detailed morphology seems to depend on the shape of the underlying slope (e.g., Dundas 2020). Unlike RSL and dark dune flows, Slope Streaks show no incremental growth between images, but simply appear in any given image at their full extent (e.g., Schorghofer et al. 2007). Also, older streaks can appear bright compared to the surrounding terrain (e.g., Aharonson et al. 2003; Baratoux et al. 2006), which is unlike RSL and dark dune flows. Slope Streaks seem to remove a thin layer of material along their path and may push some material aside (Chuang et al. 2007; Phillips et al. 2007). Slope Streaks are found in dusty, low thermal inertia areas of Mars, so are generally assumed to be dry avalanches of dust (e.g. Dundas 2020 sullivan 2001). The involvement of liquid water has been hypothesised, based on their occurrence on slopes whose temperatures can exceed 273K (Schorghofer et al. 2002), a bias in their occurrence towards hotter times of year (Heyer et al. 2019), interaction with topographic obstacles (Brusnikin et al. 2016; Kreslavsky & Head 2009), extension onto low slopes and correspondence with terrains high in Cl and Fe (i.e. availability of salts to produce brines; Bhardwaj et al. 2017). None of these observations are completely diagnostic and dry dust avalanches could have a rheology that also satisfies these constraints (Dundas 2020; Miyamoto 2004; Bhardwaj et al. 2019a).

Dark dune flows (Fig. 3a,b) are a strictly seasonal phenomena strongly linked to the defrosting phase during the retreat the seasonal ices in spring and as the name suggests are only found on dark sand dunes (near the poles in both hemispheres). They are metres to hundreds of metres in overall length and develop from dark spots that appear on the seasonal ice cover. They grow incrementally as the seasonal progresses and are no longer visible once the seasonal ice cover has sublimated away, which contrasts with RSL which tend to gradually fade (e.g., McEwen et al. 2011) and slope streaks that can persist for decades (e.g., Schorghofer et al. 2007). Their development follows the same sequence of events: a) development of a dark spot, b) propagation of the flow away from the spot, c) development of bright halos in some cases and d) as propagation progresses the tip of the flow is darker than the source spot. The general consensus is that the initial dark spots are formed by the "Kieffer model" (Kieffer et al. 2006) – this model describes the formation jets of CO_2 gas generated by basal sublimation of the seasonal translucent CO_2 slab ice. The basal sublimation builds pressure under the slab ice that when released by cracking entrains dust/sand that are then deposited around the crack forming a dark spot/fan at the surface. It is proposed that salt can also be included within these deposits and that the dark flows can be explained by the propagation of brines generated as interstitial water from cold-trapped water ice and preferential heating of the sediments forming the dark spot (Kereszturi & Appéré 2014; Kereszturi & Rivera-Valentin 2012; Kereszturi & Rivera-Valentin 2016; Kereszturi et al. 2009; Kereszturi et al. 2011b;

Kereszturi et al. 2010; Kereszturi et al. 2011a; Möhlmann 2010; Möhlmann 2004; Möhlmann 2008; Möhlmann & Kereszturi 2010). However, dry mass wasting phenomena driven by sublimation dynamics cannot be ruled out given the morphological, temperature and spectral constraints (Horvath et al. 2009; Hansen et al. 2013; Gardin et al. 2010).

Although water has been proposed for the formation of Slope Streaks and dark dune flows, the evidence presented to date favours dry avalanches and CO_2 ice sublimation mechanisms respectively.

3.2 Recurring Slope Lineae (RSL)

Recurring slope lineae are a seasonal phenomenon characterised by downslope propagating relatively low albedo streaks up to hundreds of metres in length and generally metres to tens of metres in width (Fig. 4). They were first identified thanks to repeated HiRISE images and are distinct from slope streaks and dark dune flows by growing at the warmest times of year (for a given slope and slope-orientation) and then fading until the pattern is repeated the following year (McEwen et al. 2011). It is this incremental downhill growth that led researchers to initially interpret these features as being driven by liquid water. This is because slope streaks and wind streaks, which are thought to be produced by dry granular flows (e.g., Chuang et al. 2007; Sullivan et al. 2001) or the removal of dust (Vincendon et al. 2015), respectively, do not grow, but are emplaced instantaneously (at the temporal scale of orbital observations). Although there may be mechanisms by which dry granular flows could mimic this behaviour, see Chapter DUNDAS (pages xxx-xxx). RSL occur in exclusively areas that have a low abundance of surficial dust (unlike Slope Streaks which only occur on high albedo dusty slopes) and tend to originate at rocky outcrops towards the top of steep slopes. They are found in dense concentration in the Valles Marineris (VM; Chojnacki et al. 2016; McEwen et al. 2014; Stillman et al. 2017), but also on steep slopes in the northern (Stillman et al. 2016) and southern mid-latitudes (Stillman et al. 2014; Stillman & Grimm 2018) (Fig. 2b) and at tropical latitudes outside of VM (Stillman & Grimm 2018). They often occur within the interior slopes of, on the same slopes as, or on neighbouring slopes to, mid-latitude and equatorial gullies, which are described further in Section 3.3.

RSL can be found individually or occur as dense concentrations and they tend to originate at the same place every year. Their overall length varies from year to year and neighbouring RSL can have different growth rates, and in certain locations an RSL can lengthen at the same time its neighbour is fading (Stillman et al. 2017; Stillman et al. 2020). Their path downslope deviates around obstacles (Fig. 4a-c, g-i) suggesting that they have very little momentum and that the flow is thin compared to the obstacles visible at HiRISE resolution (~25 cm/pix). RSL can come together downslope (Fig. 4c, f), split (Fig. 4c, k) and have some limited sinuosity (Fig. 4b, i). In Valles Marineris RSL are spatially and temporally associated with slumps in the loose materials over which they propagate (Chojnacki et al. 2016; Ojha et al. 2017) (Fig. 5). Such slumps extend much further downslope than RSL, have similar albedos, fading timescale, and slopes (27.5° ± 2.7°; Stillman et al. 2020). RSL are most easily identified on materials that are generally smooth at the HiRISE scale (no grains >75 cm), but can be found on slopes covered in clasts (Fig. 4d-f). They can propagate down pre-existing channels (Ojha et al. 2014), including gully channels. They tend to be restricted to slopes above the angle of repose (Dundas et al. 2017), but are found to extend to lower slopes (Schaefer et al. 2019; Stillman et al. 2020; Tebolt et al. 2020). However, RSL form on the upper reaches of scree slopes likely formed via mass wasting and are naturally at the angle of repose. Thus, just because RSL form on such a feature does not require that RSL be interpreted as a dry sediment flow (Tebolt et al. 2020). Isolated dark spots have been observed in rare cases immediately downslope of actively growing RSL, argued to be discontinuous RSL (Fig. 4e) (Ojha et al. 2015; Tebolt et

al. 2020). Stillman et al. (2017) interpreted such features as the “porpoising” of water flow, where water flowing under the surface was only sucked to the surface via capillarity in locations of low albedo.

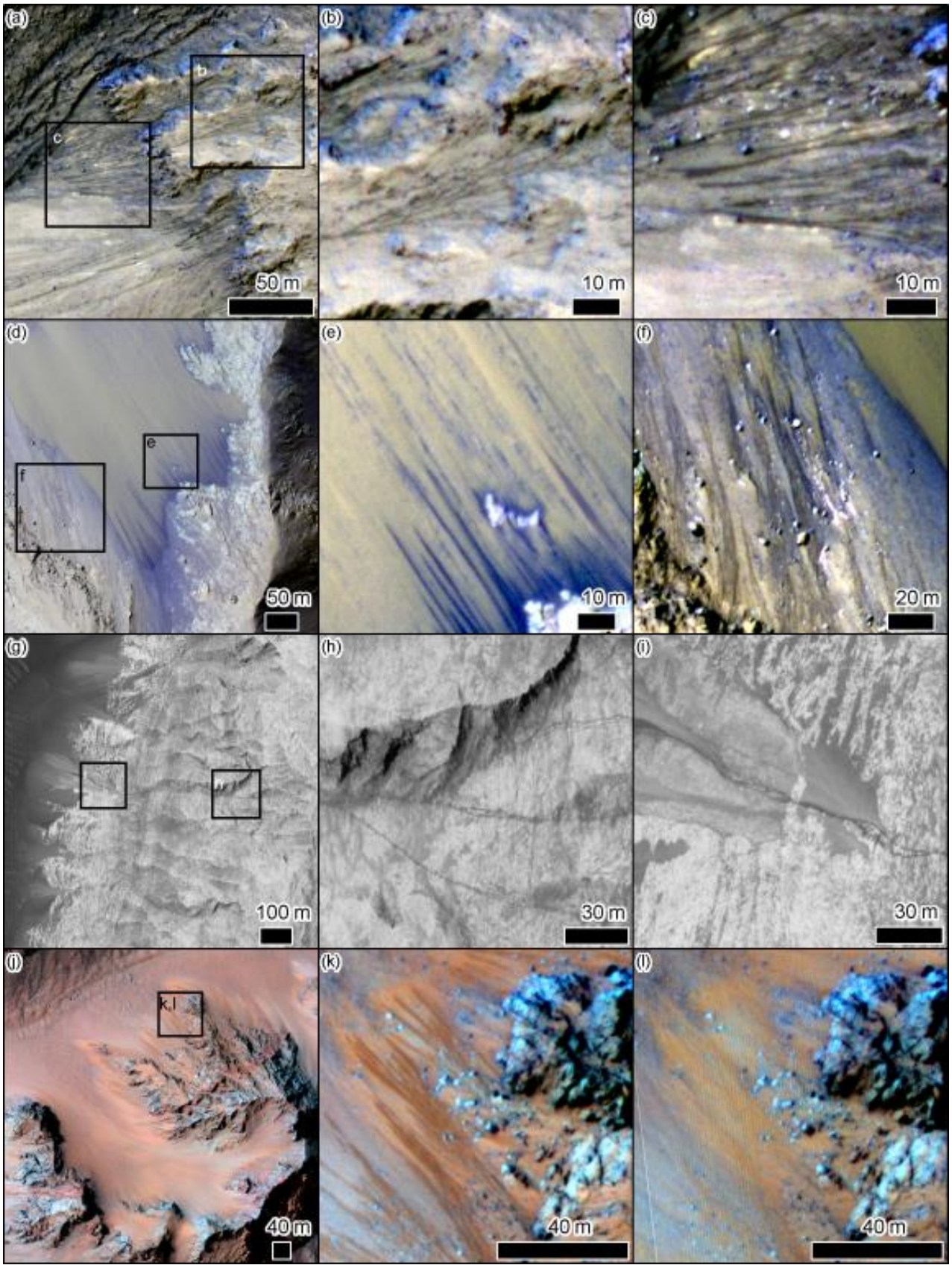
(a)
b
c
50 m
(b)
10 m
(c)
10 m
(d)
e
f
50 m
(e)
10 m
(f)
20 m
(g)
100 m
(h)
30 m
(i)
30 m
(j)
k,l
40 m
(k)
40 m
(l)
40 m

421

Figure 4: Examples of Recurring Slope Lineae (RSL), north is up in all panels. (a) RSL in the alcoves of gullies in Corozal Crater in the southern mid-latitudes with (b) showing multiple RSL coming together while deviating around obstacles and (c) showing their termini which often diverge. (a-c) False-colour HiRISE image ESP_023218_1410 where colours have been stretched to best enhance the contrast. (d) RSL extending from rocky substrates onto sand on a ridge in Coprates Chasma in Valles Marineris at the equator with (e) showing their discontinuous downslope extensions and (f) their lower contrast on the upslope rocky materials. (d-f) False-colour HiRISE image ESP_043085_1670 where colours have been stretched to best enhance the contrast. (g) RSL on the interior light-toned layered deposits in Juventae Chasma in Valles Marineris at the equator with (h) showing their propagation over the bedrock with braided sections and (i) showing their extension onto the debris fans, again showing sinuosity and braiding. (g-i) HiRISE image PSP_006915_1760 where stretch has been chosen to best enhance the contrast.(j) RSL on the central peak of Hale Crater in the southern mid-latitudes in HiRISE image ESP_047172_1440 where (k) shows their extension onto lighter albedo "fans". (l) HiRISE image ESP_046605_1440 showing the same location as in panel k, but at a season when the RSL have faded. Image credits: NASA/JPL/UofA.

Concurrent observations of dust devil tracks, boulder tracks, and RSL suggest that the distinctive dark albedo of RSL is a result of the removal of dust (Schaefer et al. 2019) and that annual atmospheric dust deposition allows their reoccurrence the following year. The dust storm of Mars Year 28 and 34 resulted in many more candidate RSL being apparent and for RSL to be in general a lot longer than in previous years (McEwen et al. 2019; Stillman et al. 2014). An alternate hypothesis is that wicking of moisture to the surface or water absorbed into salts could be the cause of the darker albedo (Heinz et al. 2016; Massé et al. 2014). In any case it is agreed that RSL do not engender any significant downslope sediment transport at the HiRISE-scale. As no sediment transport is involved, they are generally thought to represent either subsurface percolation of water, or thin granular flows.

Apart from the various dry hypotheses for RSL formation, discussed further in Chapter DUNDAS (pages xxx-xxx), water-based hypotheses require a mechanism to replenish the supply towards the top of the slope. They therefore focus around two potential mechanisms: i) atmospherically recharged source and ii) origin from aquifer seeps, which are discussed further below.

Mass balance arguments suggest that water ice frosts from the atmosphere are unlikely to be able to recharge RSL source areas, with RSL probably requiring metres cubed of water per metre of headwall, exceeding that which can be supplied from the dry martian atmosphere (Grimm et al. 2014). In addition, the kinetic barrier to melting, detailed in Section 1, would be particularly severe at the relatively warm locations of RSL occurrence in Valles Marineris – meaning the ices would need to somehow be protected by a lag in order to melt. Further, the melting of shallow subsurface ice is difficult as temperatures decrease with depth. If salt were present then melting could occur, but such melting would then flush these salts. This is unlikely because such a shallow subsurface ice would need a mechanism to recharge salt and significant amount of ice so that it could provide a source each year giving the recurrent behaviour of RSL (Stillman et al. 2014).

The surface temperature at which RSL start to grow argues that the water should be briny (i.e., have a depressed freezing point Grimm et al. 2014; Stillman et al. 2016) even though the near infra-red spectral detection of hydrated perchlorates associated with RSL from orbit (CRISM; Ojha et al. 2015) is now generally acknowledged to be due to instrument error (Leask et al. 2018; Vincendon et al. 2019) and no

systematic detection has been made of chlorine bearing salts in thermal spectra (Mitchell & Christensen 2016). The predicted abundance of salts on the martian surface is expected to be high, including chlorine-bearing species (Clark 1981; Gellert 2004; Keller et al. 2007; Kounaves et al. 2010; McSween & Keil 2000) and notably perchlorates (Glavin et al. 2013b; Glavin et al. 2013b; Hecht et al. 2009; Sutter et al. 2017; Toner et al. 2014a) which have remarkably large freezing point depression (e.g., Chevrier & Rivera-Valentin 2012). This abundance has led researchers to propose that RSL could be produced by deliquescence of these salts, i.e. the adsorption of water vapour (from the atmosphere or sublimated from ground ice) leading to the fluidisation of the salt (e.g., Bhardwaj et al. 2019b; Dickson et al. 2013). The relative humidity required for deliquescing Mars-relevant salts is on the order of >13% at 273 K (Gough et al. 2011; Heinz et al. 2016; Nuding et al. 2015; Primm et al. 2017), which for the same reasons as argued above seems high for the dry martian atmosphere. However, once these brines have formed they can form supersaturated and/or supercooled solutions with significant hysteresis prolonging their persistence in the environment (Gough et al. 2016; Primm et al. 2019; Toner et al. 2014b). Although temperatures are highest in the middle of the martian day, the relative humidity is at its lowest, so the early morning and late evening are more conducive to brine-formation by deliquesce (Gough et al. 2011; Primm et al. 2019). If RSL were caused by deliquescent salts, they should have different albedos at different times of day. This behaviour has not yet been observed with when comparing one morning CaSSIS image with an afternoon HiRISE image (Munaretto et al. 2020), but much more extensive analysis is required to substantiate this finding. Additionally, modelled water budgets using meso-scale atmospheric models coupled with deliquescence onto calcium perchlorate salts indicate an upper limit of 1 micron per sol, which is likely much too low to support any wet-dominated RSL formation mechanism (Leung et al. 2020).

Recharging sufficient salts into the source areas could be envisaged via atmospheric deposition, of notably perchlorate salts (Catling et al. 2010; Smith et al. 2014). If the brine comes from underground, there is no recharge problem for the salts, because the aquifer itself would be briny. However, repeating brine flows would be expected to continually deposit salts towards the ends of the RSL and within the subsurface. As no build-up has been detected from orbit there must be some unknown removal mechanism, if this hypothesis is true. The difficulty in recharging sufficient water (Stillman et al. 2016) and the proximity of RSL to fractures observed in the bedrock at which they originate (Abotalib & Heggy 2019) have been used as arguments to support their origin via groundwater. As discussed in Section 3.2 for gullies, a groundwater origin is hard to substantiate with confidence as we have so little knowledge on the structure of the subsurface of Mars (e.g., heatflow, permeability, lithology, fractures, cryosphere state/structure). Many of the most extensive RSL sites are found in locations that are advantageous for groundwater such as: the numerous RSL found within craters in the regional depression of Chyrse and Acidalia Planitia (Stillman et al. 2016), Garni crater on the floor of Melas Chasma (Stillman et al. 2017), and Palikir crater on the floor of the much larger Newton crater (Stillman et al. 2014). These sites could possess unconfined or confined/pressurized aquifers that could hydraulically connect to the surface via low permeability fractures. It should be noted that RSL are also found in places disadvantageous to groundwater access (Chojnacki et al. 2016). Nevertheless, such aquifers would need to possess a freezing depression that is greater than or equal to the mean annual surface temperature so that they could discharge to the surface only during the warmest part of the year (Stillman et al. 2016). Once the brine is discharged, it will then percolate downhill through the regolith. The regolith also must have an impermeable barrier to prevent the brine from seeping back into the subsurface before it shows a surface expression (Mellon & Phillips 2001). Due to the large diurnal temperature variations, the brine is

likely to completely or partially freeze at night, thus slowing its advance downhill. As discussed in Chapter DUNDAS (pages xxx-xxx) there are also RSL locations that are not likely to be connected to an aquifer such as the numerous RSL sites found on Coprates Montes (Chojnacki et al. 2016).

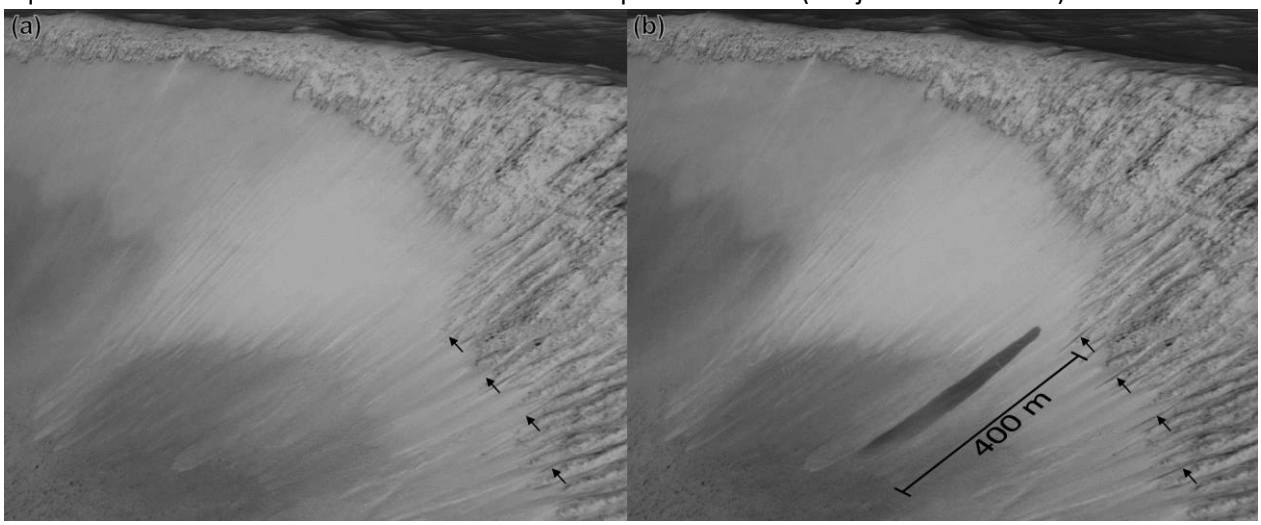

Figure 5: 3D rendering of a slump on the same slope as Recurring Slope Lineae (RSL) in Garni Crater. (a) Orthorectified HiRISE image ESP_034672_1685 showing the slope with RSL prior to the slump in MY32, Ls 65°. (a) Orthorectified HiRISE image ESP_035028_1685 showing the slope with RSL and the slump. The image was taken in MY32, Ls 77°, i.e. 26 sols after the image in panel a. Small black arrows point to the location of prominent RSL that grow between the two images. Image credits: NASA/JPL/UofA.

It is possible that liquid water is only the trigger for a motion that is then more granular, for example: the volume or weight change brought about by deliquescence could trigger a granular avalanche (Wang et al. 2019), or humidification-desiccation (water absorption-desorption) cycles could change the cohesive properties of the slope materials (Shoji et al. 2019). Experimental work has shown that boiling water or brines can cause grainflows, or eject pellets of damp material (Herny et al. 2019; Massé et al. 2016; Raack et al. 2017). These more "exotic" processes rely on the contact of liquid water with relatively warm substrates (>280K), as might be envisaged to happen at the edge of a propagating RSL flow-front, and vigorous boiling produces gas in the sediment pore-space capable of fluidising the granular bed, ejecting particles and even mobilising parts of the saturated mass. Such hybrid mechanisms would allow "dry" RSL to follow the seasonal patterns observed for RSL. However, similarly the purely dry mechanisms (Dundas et al. 2017; Schaefer et al. 2019; Schmidt et al. 2017; Vincendon et al. 2019), these granular flows would struggle to imitate the detailed growth histories of RSL (Grimm et al. 2014; Huber et al. 2020) also see Chapter DUNDAS (pages xxx-xxx).

In summary, the role of liquid water in Recurring Slope Lineae on Mars is supported by their temporal and spatial patterns of growth at the intra- and inter-seasonal scale, as well as their extension onto slopes lower than the angle of repose. The source of this water is problematic, either from the atmosphere or the subsurface. For brine-flows, a mechanism would be needed to remove the deposited salts. This outstanding problem for the "wet" hypothesis combined with new theories for the "dry" hypothesis has shifted the community's focus to resolving the issues regarding triggering and growth for the possible "dry" processes, see for example, Chapter DUNDAS (pages xxx-xxx). To date, no advanced modeling has been able to correlate the dry mechanism hypotheses with the observations.

3.3 Gullies

The term "gully" for Mars encompass a huge variety of landforms, whose uniting attribute is the presence of a channel through which material is transported from the source alcove to the debris apron or fan (see review by Conway et al. 2019b) (Fig. 6). Gullies are not to be confused with "spur and gully" morphology which was originally reported on Mars in Valles Marineris (e.g., Lucchitta 1987), but in this case the erosional and depositional parts are not connected by a channel. Spur and gully morphology with no channelisation is generally attributed to dry mass wasting processes which build talus cones in oversteepened landscapes (e.g., Thapa et al. 2017) and will not be discussed further here.

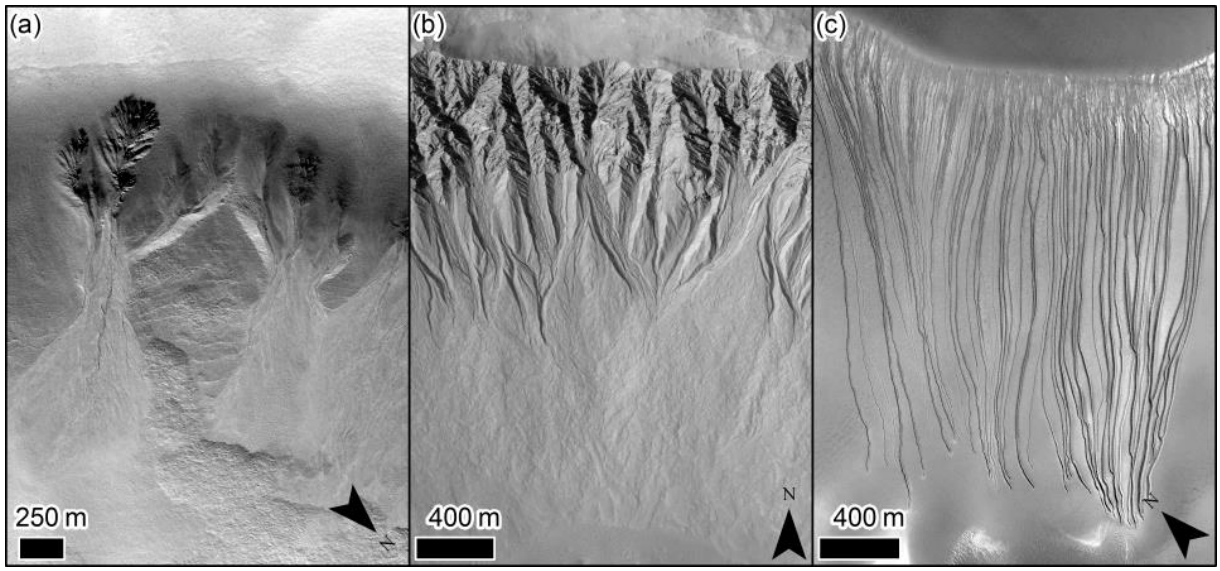

Figure 6: Examples of gullies on Mars. (a) Gullies incised into icy mantling materials on a crater wall in the northern hemisphere. Note the well-formed tributary networks, the abandoned alcoves and multiple generations of fan-deposits. HiRISE image ESP_018895_2410. (b) Gullies in Galap Crater in the southern hemisphere, where the alcoves are incised directly into the bedrock at the crater wall and no icy-mantling materials are present. HiRISE image PSP_003939_1420. (c) "Linear" gullies on the megadune located on the floor of Russell Crater in the southern hemisphere. HiRISE image ESP_038335_1255. Image credits: NASA/JPL/UofA.

Gullies, from the top of the alcove to base of the fan, are typically a kilometre in length (ranging from a hundred metres to several kilometres) and tens to hundreds of metres wide (ranging from decametres to ~kilometre). They were initially interpreted to be a result of liquid water flowing at the surface of Mars, because of their similarity to gullies carved by liquid-water on Earth and because of their latitude distribution and orientation preference (Malin & Edgett 2000). Gullies are found primarily on steep slopes at latitudes polewards of 30° north and south (Balme et al. 2006; Bridges & Lackner 2006; Dickson et al. 2007; Harrison et al. 2015; Heldmann et al. 2007; Heldmann & Mellon 2004; Kneissl et al. 2010) (Fig. 2b) and their variable spatial density in this latitude range is mainly a consequence of the availability of steep slopes (Conway et al. 2017). The sloping terrains where gullies are found comprise the relief-forming structures on Mars at kilometre-scales: impact craters (outer and inner walls, terraces, central peaks/pits), valleys and graben, mesas, buttes, collapse pits and dark sand dunes. At latitudes between 30° and 40° gullies are found primarily on pole-facing slopes and >40° they have a preference for equator-facing slopes, but can be found on slopes with all orientations (e.g., Conway et al. 2017;

Harrison et al. 2015; Heldmann & Mellon 2004). Gullies can be found in the equatorial regions, but they are generally small (hundreds of metres long for metres in channel-width), rare and only reliably identified in HiRISE images (Auld & Dixon 2016; Thomas et al. 2020), hence are not displayed with the larger landforms in Figure 2. It should be noted that Auld and Dixon (2016) classified features with an alcove and an apron but no channel as gullies which deviates from the commonly used Malin and Edgett (2000) definition that requires the presence of a channel. The latitudinal pattern in distribution and orientation of gullies (Fig. 2b) strongly suggests a climatic factor plays a role in conditioning their formation.

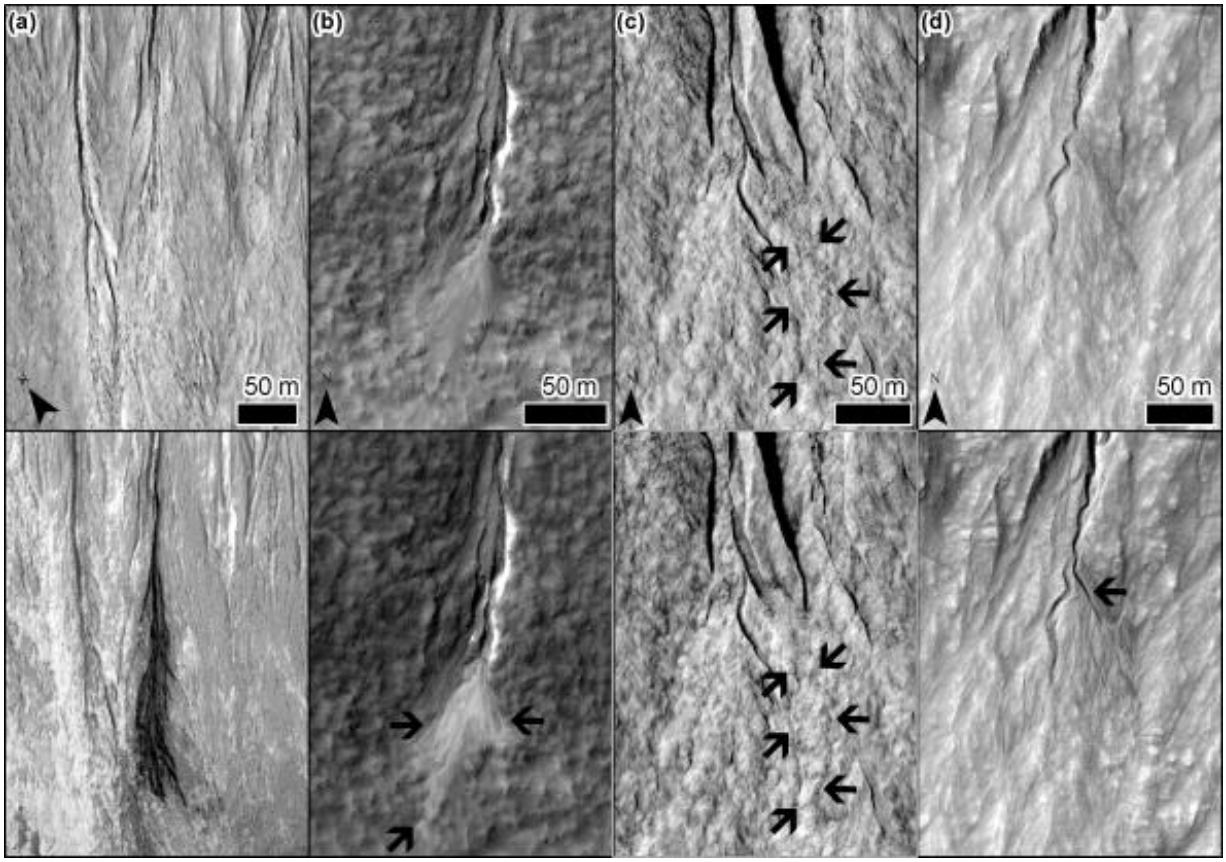

Figure 7: Examples of changes observed in martian gullies, where the top is the image before the change and at the bottom the image after the change. (a) Dark-toned deposit overlying frost in HiRISE image ESP_027567_1425 (before ESP_022688_1425). (b) Light toned deposit over an existing fan on HiRISE image ESP_031919_1435 (before ESP_014368_1435). (c) New high-relief deposit with no tonal change in HiRISE image ESP_032078_1420 (before PSP_003939_1420). (d) New channel and deposit in HiRISE image ESP_032011_1425 (before ESP_013115_1420). Note, the before-after pairs are not necessarily the closest in time but are chosen to best illustrate the changes. Image credits: NASA/JPL/UofA.

Worthy of particular attention are “linear gullies” (Fig. 6c) which are a very unusual type of martian gully, lacking a terrestrial equivalent and is only found on steeply sloping dark sand substrates (e.g., Diniega 2021; Diniega et al. 2013; Reiss & Jaumann 2003). “Classic” gullies, as described above, are also found on dunes. Linear gullies comprise a long linear to sinuous parallel-walled groove flanked by levees, which trends downslope and does not change appreciably in width along its length. The source zone is often marked by many smaller tributary grooves and the terminus either blunt or with a series of disconnected

pits, but with no obvious depositional fan/apron. They are often found near to other "classic" gullies and sometimes have morphologies that are transitional with other "classic" gullies (e.g. the channel part resembles a linear gully, whereas the source and deposit apron resembles a classic gully) (e.g., Pasquon et al. 2018). They form a relatively small proportion of the overall gully population, but are one of the most active types of gully at the present-day (Conway et al. 2019b).

Although gullies are too small to be dated directly via crater-size frequency distributions, their recent formation has been inferred by the lack of superposed impact craters. Dating of the terrains that gullies superpose has allowed authors to estimate maximum ages as 1-5 Ma (de Haas et al. 2018a; Reiss et al. 2004; Schon et al. 2009a). Gullies are composite landforms where overlapping deposits demonstrate that gullies have many multiples of formative events (e.g., de Haas et al. 2015a; Johnsson et al. 2014; Levy et al. 2010a). Inverted gully fans/channels and re-incision into mantled alcoves provide further evidence that significant hiatuses occur between different active periods in gullies (e.g., Dickson et al. 2015).

Monitoring of gullies on Mars has revealed that downslope movements of material are ongoing and predominantly occur in local winter (Diniega et al. 2010; Dundas et al. 2019b; Dundas et al. 2015b; Dundas et al. 2012; Jouannic et al. 2018; Malin et al. 2006; McEwen et al. 2007; Pasquon et al. 2019; Pasquon et al. 2018; Pasquon et al. 2016; Raack et al. 2015). Gullies on sand dunes are particularly active and most sites show some kind of motion every year. Mass balance calculations on dune gullies has highlighted that these features can be formed entirely in as little as a few hundreds of years (Pasquon et al. 2018). Only a few other sites show such cadences, with the majority of gullies showing activity having only one change within the last few decades of monitoring (e.g., Dundas et al. 2019b). Movements mostly take the form of relatively high or low albedo deposits on fans or within gully-channels (Fig. 7b), with only some identifiable by their relief (Fig. 7c,d). In a few cases the source of the sediment can be tracked back to an identifiable scarp (e.g., de Haas et al. 2019; Raack et al. 2020). Channels can be evacuated, or back-filled with sediment and new channels carved into fan-surfaces. Sites with gullies also often host RSL (Fig. 4a-c) and often small-scale equatorial gullies are also found at RSL sites (Fig. 4g-i).

Gullies have been proposed to form via both dry and wet processes, and a summary of the arguments in favour of the dry hypotheses can be found in Chapter DUNDAS (pages xxx-xxx). Due to present-day activity occurring during local winter it is very unlikely that these motions are triggered by liquid water. The only exception is that the recent activity in linear gullies does occur at a time of year when water ice can be cold-trapped and surface temperatures are rapidly rising towards the melting point (Pasquon et al. 2016), but even in this case the link with CO_2 ices provides a simpler explanation and is more widely accepted (see Chapter DUNDAS, pages xxx-xxx). It should be mentioned that some present-day activity characterised by the bright deposits, occur at times and places where CO_2 ices have not been detected, but H_2O ices have (Vincendon 2015), suggesting that water ice might be playing a role, although such deposits are found to be consistent with dry granular flows (Kolb et al. 2010; Pelletier et al. 2008). Whether the sediment transport observed at the present-day is representative of the processes that have formed the entire gully-landform still remains open to debate as gullies have a number of characteristics that are consistent with formation by flowing liquid water, as we detail below.

Martian gullies share many morphological characteristics with water-driven steepland erosional systems on Earth. Many of the detailed elements of martian gully morphology can be identified within larger terrestrial catchments, but also erosion-deposition systems that share a similar morphology can be found in permafrost to arid regions on Earth (Costard et al. 2007; Dickson et al. 2018; Hartmann et al.

2003; Hauber et al. 2018; Heldmann et al. 2010; Sinha et al. 2018). Sediment transport through such systems is typically via a cascade of different processes, including mass wasting or landsliding, debris flow and fluvial transport (e.g., Cavalli et al. 2013; Heckmann & Schwanghart 2013; May & Gresswell 2004). The upper part of martian gullies is often tributary in nature, forming an organised, hierarchical network, a typical organisation of fluvial systems on Earth. The lower part of martian gullies often comprises a fan, where multiple deposits overlap, a characteristic shared by alluvial fans on Earth (de Haas et al. 2016; de Haas et al. 2018b). Fresh individual deposits can be characterised by lobate margins and levees flanking the channel (Johnsson et al. 2014; Lanza et al. 2010; Levy et al. 2010a; Sinha et al. 2020), which are characteristic of debris flow processes on fans on Earth (e.g., Blair & McPherson 2009; de Haas et al. 2015c). In-channel deposits can show braiding, streamlining, sinuosity, abandoned channel segments, terraces, all typical features of sediment-charged streams on Earth (e.g., Bakker et al. 2019). Topographically, both in terms of along-channel profiles and in terms of contributory-characteristics martian gullies are indistinguishable from terrestrial systems dominated by debris flow or fluvial processes (Conway et al. 2015; Conway et al. 2011b; Conway & Balme 2016; Hobbs et al. 2017; Yue et al. 2014). Stratigraphic analysis has revealed that the deposits laid down in martian gully fans indicate a dominance of debris flow processes, even though typical debris flow surface morphologies, such as lobes and levees, are absent, probably as a result of surface erosion by wind (de Haas et al. 2015b).

Numerical models and experimental simulations both conclude that once liquid water is generated, it would be sufficiently stable to flow the whole length of the gullies and to transport sediment (Bargery & Gilbert 2008; Conway et al. 2011a; Heldmann et al. 2005; Herny et al. 2019; Parsons & Nimmo 2010; Raack et al. 2017). Its metastable state may result in some transport mechanisms that are rarely active on Earth, particularly those as a result of boiling, which can result in enhanced sediment transport for relatively limited quantities of water (Herny et al. 2019; Massé et al. 2016; Raack et al. 2017).

No matter the source for the liquid water, the proposed release mechanism is a result of the insolation conditions experienced by Mars under moderate to high obliquity conditions (>35°), when peak temperatures are experienced by steep pole-facing slopes in the mid-latitudes (Christensen 2003; Costard et al. 2002; Williams et al. 2009; Williams et al. 2008). Three sources of water have been considered as possible: i) groundwater, ii) ground ice, or iii) surface ice precipitates (snow, or frost).

Groundwater: Both deep (Gaidos 2001; Grasby et al. 2014) and shallow sources (Heldmann & Mellon 2004; Marquez et al. 2005; Mellon & Phillips 2001) have been proposed as the source for gullies, where in both scenarios seeps of water/brine occur when the incoming radiation is sufficient to melt the plug of ice formed where the aquifer reaches the surface, and falling winter temperatures reseal this plug. Where the radiation is too strong, water will evaporate rather than flow and where the radiation is not strong enough, the plug will never melt – these factors explain the latitude orientation trends shown by gullies (Fig. 2c). Both sources struggle to explain the emergence of gully alcoves at the top of isolated topography, where shallow aquifers would not be sufficiently voluminous to repeatedly supply sufficient water and deep aquifers would be improbable to emerge (e.g., Balme et al. 2006; Conway et al. 2019b; Treiman 2003). Although, recent arguments derived from RSL-research (Section 3.1) maintain that deep, pressurised aquifers could emerge at these elevated locations if a permeable pathway exists (Stillman et al. 2016).

Ground ice: Redistribution of the water ice from the polar caps to lower latitudes under conditions of high orbital obliquity is thought to explain the prevalence of ground ice down to 50° north and south

(Jakosky & Carr 1985; Madeleine et al. 2014; Mellon & Jakosky 1995) and its discontinuous presence to 30°N and S (Kreslavsky & Head 2000; Milliken et al. 2003; Mustard et al. 2001). The same high obliquity conditions could be conducive to its melting where peak temperatures are experienced in the subsurface on pole-facing slopes in the mid-latitudes (Costard et al. 2002; Kreslavsky & Head 2003). In this scenario the distribution and orientation of gullies with latitude is a factor of both the availability of ground ice and the conditions required for its melting. Mass balance arguments show that ground ice is being lost during gully-formation (Conway & Balme 2014), but gullies are found in zones without obvious presence of ground ice (de Haas et al. 2018a; Johnsson et al. 2014), which argues against this hypothesis. Conversely, the abrupt absence of equator-facing gullies at 40° north and south matches surprisingly well with the anticipated absence of ground ice at these locations (Conway et al. 2018b).

Snow/frost: The formation scenario for snow and/or frost (de Haas et al. 2015a; Kossacki & Markiewicz 2004; Williams et al. 2008) is similar to that for ground ice, but the source is seasonal surface deposits, rather than ice stored within the soil. For one particular site the debris flow cadence revealed by the deposit volumes and the age of the host crater is consistent with millimetres of snow over the catchment, which is broadly in accord with climate model predictions for snowfall at high obliquity (de Haas et al. 2015a). Whether atmospheric conditions in the past were conducive to melting at the surface, however, is a matter of debate.

In summary, although gullies on Mars strongly resemble terrestrial gullies carved by liquid water, it remains under debate as to whether the same processes were active on Mars. There is growing evidence that present-day activity almost certainly does not involve liquid water, but whether present-day processes are representative of the processes that have contributed to the construction of the whole gully-landform is still debated. If current modification processes of gullies cannot explain their entire formation, liquid water at high obliquity is the next most likely candidate to explain the formation of martian gullies. Periglacial landforms

Many landforms tightly associated with periglacial conditions on Earth have also been reported on Mars, including: solifluction lobes, pingos, low-centred polygons, ice-loss depressions and sorted patterned ground. For a in-depth review of these features on Mars, please refer to Balme et al. (2013). Periglacial conditions are those which are dominated by the action of freeze-thaw processes and do not necessarily imply permafrost or glacial conditions (French 2013). Integral to periglacial conditions is the occurrence of freeze-thaw cycles and the formation of an active layer – that is a layer on top of the permafrost that undergoes annual thaw – hence in apparent contraction with our understanding of the stability of liquid water on Mars. Implicit for the formation of periglacial landforms is the presence of ground ice, which as described in Section 2.2, which is a pre-requisite relatively easy to fulfil on Mars.

Below, we summarise the observations pertaining to each of these features and the way in which liquid water is thought to be involved in their generation and then introduce the concept of a landscape assemblage.

3.4 “Solifluction” lobes

Lobate forms found on hillslopes on Mars have a strong resemblance in form and scale to solifluction lobes on Earth (Gallagher et al. 2011; Johnsson et al. 2018; Johnsson et al. 2012; Soare et al. 2018b) (Fig. 8). Like their terrestrial analogues they can be sheet-like or tongue-like, extending in the downslope direction and are bounded at their lower end by a scarp or “tread”. Their margins can be picked out by relief or by clasts. The martian lobes can be larger in both width and length than solifluction lobes on

Earth (generally up hundreds of metres), but their ranges of sizes do overlap and are typically tens of metres wide and long (Gastineau et al. 2020). Even though individual lobes are small, they occur in groups that can span hundreds of metres to kilometres across and downslope. Martian lobes have the peculiarity that they are found on slopes above 10° and on average ~25°, whereas terrestrial solifluction lobes can be found on all slopes up to 35° (Gastineau et al. 2020). They occur at latitudes poleward of 60° in the northern hemisphere and at latitudes of poleward of 40° in the southern hemisphere (Fig. 2c) and are less common in the southern hemisphere (Johnsson et al. 2018).

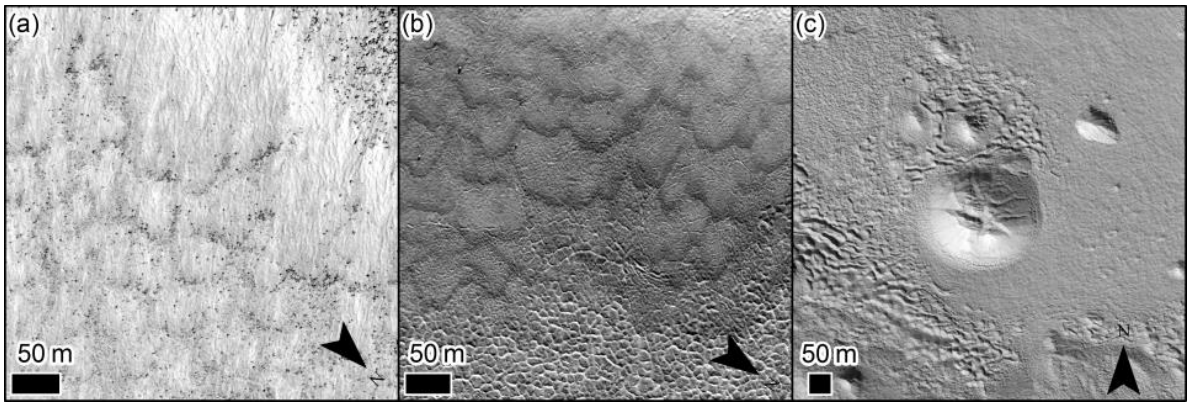

Figure 8: Examples of lobate forms and pingo-like mounds. (a) Lobate forms outlined by clasts on the wall of Heimdal Crater (Gallagher et al. 2011)*. Downslope is down-image. HiRISE image PSP_009580_2485. (b) Lobate forms marked by relief and overprinting polygonal terrain on an impact crater wall in the northern hemisphere* (Johnsson et al. 2012)*. Downslope is down-image. HiRISE image PSP_010077_2520. (c) Pingo-like mound near Moreux Crater (see Chapter SOARE, pages xxx-xxx) with prominent summit cracks. HiRISE image ESP_058140_2225. Credits: NASA/JPL/UofA.*

Solifluction lobes on Earth are sheets of material that move as a result of differential downslope movement caused by freeze-thaw cycling in the active layer (Matsuoka 2001). A range of processes lead to the formation of solifluction lobes on Earth, including: gelifluction, plug flow, frost creep and retrograde movement (Matsuoka 2001). The influence of each of these processes on the morphology of the lobes has not been isolated, but each requires extensive thaw and considering martian lobes cover hundreds of metres of areal extent, this would require equivalently extensive thaw to prevail. The age of these features is uncertain, but is presumed to be late Amazonian as they are not overlain by any other feature and there is some evidence of motion today in the form of boulder motions on the same slopes (Dundas et al. 2019a). Alternatives to thaw for generating lobate forms have not yet yielded convincing results (Gastineau et al. 2020), but some kind of creep triggered by CO_2 ice-related processes has been suggested, but remains to be substantiated (Dundas et al. 2019a).

3.5 Pingo-like mounds

Mounds with spatial extents of tens to hundreds of metres are commonplace on Mars and have been attributed to the action of a range of processes, including differential erosion, volcanism (magmatic or sedimentary), inverted impact craters and pingos (e.g., Bruno et al. 2006; Burr et al. 2009a). Of particular interest for this discussion are those that have been identified as pingos (Fig. 7) (Balme & Gallagher 2009; Burr et al. 2009b; Dundas et al. 2008; Dundas & McEwen 2010; Soare et al. 2013b; Soare et al. 2013a; Soare et al. 2014a; Soare et al. 2005), see also Chapter SOARE (pages xxx-xxx). These landforms

747 have been reported mainly in the mid-to-high-latitudes on Mars with the exception of one report near
748 the equator (Balme & Gallagher 2009).

749 Pingos on Earth can be formed by the impingement of permafrost upon a near-surface liquid water body
750 (talik) generating hydrostatic pressure (closed system) or by artesian pressure developed in a talik
751 connected to the surface (open system). Typically closed system pingos are developed when an alas, or
752 thermokarst lake, catastrophically drains and the permafrost re-advances into the saturated sediments
753 (e.g., Mackay 2002). Open system pingos develop where sub-permafrost meltwater is pushed to the
754 surface by an elevated hydrostatic gradient generated by surrounding topography, for example in the
755 forefields of retreating glaciers (Christiansen 1995; French 2013). In both cases massive ice is formed in
756 the core of the pingo which pushes up the surface above it, forming a mound. The mounds can be
757 circular, elongate or form complexes in planform. On Earth, pingos can grow to heights of tens of metres
758 with widths of hundreds of metres to nearly a kilometre (Gosse & Jones 2011; Jones et al. 2012). As they
759 grow via injection of water and deformation of the ground, they often display summit cracks where the
760 deformation is greatest (e.g., Mackay 1987). Their flanks slopes can increase beyond the angle of repose
761 then causing mass wasting of the flanks. The cracks in the overburden can engender the destabilisation
762 of the interior ice, forming a summit pit. If the ice at the core melts then the pingo can completely
763 deflate leaving a shallow raised rim depression or pingo scar (Flemal 1976).

764 Similarly, pingos on as Mars have been differentiated from other mounds, such as rootless cones,
765 principally by their summit cracks (Fig. 8) and pits, with some displaying flank mass wasting and irregular
766 planforms. Such mounds have been reported in closed topographic environments, such as crater floors
767 (Soare et al. 2013a), as well as at the base of slopes in more open topographic environments (Soare et al.
768 2014a). The implication of pingos on Mars is that there was sufficient melt to generate the talik, but no
769 long-lived sub-surface water is required once they are formed. The age of the mounds on Mars is
770 unknown, but they are not superposed by any other feature, so are presumably Late Amazonian in age.
771 No alternative mechanism for ground-uplifting has been proposed as an alternative to the liquid water
772 hypothesis, but the interpretation of these mounds as being a result of heave (and not one of the other
773 potential and numerous mound-forming processes) remains under question, as liquid water is
774 considered unlikely.

775 3.6 Patterned ground

776 Patterned grounds on Earth are characterised by the separation of the surface soils into relatively fine
777 and clastic domains with regular, repeating patterns. These take the form of, sorted stone circles,
778 labyrinths, polygon-nets or piles, which can evolve into clastic stripes on sloping terrain. The ratio
779 between the fines and clasts, the amount of confinement and the slope are all factors that play a role in
780 determining the patterns that are expressed at the surface (Kessler & Werner 2003). The mechanism
781 that leads to the sorting is a feedback that involves frost heave combined with differing thermal inertias
782 of saturated soil and stones (Hallet 1990) and necessarily involves freeze-thaw cycles. On Mars surface
783 patterns resembling those of sorted patterned ground on Earth have been identified at the equator
784 (Balme & Gallagher 2009), but more pervasively in the northern plains at >35 °N (Barrett et al. 2018;
785 Barrett et al. 2017; Gallagher et al. 2011; Gallagher & Balme 2011; Soare et al. 2018a), but also in the
786 southern hemisphere (Soare et al. 2016). The martian landforms include clastic polygons, stripes and
787 boulder piles (Fig. 9) and tend to be at the larger end of the scale of the sorted patterned grounds
788 observed on Earth, with length-scales of tens of metres, as opposed to metres as usually seen on Earth

(Barrett et al. 2018). The patterns follow the expected transition to stripes on sloping terrain on Mars as they do on Earth.

The presence of these landforms on Mars suggests a climatic episode where freeze-thaw cycles were common allowing the development of these landforms. An alternate CO_2 ice driven process is described in Chapter DUNDAS (pages xxx-xxx) (Orloff et al. 2011; Orloff et al. 2013), but no experimental or field evidence is available to test its efficacy, hence remains difficult to assess its likelihood. Whether these landforms are active at the present-day is unknown and their age is difficult to determine but given their uncratered and pristine appearance it is assumed to be late Amazonian.

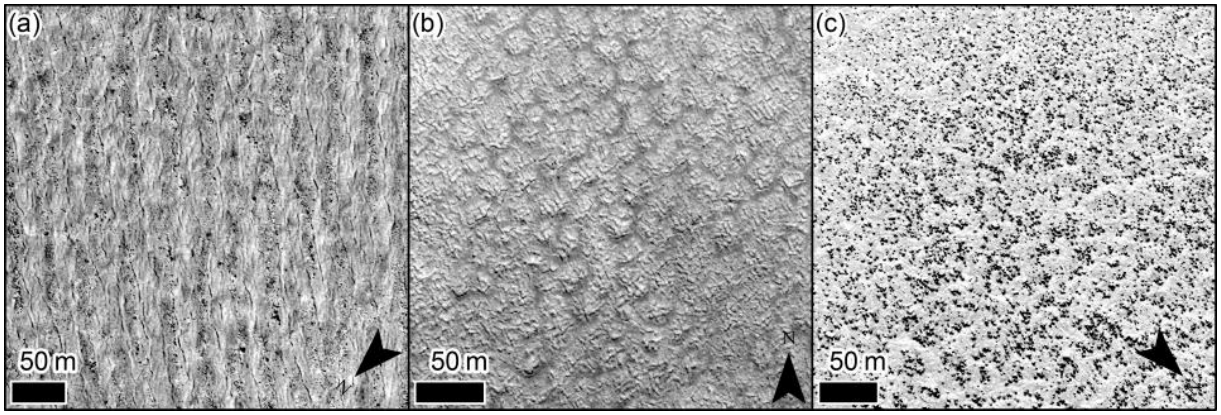

Figure 9: Examples of sorted forms on Mars. (a) Sorted stripes in Heimdal crater (Gallagher et al. 2011)*, where the stripes are picked out by clasts, downslope is to the bottom of the image. HiRISE image PSP_009580_2485. (b) Sorted circles on the plains outside Heimdal Crater* (Gallagher et al. 2011)*. HiRISE image PSP_009580_2485. (c) Sorted nets near Lomonosov Crater* (Barrett et al. 2017)*, where clasts are arranged into polygonal patterns. HiRISE image ESP_017131_2485. Image credits: NASA/JPL/UofA.*

3.7 Low-centred polygons

In Section 2.3.2 we described the prevalence of polygonal patterns in the martian mid-to-high latitudes, which are believed to be a direct result of thermal contraction cracking of perennially frozen ground (Mellon 1997). The polygons are generally metres to tens of metres in diameter (Mangold 2005). In many areas the centres of these polygons are at lower elevations than their edge often with a double raised rim (Levy et al. 2010b; Levy et al. 2009a; Soare et al. 2014b; Soare et al. 2018b) (Fig. 10d-f), "low-centred polygons", a phenomenon on Earth that is linked to active ice-wedge or sand-wedge polygons. Ice-wedge polygons form when liquid water penetrates cracks formed by thermal contraction and expands to both force the crack further apart and pushes up the material above it (MacKay 2002). Sand-wedges form when sand is repeatedly transported into the contraction crack and raised rims can be formed when the thermal re-expansion of the ground pushes against the additional material that has accumulated in the wedge causing the soil to be displaced upwards at the margin (Murton et al. 2000; Pewe 1959). Without in situ investigation it remains unknown if the low centred polygons on Mars comprise ice or sand wedges and however, the presence of ice-wedges has been inferred by the landscape context of the low-centred polygons, a concept discussed further in Section 3.3.6. On their own low-centred polygons are ambiguous and have not been used to argue for the action of liquid water, but have been incorporated as part of a landscape assemblage that has been used to argue for the action of liquid water, see Section 3.3.6.

3.8 Ice-loss depressions

We refer readers to Chapter VIOLA (pages xxx-xxx) for a complete description of landforms interpreted to be a result of ice-loss collapse processes on Mars, but for completeness we provide an abridged description here as well. These landforms are often referred to as "thermokarst", which on Earth refers to landscapes created by collapse induced by thaw (increase in temperature), and on Mars this is likely not the case, so we do not use this term for Mars. "Cryokarst" is another term that has been used for these landforms (Costard 2007), but is a term usually restricted to collapse features engendered by the loss of glacial ice via melting (e.g., Corbel & Gallo 1970), hence we do not apply this term either. For collapse to occur the ground must contain excess ice, that is ice in excess of the pore-space, hence when it is lost a decrease in volume occurs. On Earth, ice-loss in thermokarst occurs via thaw, but on Mars ice-loss is more likely to occur by sublimation (e.g., Dundas et al. 2015a). This is in accord with observations, as no evidence of lakes or drainage channels have been observed. On Earth, thermokarst landforms are varied (e.g., Kokelj & Jorgenson 2013), but of particular relevance to Mars are three features: terrain comprised of circular to oblate depressions often filled with water "alases" resulting from the degradation of excess ice, high centred polygons resulting from ice-loss at the polygon margins and beaded streams that are a result of the melting of ice in ice-wedge polygons. So called "scalloped depressions" are found on Mars (Fig. 10b,c,e) and parallels have been drawn between these and alases on Earth (e.g., Lefort et al. 2010; Soare et al. 2008; Ulrich et al. 2010). These depressions are found polewards of 40°N (Orgel et al. 2018; Ramsdale et al. 2018; Séjourné et al. 2018) and poleward of 35°S (Voelker et al. 2017; Zanetti et al. 2010). A related feature is expanded craters (Fig. 10a), which are circular resembling impact craters yet have an identifiable terrace (Viola et al. 2015; Viola & McEwen 2018), and they have similar latitudinal distribution to scalloped depressions. High-centred polygons (Fig. 10e) are found both in association with other ice-loss depressions on Mars and as isolated landforms, but as on Earth are associated with ice-loss at the polygon margins (e.g., Levy et al. 2009b; Soare et al. 2014b). On Earth, this loss can be from an ice-wedge (e.g., Ulrich et al. 2011), but also simply general loss of underlying massive or excess ice focused via the thermal contraction crack at the polygon margin (Marchant et al. 2002). Polygon junction pits (Fig. 10b) are observed in Utopia Planitia (Costard et al. 2016; McGill 1986; Soare et al. 2012; Soare et al. 2011) and parallels have been drawn between these expanded polygon margins and degraded ice-wedge polygons on Earth which form beaded-streams. All these ice-loss features are found in the mid-latitudes and also show concentrations at certain longitudes: Utopia and Acidalia Planitae in the northern hemisphere and Malea Planum in the southern hemisphere. The age of the ice-loss depressions is not easy to determine – they superpose all other landscape features, so are thought to be Late Amazonian (see Chapter VIOLA, pages xxx-xxx).

Although it is likely that the ice-loss depressions on Mars do not involve the generation of liquid water, their presence is a strong indicator of excess ice and the generation of excess ice on Earth involves the presence of saturated ground (e.g., Rempel 2007). Excess ice is differentiated from glacial or massive ice as it requires development of ice within the soil column, rather than deposition of ice directly at the surface. Ice-loss terrain cannot develop in glacial ice as there would not be sufficient material left behind after thaw/sublimation to maintain the landform relief. Porous ice (analogous to firn) has been inferred to be present in areas with ice-loss terrain to depths of around a hundred metres from radar sounding data (Bramson et al. 2017; Bramson et al. 2015; Stuurman et al. 2016), and could have up to 20% lithic material, however this is at odds with geomorphic evidence showing that ice could not have been precipitated from the atmosphere (e.g., boulders at the surface; Sizemore et al. 2015). Enriching the martian soil column to tens of metres of depth with ice in the absence liquid water is challenging

because ice diffused into the pore-space tends to seal the underlying soil column from further deposition (Jakosky 1983; Zent et al. 1986), even if migration through thermal contraction cracks is taken into account (Fisher 2005). Segregation ice has been observed at the Phoenix landing site and can be generated without thaw (Mellon et al. 2009; Sizemore et al. 2015), but such diffusive processes are only thought to be able to produce excess ice in the first metre of the soil.

Note, that a porous medium with salt and ice in its pores will contain some residual liquid. The amount of unfrozen water depends on the temperature, salt concentration, salt type, and surface area of the medium. This water stays unfrozen due to freezing point depression due to the dissolved salts and because of the effects of surface energy along curved interfaces (Rempel 2012; Sizemore et al. 2015). When a porous media with an appreciable amount of unfrozen water and permeability below freezing undergoes temperature cycling near 273 K, it can form segregated ice (i.e. ice lenses). This process is called cryosuction and occurs under a temperature gradient, where unfrozen water is suctioned to colder temperatures when the liquid veins in the colder soil constrict due to the colder temperature. This new water is then frozen and more water is drawn into the colder porous media. With the very cold temperatures of Mars, temperature cycling near 273 K only occurs within the first metre of the soil.

Hence, although ice-loss depressions are not thought to be engendered by melt, it is still an open question as to whether the generation of the terrain hosting these depressions implies enrichment of the ground in ice via migration of unfrozen water. The timing of the emplacement of the terrain hosting the ice-loss depressions is hard to determine, but is most likely to be during the Amazonian (Soare et al. 2015; Willmes et al. 2012) (see Chapter VIOLA, pages xxx-xxx and Chapter SOARE, pages xxx-xxx), although could be older.

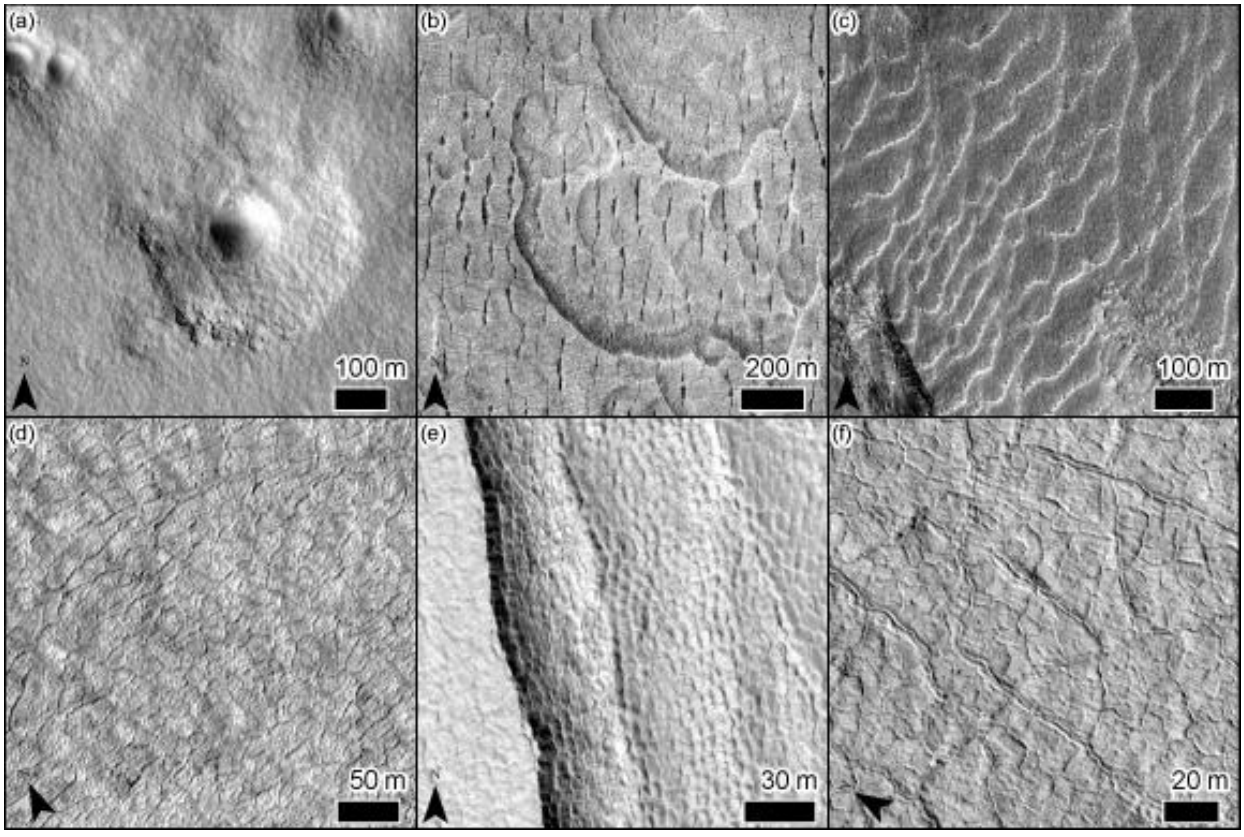

Figure 10: Examples of martian ice-loss depressions and different polygonal patterns. (a) Expanded secondary craters, where a polygonised basin can be seen extending away from the central bowl-shaped depression (REF). HiRISE image ESP_028411_2330. (b) "Scalloped" depressions in Utopia Planitia intersected by polygon-junction pits. HiRISE image PSP_007740_2250. (d) "Wavy" and polygonised depressions associated with gullies in the Argyre Basin. HiRISE image ESP_040974_1395. (e) Low-centred polygons on the inter-crater plains in the high southern latitudes. HiRSE image ESP_022381_1100. (e) Scalloped depression in Utopia Planitia with low-centred polygons near its wall and high-centred polygons on its floor. HiRISE image ESP_034164_2260. (f) Polygon margins marked by a double-raised rim. HiRISE image PSP_005821_1095. Image credits: NASA/JPL/UofA.

3.9 Landscape Assemblage

Above, we have examined each landform independently and examined the likelihood that each could be a result of processes involving liquid water. However, landforms do not occur in isolation and both the context and the association between landforms can favour one interpretation over another. This concept of a landscape assemblage has been used to argue for the involvement of liquid water in the generation of landscapes on Mars (Balme et al. 2013; Gallagher & Balme 2011; Hauber et al. 2011a; Hauber et al. 2011b; Soare et al. 2014b; Soare et al. 2018b; Soare et al. 2018a; Soare et al. 2016; Soare et al. 2005) (see Chapter SOARE, pages xxx-xxx), where gullies, sorted patterned ground, lobate forms, low-centred polygons, pingos and/or ice-loss depressions are found in close proximity suggesting a common suite of processes in their origin. Figure 11 outlines such a scenario where freeze-thaw cycles within the materials in the crater wall, brings about sorting (to form stripes) and gelifluction to create solifluction lobes – extreme melting events lead to generation of gullies, whose melt water drives the formation of pingos at the base of the slope. The context of many of these assemblages is interpreted to be post-glacial, because of the following attributes: "washboard" texture on slopes (indicative of downslope deformation), polygonal surface textures and ice-loss-depressions (indicating high ice content), expanded fractures (which could be crevasses), all upslope of arcuate ridges with spatulate depressions (interpreted to be moraines, e.g., Berman et al. 2005) and often stratigraphically above older glacial units (Head et al. 2008; Jawin et al. 2018).

The fact that CO_2 ice processes and sublimation landscape assemblages are not found on Earth means an equivalent comparison cannot be made, a point that will be discussed further in Section 4.

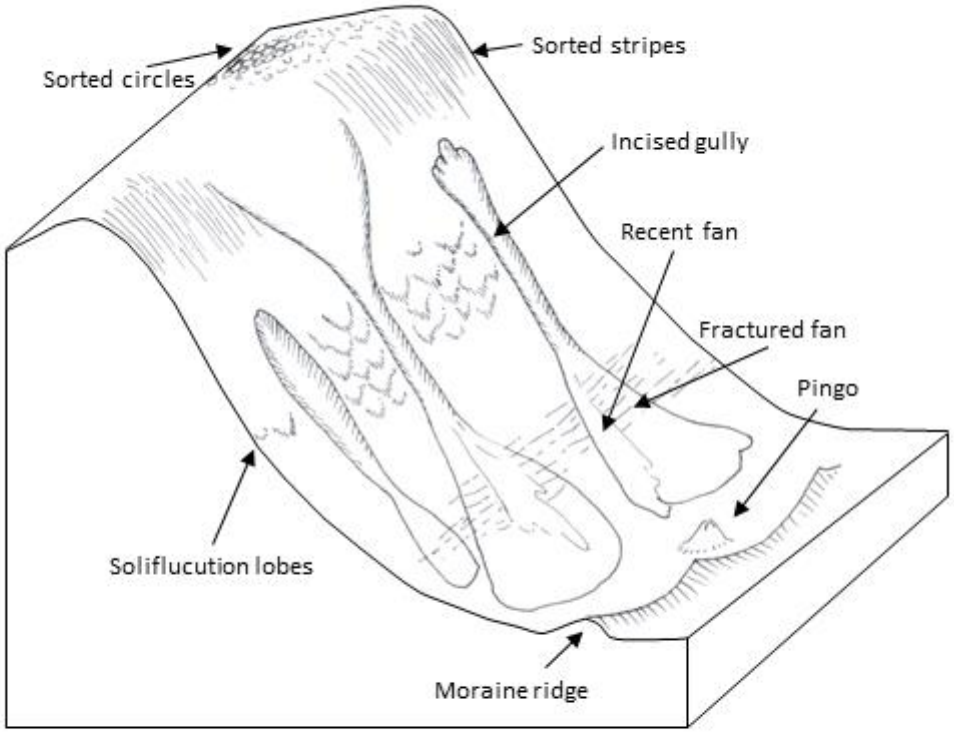

Figure 11: Sketch of landscape assemblage on a crater wall, with (from top to bottom), sorted circles leading into sorted stripes then solifluction lobes. Hillslope is incised by gullies, whose fans are partially overprinted by extensional fractures. At the base of the gullies are arcuate ridges and in the intervening basin, a pingo.

3.10 Evidence for melting of martian icecaps or glaciers

Evidence for melting of martian icecaps or glaciers spans from the present-day, to contemporaneous with gullies (millions of years ago), contemporaneous with extant martian glaciers (hundreds of millions of years ago) to much earlier in martian history (billions of years ago). Orosei et al. (2018) and Lauro et al. (2020) reported radar evidence which suggested the presence of lakes of liquid brine underneath the south polar cap of Mars at the present-day. Recent modelling work has highlighted that the position of the proposed lake is not located in a local depression, but is connected to the hydrological system, hence is more likely a pocket of brine caused by locally elevated geothermal flux (Arnold et al. 2019). While

MARSIS detects a significant radar return, it is unfortunate that the higher frequency radar sounder SHARAD has not detected this anomaly. SHARAD cannot always image the floor of the SPLD, however, given such a large signal one would expect a detection. Hence, although not substantiated by other evidence, it remains plausible that liquid water can be generated at the base of the martian polar caps, even under present-day conditions. Various lines of evidence already point to the fact that the south polar cap has undergone basal melting in the Early Hesperian – Late Noachian (e.g., Kress & Head 2015). Sinuous ridges emanating away from the boundary of the south polar cap have been interpreted to be eskers – deposits laid down in sub-glacial channels (Butcher et al. 2016; Kress & Head 2015; Scanlon et al. 2018; Scanlon et al. 2015). Scenarios in which elevated geothermal heat flux is required in the form of volcano-ice interaction (Ackiss & Wray 2014; Ghatan & Head III 2002; Wray et al. 2009) and passive climate-driven melting with a generally larger Noachian geothermal heat-flux (Fastook et al. 2012) have been explored and found to be plausible.

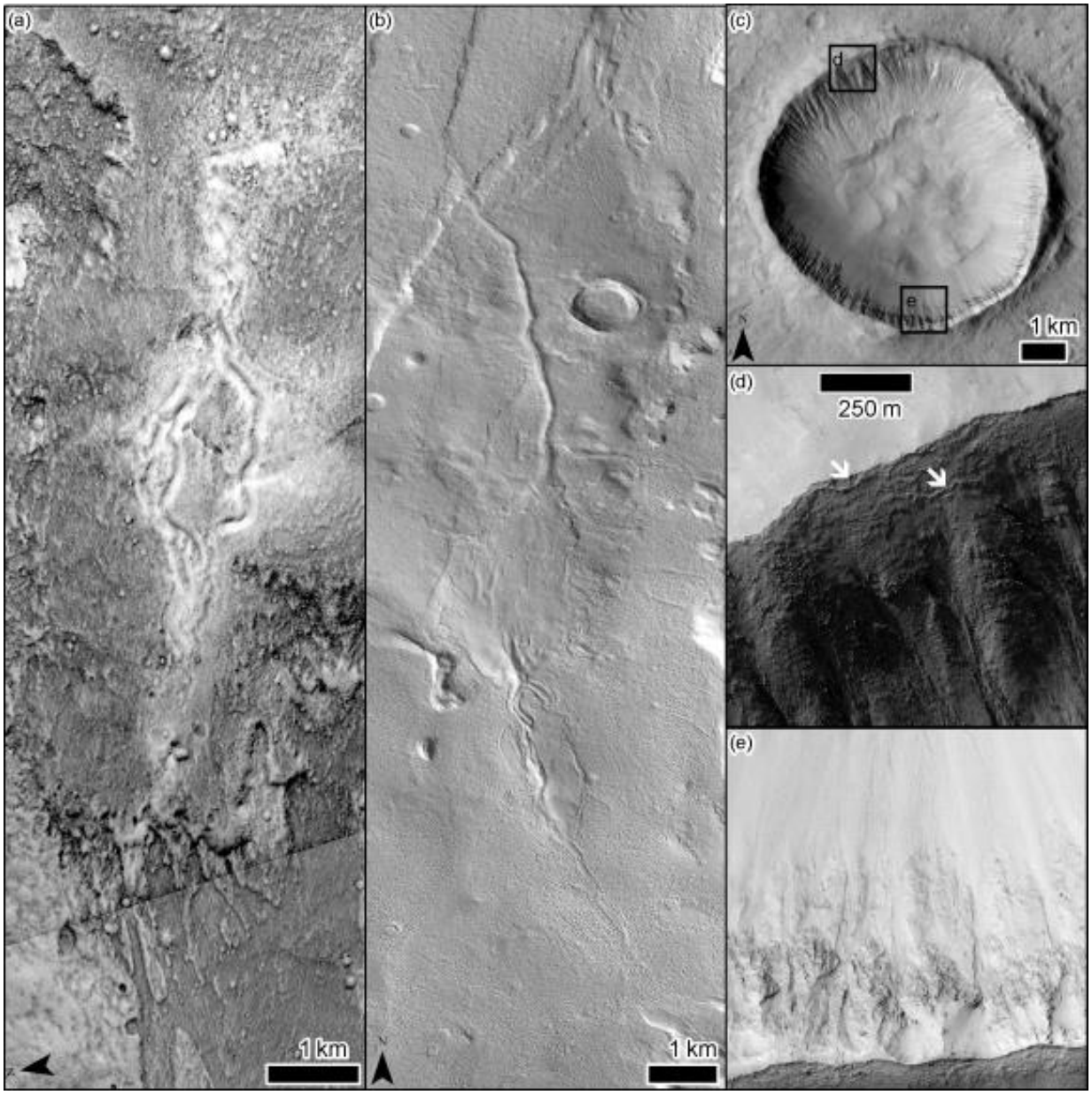

Figure 12: Evidence of basal melting of glaciers on Mars. (a) Sinuous ridge in Phlegra Montes (Gallagher & Balme 2015) *interpreted as an esker, whose parent glacier is located off the bottom of the image. CTX Images G20_026224_2116 and P22_009583_2132. (b) Sinuous ridge emerging from parent glacier located in lower half of image in Tempe Terra* (Butcher et al. 2017)*. CTX image P05_002907_2258. (c) Crater in the southern mid-latitudes in CTX image G09_021563_1427 showing evidence of glacial erosion, where the glaciated pole-facing slope in (d) has a lower slope-angle with the bedrock spurs planed off (arrows) directly above arcuate ridges interpreted to be moraines, and the non-glaciated equator-facing slope in (e) has preserved bedrock spurs exhibiting a higher slope angle* (Conway et al. 2018a)*. (d-e) HiRISE image PSP_006663_1425. Image credits: NASA/JPL/UofA/MSSS.*

Sub-glacial or sub-ice-cap melting has also been proposed as an alternative to "the warm wet early Mars" explanation for the valley networks (Section 1) which are a global surface feature (e.g., Cassanelli & Head 2015; Fastook & Head 2015; Weiss & Head 2015; Wordsworth et al. 2013; Grau Galofre et al. 2020). In contrast, the presently visible glaciers on Mars are generally believed to be cold-based, that is, their interior temperature never rises above the freezing point of water, hence their deformation progresses via the plastic deformation of ice integrated over long time periods. As described in Section 2.2, the martian mid-latitudes are host to a huge number of glacial forms (Fig. 2d), which are believed to be several tens to hundreds of million years old (see Hepburn et al. 2019 and references therein). Some evidence for surface melting of these features comes in the identification of tens of small supraglacial and pro-glacial channels (Fassett et al. 2010), but such channels do not imply the long-lived liquid water involved in basal melting. Recent work has questioned the cold-based paradigm for Amazonian glaciers in two ways: firstly examples of Amazonian debris covered glaciers directly associated with eskers have been reported (Butcher et al. 2017; Gallagher & Balme 2015), and evidence has been found for enhanced erosion of mid-latitude crater walls which is consilient with wet-based glaciation in the last 5-10 Ma (Conway et al. 2018a).

In Phlegra Montes and Tempe Terra, sinuous ridges emerge from extant debris covered glaciers found within fault-bounded graben (Fig. 12). These ridges are interpreted as being eskers, not just because of their intimate association with the glaciers, but because their morphological and topographic relationships are consistent with expectations from terrestrial glaciers/ice sheets (Butcher et al. 2020; Butcher et al. 2017; Gallagher & Balme 2015). The formation of eskers requires substantial amounts of liquid water and its fate once it emerged from under the ice would have likely been quick evaporation and freezing, although no geomorphic evidence is apparent to support or refute this inference. It should be noted that on Earth catastrophic outbursts from sub-glacial conduits do not produce terminal deposits, in contrast to long-lived more stable flows (Burke et al. 2012; Butcher et al. 2020). As both systems are within fault-bounded graben, elevated geothermal heat flux associated with the crustal-thinning could be the reason that only these isolated individual esker systems have been found.

Analysis of high resolution digital elevation models has revealed systematic lowering of the bedrock slopes of pole-facing crater walls in the mid-latitudes intimately associated with the removal of bedrock spurs and transformation of the texture of the exposed bedrock (Conway et al. 2018a)(Fig. 12). The amount of horizontal retreat required to explain the observed slope-lowering ranged up to 10^2 m/Myr and this elevated value is consistent with erosion rates of wet-based glaciers on Earth. Cold-based glaciers on Earth have erosion rates of tens of metres per million years and rates on Mars are expected to similar or lower because of the lower gravity and lower mean average temperature making the ice more rigid (Karlsson et al. 2015). The parts of the craters affected by the slope-lowering are intimately

associated with the presence of a "pasted-on" mantling deposit located downslope of the removed bedrock, which can be interpreted to be an ice-rich till-like deposit due to the presence of downslope lineaments (striations). Where this mantle-deposit interacts with older glacial deposits (LDA or CCF) located on the crater floor there are arcuate ridges interpreted to be moraines (Arfstrom & Hartmann 2005; Berman et al. 2008; Berman et al. 2005; Head et al. 2008; Jawin et al. 2018; Whalley & Azizi 2003). On Earth, terminal moraine ridges are formed by thrusting of the basal sediments towards the glacial surface, which is facilitated by the presence of liquid water (e.g., Benn & Evans 2010), but recent research has revealed they can occur due to deceleration in entirely frozen cold-based glaciers (Fitzsimons & Howarth 2020).

The implication of this work is that a limited amount of melting occurred within the top decametres of the ground in the last 5-10 Ma over a widespread area on Mars. The exact trigger for this "event" is unknown, but seems to be related to the shift of Mars to lower average obliquity at 4.5 Ma (Laskar et al. 2004; Laskar et al. 2002). Another possibility is that periglacial processes have caused the observed slope-lowering (which would still involve liquid water) or some other process driven by H_2O or CO_2 frost-driven rock-breakdown, but at present no viable mechanism has been proposed. Unlike the phase-change from liquid water to solid water, direct condensation from gas to solid does not involve a volume change so rock-breakdown could only be engendered by deposition of frost within cracks opened by thermal contraction whose closure on warming is then limited by the presence of the ice. It should be noted that direct condensation of water ice at extremely low vapour pressures has been shown to always pass via the liquid phase and only in porous particles in the terrestrial atmosphere (David et al. 2019). Given the close association of this suite of landforms with gullies it is tempting to implicate melting for the whole suite of landforms, but whether this is reasonable is certainly debatable.

3.11 Assemblages of pitted cones, flows, ridges and fractures

Sedimentary volcanism is the mobilisation of sediments by groundwater circulation and is usually engendered on Earth pressurised aquifers caused by dense sediments overlying less-dense saturated sediments. Most eruptions are facilitated by gas production (usually methane) and/or tectonic activity. When this process involves clay-sized sediments it is referred to as mud-volcanism. Pitted cones interpreted to be mud-volcanoes have been reported in all three basins in the northern plains of Mars: Acidalia Planitia (e.g., Hemmi & Miyamoto 2018; Oehler & Allen 2010)Fig. 13a), Chryse Planitia (e.g. Brož et al. 2019; Komatsu et al. 2016; Martínez-Alonso et al. 2011) and Utopia Planitia (e.g., McGowan 2011; Skinner & Tanaka 2007) (Fig. 13b). These basins are at a lower elevation than the southern highlands (Fig. 2d) and form a depositional trap for the sediments eroded from the highlands by the valley networks and outflow channels (e.g., Tanaka et al. 2005). At other sites, such as Candor and Coprates Chasmata (Okubo 2016) and Terra Sirenum (Hemmi & Miyamoto 2017) the pitted cones are located in sedimentary fill in other smaller basins. Sedimentary volcanism is thought to mobilise the sediments accumulated in these various basins to form cones and flows. In Acidalia the mud-volcanoes are also associated with polygonal patterns tens of kilometres in diameter, which could represent fluid expulsion pathways (Allen et al. 2013). Fractures and spatially associated pitted cones are also interpreted to be a result of sedimentary volcanism in the Galaxias region (Fig. 13c) (Gallagher et al. 2018) and sedimentary volcanism is a common interpretation of such enigmatic assemblages of km-scale polygonal fractures, ridges and aligned-cones (e.g., De Toffoli et al. 2018; Ivanov et al. 2014; Salvatore & Christensen 2014; Skinner & Mazzini 2009).

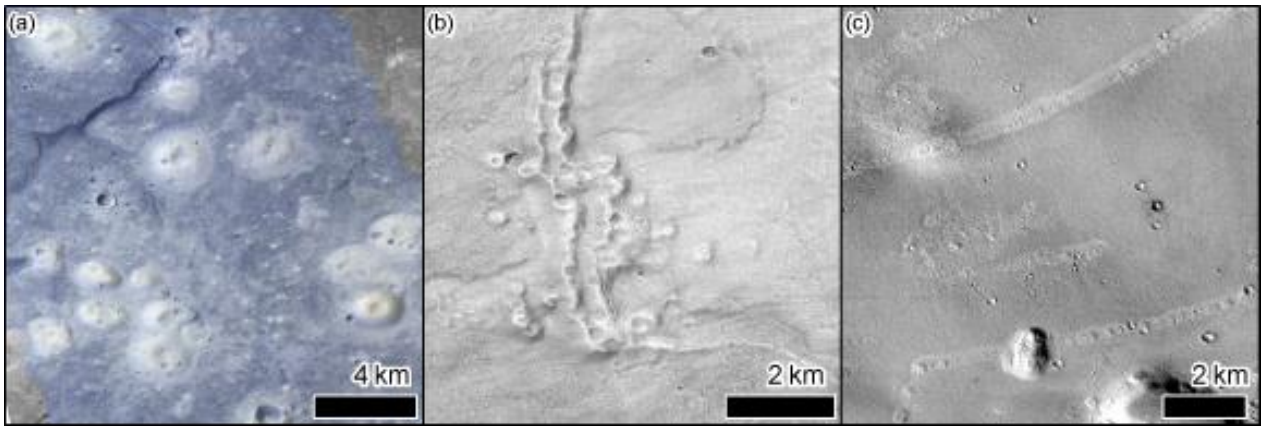

Figure 13: Examples of evidence for sedimentary volcanism on Mars. (a) Pitted cones in Acidalia Planitia with a fracture-junction visible top-left. CaSSIS image MY35_009369_141_0 with channels NIR, PAN and BLU mapped to RGB. (b) Pitted cones and ridges in southern Utopia Planitia. HiRSE image ESP_053364_2135. (c) Aligned cones in Galaxias region, CTX image B05_011746_2156. Image credits: NASA/JPL/UofA/MSSS/ESA/Unibe.

Present-day detections of methane in the martian atmosphere are still heavily debated (e.g., Webster et al. 2018 and references therein), but the discussion of methane has reignited interest in finding and analysing the surface expression of sedimentary volcanism on Mars, as methane gas can be a key driver of sedimentary volcanism on Earth. However, many of these features are estimated as being Amazonian in age or older (Ivanov et al. 2014; Komatsu et al. 2016; Oehler & Allen 2010; Senthil Kumar et al. 2019), and in general are older than gullies and the most recent periglacial and glacial landforms, which means they cannot be *directly* linked to present-day atmospheric methane detections. Sedimentary volcanism implies a source of pressurised liquid water underground whose supply could be engendered by a wide-range of processes including: the impingement of the cryosphere on the hydrosphere due to long-term climate-shifts, destabilisation of clathrates (e.g., De Toffoli et al. 2019) via localised increases in geothermal heat flux or seismic/tectonic/magmatic activity, or simply diapirism of trapped saturated sediments (see summary in Skinner & Tanaka 2007).

Sedimentary volcanism and by association liquid water, is not the only hypothesis for the generation of this suite landforms. Mud-volcanoes could easily be confused with magmatic cones, especially as the behaviour of mud is not well-constrained under martian surface conditions (Brož et al. 2020) and similarly the associations of cones, ridges and fractures have been attributed to a range of processes, e.g. volcanic (e.g., Fagents et al. 2002; Frey & Jarosewich 1982; Ghent et al. 2012), tsunamigenic (Costard et al. 2017) and glacial (e.g., Guidat et al. 2015; Kargel et al. 1995; Rossbacher & Judson 1981). These alternates also imply liquid water, as the volcanic hypothesis requires volatile enrichment to cause the explosive eruptions making the cones (lava-ice or lava-water interaction). The alternates generally imply short-lived episodes of water generation, as opposed to the long-lived aquifer implied in sedimentary volcanism. Liquid water is consistent with the morphology of these features and it is difficult to assess if the sub-surface conditions of Mars could have been conducive to their formation via sedimentary volcanism, as we know so little about the internal structure of Mars (cf. Section 3.2).

3.12 Liquid water related morphologies associated with impacts

Hypervelocity impacts by bolides into planetary surfaces deposit huge amounts of energy into the target body, of which most is converted into heat (Melosh 1989). The lack of substantial atmosphere on Mars means that bolides reach the surface with greater energy than they do on Earth. As discussed in Section 2 we know that there are substantial amounts of water ice in the near-surface of the martian crust and potentially a deep cryosphere, and so the heat deposited into the crust by impacts could generate liquid water by melting. This could be melting immediately during the impact in the cavity and the ejecta (e.g., Boyce et al. 2012; Newsom 1980; Weiss & Head 2016), vaporisation of the ice could inject vapour into the surrounding atmosphere and create a transient and localised hydrological cycle (e.g., Kite et al. 2011; Segura 2002; Segura et al. 2008; Steakley et al. 2019) and finally the thermal anomaly could maintain hydrothermal circulation within the crust for thousand or millions of years post impact (e.g., Abramov & Kring 2005; Barnhart et al. 2010; Osinski et al. 2013; Rathbun & Squyres 2002).

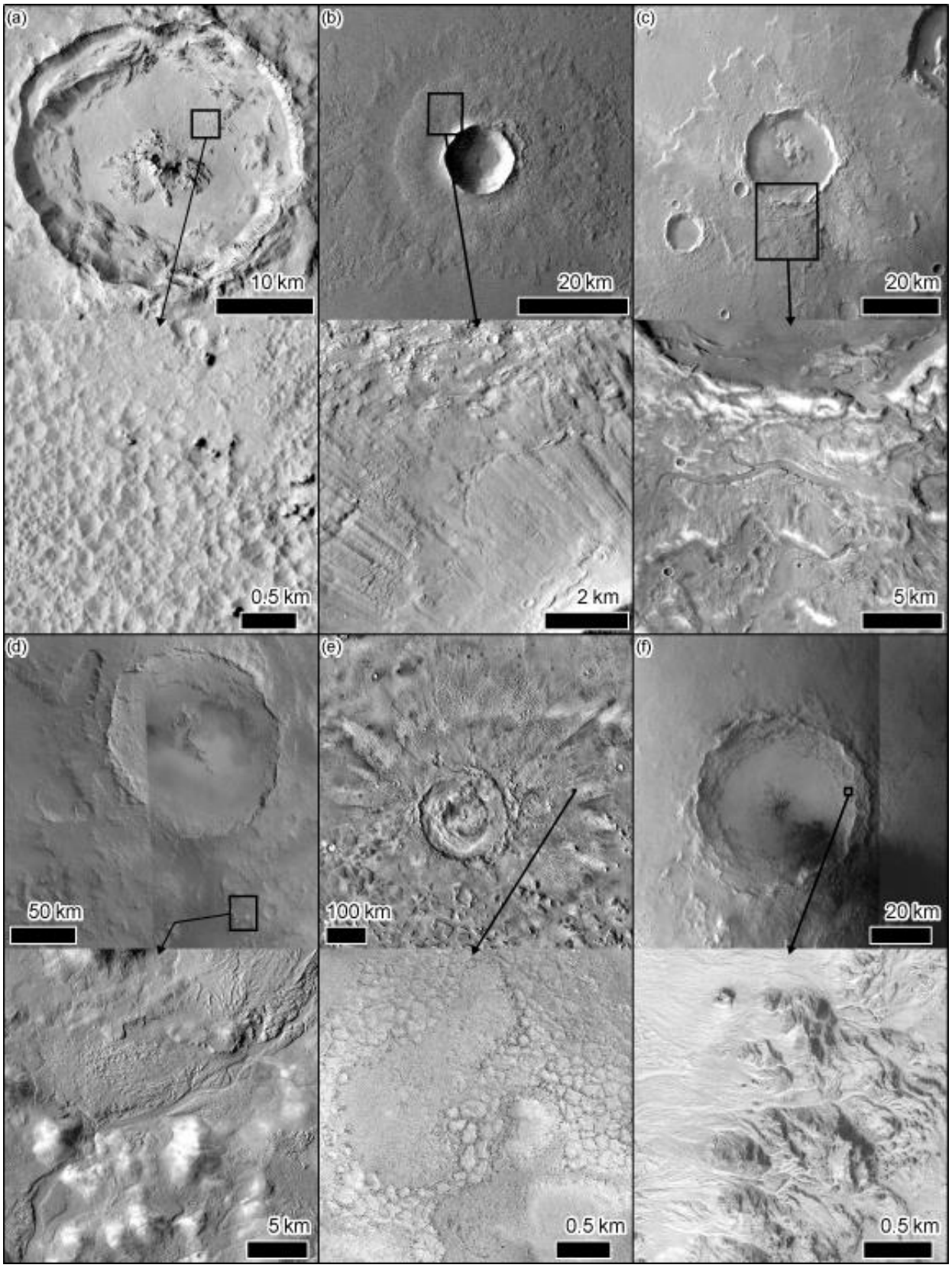
(a)
10 km
0.5 km
(b)
20 km
2 km
(c)
20 km
5 km
(d)
50 km
5 km
(e)
100 km
0.5 km
(f)
20 km
0.5 km

1070

Figure 14: Crater-related liquid water morphologies. (a) Pits on the floor of <10 Ma Tooting Crater (Mouginis-Mark & Boyce 2012)*. CTX image P01_001538_2035. (b) Double-layered ejecta crater in northern plains, with lobate margins and radiating grooves* (Weiss & Head 2014)*. Top HRSC image h2878_0000 and bottom CTX image P20_008833_2149. (c) Multilayer ejecta crater in southern hemisphere with channels incised into its ejecta blanket* (Mangold 2012)*. Top, HRSC image ha313_0000, bottom CTX image B16_015984_2149. (d) Hale Crater with channels incising the ejecta. Top HRSC images h2526_0001 and h0533_0000, bottom CTX image P03_002220_1418. (e) Lyot Crater with clastic polygonal networks in the ejecta. Top THEMIS day IR controlled mosaic image from the USGS and bottom HiRISE image ESP_016985_2315. (f) Mojave Crater with alluvial fans on the inner craters slopes. Top HRSC images hd605_0000 and h1991_0000 and bottom HiRISE image ESP_012834_1875. Image credits: NASA/JPL/MSSS/ESA/DLR/UofA.*

Geomorphological evidence for these processes in the Amazonian epoch is abundant. Craters only a few million years old display pits on their floors (Fig. 14a) and within their ejecta materials interpreted to be a result of volatile-release as steam (Boyce et al. 2012; Morris et al. 2010; Mouginis-Mark & Boyce 2012; Tornabene et al. 2012). These pits can be associated with incised channels, alluvial fans (Fig. 14f) and debris lobes emanating from high points inside the crater cavity, thought to represent the flow of water-rich materials immediately post-impact, e.g. alluvial fans in Tooting and Mojave Craters both dated to < 10 Ma (Goddard et al. 2014; Morris et al. 2010; Williams & Malin 2008). Channels incising into and emanating from ejecta blankets are used as evidence for water escaping from the melting cryosphere beneath (Fig. 14c,d) (El-Maarry et al. 2013; Harrison et al. 2010; Jones et al. 2011; Mangold 2012; Weiss et al. 2017). Clastic polygonal networks in the ejecta of Lyot Crater (Fig. 14e) even suggest that water in the ejecta blanket could result in longer-term ice-segregation processes (Brooker et al. 2018) and conical landforms in the ejecta flows at Hale Crater may also be suggestive of longer-term ice-loss processes (Conway et al. 2019a).

Lobate ejecta morphologies (e.g., multi-layer ejecta, double-layer ejecta - Fig. 14b) are interpreted to be the result of fluidisation and are observed almost exclusively at the mid- to high-latitudes (e.g., Barlow 2006; Barlow 2005; Barlow & Perez 2003; Costard 1989; Mouginis-Mark 1981; Mouginis-Mark 1979). Numerical models generally find this morphology to be consistent with either melting or a volatile-rich layer (e.g., Baratoux et al. 2002; Oberbeck 2009; Weiss & Head 2014; Weiss & Head 2013). However, other modelling studies find that the fluidisation is unrelated to water and could be due to increased fragmentation (Rager et al. 2014) or the presence of an erodible surface (Wada & Barnouin-Jha 2006) – yet both require preconditioning of the surface by water or water ice to explain the latitudinal distribution.

Spectral evidence for hydrothermal alteration is common in craters prior the Amazonian, but is lacking in Amazonian craters (Turner et al. 2016). Similarly, evidence for crater-bound paelolakes, which could result from hydrothermal circulation are lacking particularly from the late Amazonian epoch (e.g., Cabrol 1999).

Craters also host numerous fluvial channels or fans that cannot necessarily directly be linked to the impact event itself but could be formed as a result of the impact's topography (microclimate, and/or sink) or its interaction with groundwater. Examples include: regional drainage networks of Lyot Crater linked to surface ice accumulation and melt in a climatic microenvironment (Dickson et al. 2009), valleys

draining into craters' central pit (Peel & Fassett 2013), and alluvial fans dated to around ~1 Ga resulting from prolonged runoff (e.g., Grant & Wilson 2011; Kite et al. 2019; Kite et al. 2017; Mangold et al. 2012).

In summary, impact crater related morphologies in the late Amazonian represent very transient melting of ground ice mobilised by the impact event, with more substantial evidence for sustained liquid water environments tending to come from the early Amazonian. In essence, most of these landform interpretations are consistent with our expectations for the existence of liquid water on Mars, as impacts are almost intuitively expected to cause melting if they interact with ice, but some of the details of exactly how much water and its origin are more the focus of debate.

3.13 Other evidence for liquid water in the Amazonian

Other morphological evidence for liquid water dates to the early Amazonian with both valley networks and outflow channels having been reported to have been active at this time. It is generally acknowledged that water in such systems was short-lived and ephemeral in contrast to the Noachian valley networks (e.g., Hauber et al. 2013; Wilson et al. 2016). For example, shallow snowmelt has been proposed to explain valleys in Gorgonum and Newton basins (Howard & Moore 2011), for Kārūn Valles (Adeli et al. 2016) and valley networks on the flanks of martian volcanos (Fassett & Head III 2008). A liquid water origin for these landforms represents the consensus even if its source is debated and varied.

Some of the martian outflow channels are also dated to the Amazonian (particularly those on the flanks of the martian volcanos) and their interpretation is less consensual. A detailed discussion of the competing hypotheses can be found in Chapters LEVERINGTON (pages xxx-xxx) and GALLAGHER (pages xxx-xxx). In brief the crux of the debate is whether these outflow morphologies can be ascribed to outpourings of water or mud triggered by lava-ice interaction (e.g., Balme et al. 2011; Burr 2002; Vijayan & Sinha 2017; Wilson & Head 2002) or deep aquifer sources (e.g., Hanna & Phillips 2006; Marra et al. 2015; Marra et al. 2014), or low viscosity lava (Leverington 2011; Leverington 2009). The debate arises from the observation that these outflow channels are covered in basalt and not apparently sedimentary facies, as might be expected from outpourings of liquid water.

4 Synthesis and outlook

The reason that the debate around the evidence for liquid water in Mars is still a hot topic is because the search is motivated by not only scientific curiosity, but can be framed in the larger question of whether life exists or arose elsewhere in the Solar System. In the search for present or past life beyond our planet, finding evidence of present or past liquid water on Mars has been a preoccupation of planetary scientists since the beginning of orbital observations and has been the reason that various space agencies have sent missions to Mars (e.g., ESA's ExoMars missions; Kereszturi et al. 2016; Vago et al. 2017; and NASA's motto "follow the water"; Hubbard et al. 2002). Without a protective atmosphere the surface of Mars is bathed in ionising radiation and solar particles, making it a particularly challenging surface environment for life at the present-day (e.g., Teodoro et al. 2018). However, finding evidence that liquid water has appeared periodically at the surface could indicate that Mars has subsurface water reservoirs that could be harbours for extant life. Recent activity of liquid water also bolsters the probability of liquid water activity in the past and the longevity of habitable conditions. The presence of habitable conditions also increases the chance that the space probes we send to Mars could contaminate these likely uninhabited habitats (Cockell et al. 2012) and out of this concern have arisen planetary protection regulations (National Aeronautics and Space Administration 2005). These regulations

determine the level of sterilisation to which a spacecraft must be submitted to reduce the likelihood of cross-contamination. This effectively prohibits the direct exploration of zones that could have liquid water, for example sites with RSL and gullies are subject to these rules (Kminek et al. 2010; Rummel et al. 2014). Water is also an important resource for future human investigations, even in its solid state (e.g., Heldmann et al. 2014) and hence finding zones where relatively pure water ice would be easily accessible has attracted some recent attention (e.g. SWIM project; Perry et al. 2019).

While none of the features described here have been proven beyond all doubt to require the activity of liquid water, in the aggregate it is challenging to explain all of them without any liquid water on an ice-rich planet that has straddled the triple point of water for all of the Amazonian. Liquid water is more generally agreed to be responsible for early Amazonian features including valleys, channels, alluvial fans and deltas. Most of which are thought to originate from punctual or rare events. However, a consensus view has not been reached over the role, or not, of sedimentary volcanism in building landforms over this period. In the late Amazonian to present-day, the role of water is much less certain, with practically all landforms interpreted as being linked to liquid water having substantial alternate hypotheses. The exceptions are solifluction lobes and pingos where to-date there is no alternate hypothesis to those involving liquid water has been proposed. The evidence for sub-glacial melting in the Late Amazonian is a topic that has only recently been opened and will likely receive more attention as more observations are collected. For presently active features, the focus is currently on processes that do not involve liquid water, but the behaviour of certain downslope flows means that liquid water has not been entirely ruled out. RSL continue to be the most likely of presently active surface features to be linked to liquid water. For the reasons outlined above it is important to continue studying these landforms and continually assess the balance of evidence as new data are collected.

The long-lived and ongoing debate over the presence of recent liquid water at the martian surface raises a couple of important questions for planetary science:

- What level of knowledge do we need to determine (with a reasonable level of confidence) whether liquid water could be present at the surface?
- Are we being misled by Earth analogues and our *a priori* knowledge of terrestrial geomorphology?

For the existence of present-day liquid water, RSL are the primary focus of debate, although periodically other features are proposed (Bhardwaj et al. 2017; Heyer et al. 2019; Kossacki & Markiewicz 2010; Kreslavsky & Head 2009). Progress on RSL is being hindered by:

- Lack of high temporal resolution monitoring (imaging, SAR, IR and VIS-NIR spectral) at the spatial resolution of CaSSIS-HiRISE, observations at different times of day or even better continuous monitoring
- Lack of knowledge of the near-surface atmosphere apart from the handful of places where we have landed missions with meteorology instruments. This limits our knowledge on the influence of micro-environments in the steep topography where RSL are found.
- Lack of knowledge of the basic attributes of the martian subsurface, including the crustal heat flow, porosity, permeability of the regolith with depth, the presence and structure of a potential cryo-hydro-sphere.

Debates over water in the recent past also depend on the above lacunae and we can also add:

- Limits/uncertainties in our ability to model the martian climate at the present-day are magnified when applied to the past and limit our ability to understand past environments. Hence, we are reliant on geomorphic evidence for informing us about the activity of liquid water at the surface, which in and of itself is reliant on our knowledge of what processes form landscapes on Earth.

The existing hardware in orbit around Mars and on its surface combined with their operational constraints and observational modes cannot resolve these problems. New hardware could address some of these issues, for example in orbit: a CaSSIS-HiRISE imager on a spacecraft with a lower orbital inclination to provide higher frequency imaging and time of day coverage (McEwen et al. 2012) , high-resolution (10 m/pix) thermal imager to better constrain thermal inertia and possibly the temperature of shallow brine, Synthetic Aperture Radar (SAR) with high resolution (18 m/pix) orbital radar to detect shallow ice or liquid water, or an imaging spectrometer capable of distinguishing ices and their structure at high resolution. Surface measurements could include: a network of heat flow probes to determine how heat flow varies over Mars and better constrain its value, to measure the volume of subsurface ice (Grimm & Stillman 2015), ground penetrating radar (GPR) to detect the structure of segregated ice and possibly any shallow aquifers, a transient electromagnetic sounder (TEM) capable of detecting aquifers to a depth of a few kilometres (e.g., Stamenkovic et al. 2020), or use of the magnetotelluric (MT) method to passively sense deep conductive bodies and is capable of detecting a subsurface aquifer within the first 5 km of the crust (e.g., Grimm et al. 2020; Grimm 2002).

Our knowledge from terrestrial geomorphology inevitably leaves us with a biased view of the landscapes and landforms we find on Mars. Not only that, but even on Earth multiple processes can lead to similar looking landforms “equifinatlity” – a problem usually resolved on Earth by employing a multidisciplinary investigation. For example, hummocky landforms can be the result of rock avalanches or be the vestiges of glacial terminal moraines (e.g., McColl et al. 2019; McColl & Davies 2011). These conundra are resolved using sedimentology, stratigraphy, geophysical techniques and cosmogenic or other dating techniques, in combination with field and remote sensing observations (e.g., images, digital terrain models). On Mars we only have remote sensing data to rely on and sometimes even with images, spectral data, radar and digital terrain models the interpretation can remain ambiguous. We are also confronted with an environment where the processes acting on it could, and should, be very different to those on Earth. For example, the lack of plate tectonics on Mars means that evidence of surface processes is preserved longer at the surface than we are used to on Earth, meaning landforms with a “fresh” appearance could date to hundreds of thousands if not millions of years. The generation of relief on Earth is dominated by the continuous action of plate tectonics and its associated volcanism, whereas on Mars the relief is created by stochastic impact events and in the past the development of outsized volcanoes and fault-systems. This means the overall structure of the landscapes of the two planets is fundamentally different starting at the continental scale.

Despite these differences, as demonstrated in Section 3, remarkably similar landscapes and landforms are found on the two planets at scales of kilometres to metres. Terrestrial analogues have therefore helped us to deduce what kinds of processes are active to produce these landscapes. A philosophical analysis of the utility of Earth analogues for informing planetary investigations is beyond the scope of this work, but interested readers are referred to the analyses of Baker (2014). Nevertheless, whether or not “something else” can produce the same landscapes and landforms as liquid water is unknown and is one of the core uncertainties stemming from our use of terrestrial analogues. For example, for martian gullies we know the flows at the present-day are fluidised to the same degree as water-saturated debris

flows on Earth (de Haas et al. 2019), but we do not know if sublimating CO_2 could mimic this fluidisation despite being controlled by different physics (de Haas et al. 2019).

Another method of addressing the range of environmental conditions under which water (or brine) can result in landform development is to perform controlled laboratory experiments. Such experiments need to have two complementary outlooks. Firstly, experiments to address very basic physical questions (how fast can brines form by deliquesce in presence of Mars sediments?) in order to test our parameterisation and understanding of the physical laws underpinning the kinetics of individual processes. The aim is to understand the basis physics in a realistic transient environmental setting for Mars. Additionally, understand the metastability of brine can be very important as brine can remain liquid for an extended period of time (e.g., Gough et al. 2011; Toner et al. 2014b; Primm et al. 2017; Primm et al. 2019). Secondly, more complex simulations, analogous to flume experiments, where processes can be transient and interlinked in order to address the open questions in an empirical fashion. For example, laboratory work can be used to compare the action of water as a fluidising agent to that of gas supported flows. Particularly in this second case, care needs to be taken to appropriately scale the experiments and consider the limits of their application to Mars (Paola et al. 2009).

5 Conclusions

If we used geomorphological arguments in isolation the case for liquid water on Mars would be hard to counter. The main argument against liquid water is that martian environmental conditions should not allow its production, so either we have some fundamental misunderstanding of the martian surface/subsurface conditions at the present and/or in the recent past, or some other agent(s) is(are) acting like liquid water does on Earth. For some of the landforms examined in this chapter alternative processes have been identified, but for others, namely “solifluction” lobes and pingo-like mounds, liquid water remains the only suggested agent. The lack of agent does not imply one does not exist, but it could remain to be elucidated. We maintain that liquid water is a viable contender to explain the present-day activity of RSL, the recent formation of gullies, periglacial landforms and subglacial landforms and the formation of certain impact-related features and sedimentary volcanism in the deeper past. The implication being that, although a lot less active than in the past, liquid water remains an active geomorphological agent on Amazonian Mars. In order to consolidate this position, we argue that the most progress can be made in the short-term by focussing research efforts on experimental work informed by remote sensing observations and in the long-term by better equipped Mars-missions in the future. Additionally, sending a small mission to determine, if Mars still possesses deep groundwater would be greatly beneficial as it can serve as an end member for the likelihood of water to have survived in the ground for 100 Ma to Ga.

6 References cited

Abotalib, A.Z. & Heggy, E., 2019. A deep groundwater origin for recurring slope lineae on Mars. *Nature Geoscience*, 12(4), p.235–241.

Abramov, O. & Kring, D.A., 2005. Impact-induced hydrothermal activity on early Mars. *J. Geophys. Res.*, 110(E12), p.doi:10.1029/2005je002453.

Abrevaya, X.C. et al., 2016. The Astrobiology Primer v2.0 S. D. Domagal-Goldman et al., eds. *Astrobiology*, 16(8), p.561–653.

1277 Ackiss, S.E. & Wray, J.J., 2014. Occurrences of possible hydrated sulfates in the southern high latitudes of
1278 Mars. *Icarus*, 243, p.311–324.

1279 Adeli, S. et al., 2016. Amazonian-aged fluvial system and associated ice-related features in Terra
1280 Cimmeria, Mars. *Icarus*, 277, p.286–299.

1281 Aharonson, O. & Schorghofer, N., 2006. Subsurface ice on Mars with rough topography. *J. Geophys. Res.-*
1282 *Planets*, 111(E11), p.10.

1283 Aharonson, O., Schorghofer, N. & Gerstell, M.F., 2003. Slope streak formation and dust deposition rates
1284 on Mars. *Journal of Geophysical Research (Planets)*, 108, p.5138.

1285 Allen, C.C. et al., 2013. Fluid expulsion in terrestrial sedimentary basins: A process providing potential
1286 analogs for giant polygons and mounds in the martian lowlands. *Icarus*, 224(2), p.424–432.

1287 Andrews-Hanna, J.C. & Phillips, R.J., 2007. Hydrological modeling of outflow channels and chaos regions
1288 on Mars. *Journal of Geophysical Research (Planets)*, 112, p.doi: 10.1029/2006JE002881.

1289 Appéré, T. et al., 2011. Winter and spring evolution of northern seasonal deposits on Mars from OMEGA
1290 on Mars Express. *J. Geophys. Res.*, 116(E5), p.E05001.

1291 Arfstrom, J. & Hartmann, W.K., 2005. Martian flow features, moraine-like ridges, and gullies: Terrestrial
1292 analogs and interrelationships. *Icarus*, 174(2), p.321–335.

1293 Arnold, N.S. et al., 2019. Modeled Subglacial Water Flow Routing Supports Localized Intrusive Heating as
1294 a Possible Cause of Basal Melting of Mars' South Polar Ice Cap. *Journal of Geophysical Research:*
1295 *Planets*, 124(8), p.2101–2116.

1296 Auld, K.C. & Dixon, J.C., 2016. A Classification of Martian Gullies from HiRISE Imagery. *Planetary and*
1297 *Space Science*, 131, p.88–101.

1298 Baker, D.M.H. & Carter, L.M., 2019a. Probing supraglacial debris on Mars 1: Sources, thickness, and
1299 stratigraphy. *Icarus*, 319, p.745–769.

1300 Baker, D.M.H. & Carter, L.M., 2019b. Probing supraglacial debris on Mars 2: Crater morphology. *Icarus*,
1301 319, p.264–280.

1302 Baker, D.M.H., Head, J.W. & Marchant, D.R., 2010. Flow patterns of lobate debris aprons and lineated
1303 valley fill north of Ismeniae Fossae, Mars: Evidence for extensive mid-latitude glaciation in the
1304 Late Amazonian. *Icarus*, 207(1), p.186–209.

1305 Baker, V.R. et al., 1991. Ancient oceans, ice sheets and the hydrological cycle on Mars. *Nature*,
1306 352(6336), p.589–594.

1307 Baker, V.R., 1979. Erosional processes in channelized water flows on Mars. *Journal of Geophysical*
1308 *Research*, 84(B14), p.7985.

1309 Baker, V.R., 2014. Terrestrial analogs, planetary geology, and the nature of geological reasoning.
1310 *Planetary Geology Field Symposium, Kitakyushu, Japan, 2011: Planetary Geology and Terrestrial*
1311 *Analogs*, 95, p.5–10.

1312 Baker, V.R. & Milton, D.J., 1974. Erosion by catastrophic floods on Mars and Earth. *Icarus*, 23(1), p.27–41.

1313 Bakker, M. et al., 2019. Morphological Response of an Alpine Braided Reach to Sediment-Laden Flow
1314 Events. *Journal of Geophysical Research: Earth Surface*, 124(5), p.1310–1328.

1315 Balme, M. et al., 2006. Orientation and distribution of recent gullies in the southern hemisphere of Mars:
1316 Observations from High Resolution Stereo Camera/Mars Express (HRSC/MEX) and Mars Orbiter
1317 Camera/Mars Global Surveyor (MOC/MGS) data. *Journal of Geophysical Research: Planets*,
1318 111(E5), p.doi:10.1029/2005JE002607.

1319 Balme, M.R. et al., 2011. Fill and spill in Lethe Vallis: a recent flood-routing system in Elysium Planitia,
1320 Mars. *Geological Society, London, Special Publications*, 356(1), p.203–227.

1321 Balme, M.R. & Gallagher, C., 2009. An equatorial periglacial landscape on Mars. *Earth and Planetary*
1322 *Science Letters*, 285(1–2), p.1–15.

1323 Balme, M.R., Gallagher, C.J. & Hauber, E., 2013. Morphological evidence for geologically young thaw of
1324 ice on Mars: A review of recent studies using high-resolution imaging data. *Progress in Physical*
1325 *Geography*, 37(3), p.289–324.

1326 Bapst, J., Byrne, S. & Brown, A.J., 2018. On the icy edge at Louth and Korolev craters. *Icarus*, 308, p.15–
1327 26.

1328 Baratoux, D. et al., 2006. The role of the wind-transported dust in slope streaks activity: Evidence from
1329 the HRSC data. *Icarus*, 183(1), p.30–45.

1330 Baratoux, D., Delacourt, C. & Allemand, P., 2002. An instability mechanism in the formation of the
1331 Martian lobate craters and the implications for the rheology of ejecta: EJECTA RHELOGY FROM
1332 AN INSTABILITY MECHANISM. *Geophysical Research Letters*, 29(8), p.51-1-51–4.

1333 Bargery, A.S. & Gilbert, J.S., 2008. *Aqueous eruption and channel flow on Mars during the Amazonian*
1334 *epoch*. Lancaster, UK: University of Lancaster, Department of Environmental Science.

1335 Barlow, N.G., 2005. A review of Martian impact crater ejecta structures and their implications for target
1336 properties. *Geological Society of America Special Papers*, 384, p.433–442.

1337 Barlow, N.G., 2006. Impact craters in the northern hemisphere of Mars: Layered ejecta and central pit
1338 characteristics. *Meteorit. Planet. Sci.*, 41(10), p.1425–1436.

1339 Barlow, N.G. & Perez, C.B., 2003. Martian impact crater ejecta morphologies as indicators of the
1340 distribution of subsurface volatiles. *J. Geophys. Res.-Planets*, 108(E8),
1341 p.doi:10.1029/2002JE002036.

1342 Barnhart, C.J., Nimmo, F. & Travis, B.J., 2010. Martian post-impact hydrothermal systems incorporating
1343 freezing. *Icarus*, 208(1), p.101–117.

1344 Barrett, A.M. et al., 2017. Clastic patterned ground in Lomonosov crater, Mars: examining fracture
1345 controlled formation mechanisms. *Icarus*, 295, p.125–139.

1346 Barrett, A.M. et al., 2018. The distribution of putative periglacial landforms on the martian northern
1347 plains. *Icarus*, 314, p.133–148.

1348 Becerra, P., Sori, M.M. & Byrne, S., 2017. Signals of astronomical climate forcing in the exposure
1349 topography of the North Polar Layered Deposits of Mars: Astronomical Forcing of Mars' NPLD.
1350 *Geophysical Research Letters*, 44(1), p.62–70.

1351 Benn, D.I. & Evans, D.J.A., 2010. *Glaciers & Glaciation* Second Edition., London: Hodder Education.

1352 Berman, D.C. et al., 2005. The role of arcuate ridges and gullies in the degradation of craters in the
1353 Newton Basin region of Mars. *Icarus*, 178, p.465–486.

1354 Berman, D.C., Crown, D.A. & Bleamaster, L.F., 2008. Degradation of Mid-Latitude Craters on Mars:
1355 Gullies, Arcuate Ridges, and Small Flow Lobes. Available at:
1356 http://adsabs.harvard.edu/abs/2008LPICo1303...13B.

1357 Berman, D.C., Crown, D.A. & Joseph, E.C.S., 2015. Formation and mantling ages of lobate debris aprons
1358 on Mars: Insights from categorized crater counts. *Planetary and Space Science*, 111, p.83–99.

1359 Bhardwaj, A. et al., 2019a. Are Slope Streaks Indicative of Global-Scale Aqueous Processes on
1360 Contemporary Mars? *Reviews of Geophysics*, 57(1), p.48–77.

1361 Bhardwaj, A. et al., 2019b. Discovery of recurring slope lineae candidates in Mawrth Vallis, Mars.
1362 *Scientific Reports*, 9(1), p.2040.

1363 Bhardwaj, A. et al., 2017. Martian slope streaks as plausible indicators of transient water activity.
1364 *Scientific Reports*, 7(1). Available at: http://www.nature.com/articles/s41598-017-07453-9
1365 [Accessed March 23, 2020].

1366 Bierson, C.J. et al., 2016. Stratigraphy and evolution of the buried CO_2 deposit in the Martian south polar
1367 cap: MARS SPLD HISTORY. *Geophysical Research Letters*, 43(9), p.4172–4179.

1368 Bishop, J.L. et al., 2004. Multiple techniques for mineral identification on Mars: *Icarus*, 169(2), p.311–
1369 323.

1370 Blair, T.C. & McPherson, J.G., 2009. Processes and Forms of Alluvial Fans. In A. J. Parsons & A. D.
1371 Abrahams, eds. *Geomorphology of Desert Environments*. Dordrecht: Springer Netherlands, pp.
1372 413–467. Available at: https://doi.org/10.1007/978-1-4020-5719-9_14.

1373 Blasius, K.R., Cutts, J.A. & Howard, A.D., 1982. Topography and stratigraphy of Martian polar layered
1374 deposits. *Icarus*, 50(2–3), p.140–160.

1375 Boxe, C.S. et al., 2012. Adsorbed water and thin liquid films on Mars. *International Journal of*
1376 *Astrobiology*, 11(3), p.169–175.

1377 Boyce, J.M. et al., 2012. Origin of small pits in martian impact craters. *Icarus*, 221(1), p.262–275.

1378 Boynton, W.V. et al., 2002. Distribution of Hydrogen in the Near Surface of Mars: Evidence for
1379 Subsurface Ice Deposits. *Science*, 297(5578), p.81–85.

1380 Bramson, A.M. et al., 2019. A Migration Model for the Polar Spiral Troughs of Mars. *Journal of*
1381 *Geophysical Research: Planets*, 124(4), p.1020–1043.

1382 Bramson, A.M. et al., 2015. Widespread excess ice in Arcadia Planitia, Mars. *Geophysical Research*
1383 *Letters*, 42(16), p.6566–6574.

1384 Bramson, A.M., Byrne, S. & Bapst, J., 2017. Preservation of Midlatitude Ice Sheets on Mars: Mars
1385 Midlatitude Ice Sheet Preservation. *Journal of Geophysical Research: Planets*, 122(11), p.2250–
1386 2266.

1387 Bridges, J.C. et al., 2001. Alteration Assemblages in Martian Meteorites: Implications for Near-Surface
1388 Processes. *Space Science Reviews*, 96(1/4), p.365–392.

1389 Bridges, N.T. & Lackner, C.N., 2006. Northern hemisphere Martian gullies and mantled terrain:
1390 Implications for near-surface water migration in Mars' recent past. *Journal of Geophysical*
1391 *Research (Planets)*, 111, p.09014.

1392 Brooker, L.M. et al., 2018. Clastic polygonal networks around Lyot crater, Mars: Possible formation
1393 mechanisms from morphometric analysis. *Icarus*, 302, p.386–406.

1394 Brothers, T.C. & Holt, J.W., 2016. Three-dimensional structure and origin of a 1.8 km thick ice dome
1395 within Korolev Crater, Mars: STRUCTURE AND ORIGIN OF KOROLEV ICE DOME. *Geophysical*
1396 *Research Letters*, 43(4), p.1443–1449.

1397 Brothers, T.C., Holt, J.W. & Spiga, A., 2013. Orbital radar, imagery, and atmospheric modeling reveal an
1398 aeolian origin for Abalos Mensa, Mars: AEOLIAN ORIGIN FOR ABALOS MENSA, MARS.
1399 *Geophysical Research Letters*, 40(7), p.1334–1339.

1400 Brough, S., Hubbard, B. & Hubbard, A., 2016. Former extent of glacier-like forms on Mars. *Icarus*, 274,
1401 p.37–49.

1402 Brown, A.J. et al., 2010. Compact Reconnaissance Imaging Spectrometer for Mars (CRISM) south polar
1403 mapping: First Mars year of observations. *J. Geophys. Res.*, 115(E2), p.E00D13.

1404 Brown, A.J. et al., 2008. Louth crater: Evolution of a layered water ice mound. *Icarus*, 196(2), p.433–445.

1405 Brown, A.J., Calvin, W.M. & Murchie, S.L., 2012. Compact Reconnaissance Imaging Spectrometer for
1406 Mars (CRISM) north polar springtime recession mapping: First 3 Mars years of observations. *J.*
1407 *Geophys. Res.*, 117, p.E00J20.

1408 Brož, P. et al., 2020. Experimental evidence for lava-like mud flows under Martian surface conditions.
1409 *Nature Geoscience*, 13, p.403–407.

1410 Brož, P. et al., 2019. Subsurface Sediment Mobilization in the Southern Chryse Planitia on Mars. *Journal*
1411 *of Geophysical Research: Planets*, 124(3), p.703–720.

1412 Bruno, B.C. et al., 2006. Identification of volcanic rootless cones, ice mounds, and impact craters on Earth
1413 and Mars: Using spatial distribution as a remote sensing tool. *J. Geophys. Res.*, 111(E6),
1414 p.E06017.

1415 Brusnikin, E.S. et al., 2016. Topographic measurements of slope streaks on Mars. *Icarus*, 278, p.52–61.

1416 Buhler, P.B. et al., 2019. Coevolution of Mars's atmosphere and massive south polar CO2 ice deposit.
1417 *Nature Astronomy*. Available at: http://www.nature.com/articles/s41550-019-0976-8 [Accessed
1418 March 3, 2020].

1419 Buhler, P.B. et al., 2017. How the martian residual south polar cap develops quasi-circular and heart-
1420 shaped pits, troughs, and moats. *Icarus*, 286, p.69–93.

1421 Burke, M.J., Brennand, T.A. & Perkins, A.J., 2012. Transient subglacial hydrology of a thin ice sheet:
1422 insights from the Chasm esker, British Columbia, Canada. *Quaternary Science Reviews*, 58, p.30–
1423 55.

1424 Burr, D.M. et al., 2009a. Mesoscale raised rim depressions (MRRDs) on Earth: A review of the
1425 characteristics, processes, and spatial distributions of analogs for Mars. *Planetary and Space*
1426 *Science*, 57(5–6), p.579–596.

1427 Burr, D.M., 2002. Recent aqueous floods from the Cerberus Fossae, Mars. *Geophysical Research Letters*,
1428 29(1). Available at: http://doi.wiley.com/10.1029/2001GL013345 [Accessed March 24, 2020].

1429 Burr, D.M., Tanaka, K.L. & Yoshikawa, K., 2009b. Pingos on Earth and Mars. *Planetary and Space Science*,
1430 57(5–6), p.541–555.

1431 Butcher, F.E.G. et al., 2020. Morphometry of a Glacier-Linked Esker in NW Tempe Terra, Mars, and
1432 Implications for Sediment-Discharge Dynamics of Subglacial Drainage. *Earth and Planetary*
1433 *Science Letters*, 542, p.116325.

1434 Butcher, F.E.G. et al., 2017. Recent Basal Melting of a Mid-Latitude Glacier on Mars. *Journal of*
1435 *Geophysical Research: Planets*. Available at: http://dx.doi.org/10.1002/2017JE005434.

1436 Butcher, F.E.G., Conway, S.J. & Arnold, N.S., 2016. Are the Dorsa Argentea on Mars eskers? *Icarus*, 275,
1437 p.65–84.

1438 Byrne, S., 2003. A Sublimation Model for Martian South Polar Ice Features. *Science*, 299(5609), p.1051–
1439 1053.

1440 Byrne, S. et al., 2009. Distribution of mid-latitude ground ice on mars from new impact craters. *Science*,
1441 325(5948), p.1674–1676.

1442 Cabrol, N., 1999. Distribution, Classification, and Ages of Martian Impact Crater Lakes. *Icarus*, 142(1),
1443 p.160–172.

1444 Carr, M. & Head, J., 2019. Mars: Formation and fate of a frozen Hesperian ocean. *Icarus*, 319, p.433–443.

1445 Carr, M.H., 1996. Channels and valleys on Mars: cold climate features formed as a result of a thickening
1446 cryosphere. *Planetary and Space Science*, 44(11), p.1411–1417.

1447 Carr, M.H., 1979. Formation of Martian flood features by release of water from confined aquifers.
1448 *Journal of Geophysical Research*, 84, p.2995–3007.

1449 Carter, J. et al., 2015. Widespread surface weathering on early Mars: A case for a warmer and wetter
1450 climate. *Icarus*, 248, p.373–382.

1451 Cassanelli, J.P. & Head, J.W., 2015. Firn densification in a Late Noachian "icy highlands" Mars:
1452 Implications for ice sheet evolution and thermal response. *Icarus*, 253, p.243–255.

1453 Catling, D.C. et al., 2010. Atmospheric origins of perchlorate on Mars and in the Atacama. *Journal of*
1454 *Geophysical Research*, 115, p.E00E11.

1455 Cavalli, M. et al., 2013. Geomorphometric assessment of spatial sediment connectivity in small Alpine
1456 catchments. *Sediment sources, source-to-sink fluxes and sedimentary budgets*, 188(0), p.31–41.

1457 Chan, M.A. et al., 2004. A possible terrestrial analogue for haematite concretions on Mars. *Nature*,
1458 429(6993), p.731–734.

1459 Chevrier, V.F. & Rivera-Valentin, E.G., 2012. Formation of recurring slope lineae by liquid brines on
1460 present-day Mars. *Geophys. Res. Lett.*, 39(21), p.L21202.

1461 Chojnacki, M. et al., 2016. Geologic context of recurring slope lineae in Melas and Coprates Chasmata,
1462 Mars: GEOLOGY OF MELAS AND COPRATES RSL. *Journal of Geophysical Research: Planets*, 121(7),
1463 p.1204–1231.

1464 Christensen, P.R., 2003. Formation of recent martian gullies through melting of extensive water-rich
1465 snow deposits. *Nature*, 422(6927), p.45–48.

1466 Christiansen, H.H., 1995. Observations of Open System Pingos in a Marsh Environment, Mellemfjord,
1467 Disko, Central West Greenland. *Geografisk Tidsskrift-Danish Journal of Geography*, 95(1), p.42–
1468 48.

1469 Chuang, F.C. et al., 2007. HiRISE observations of slope streaks on Mars. *Geophysical Research Letters*,
1470 34(20), p.doi:10.1029/2007GL031111.

1471 Clark, B., 1981. The salts of Mars. *Icarus*, 45(2), p.370–378.

1472 Clifford, S.M. et al., 2010. Depth of the Martian cryosphere: Revised estimates and implications for the
1473 existence and detection of subpermafrost groundwater. *J. Geophys. Res.*, 115(E7),
1474 p.doi:10.1029/2009JE003462.

1475 Clifford, S.M. & Parker, T.J., 2001. The evolution of the Martian hydrosphere: Implications for the fate of
1476 a primordial ocean and the current state of the northern plains. *Icarus*, 154(1), p.40–79.

1477 Cockell, C.S. et al., 2012. Uninhabited habitats on Mars. *Icarus*, 217(1), p.184–193.

1478 Coleman, N.M., 2005. Martian megaflood-triggered chaos formation, revealing groundwater depth,
1479 cryosphere thickness, and crustal heat flux. *Journal of Geophysical Research*, 110(E12), p.E12S20.

1480 Conway, S., Wright, J. & Morino, C., 2019a. Conical landforms on Mercury and Mars - indicators of
1481 volatile release. In *EPSC-DPS Joint Meeting 2019*. p. EPSC-DPS2019-1827. Available at:
1482 https://ui.adsabs.harvard.edu/abs/2019EPSC...13.1827C.

1483 Conway, S.J. et al., 2012. Climate-driven deposition of water ice and the formation of mounds in craters
1484 in Mars' north polar region. *Icarus*, 220(1), p.174–193.

1485 Conway, S.J. et al., 2011a. Enhanced runout and erosion by overland flow under subfreezing and low
1486 pressure conditions: experiments and application to Mars. *Icarus*, 211(1), p.443–457.

1487 Conway, S.J. et al., 2018a. Glacial and gully erosion on Mars: A terrestrial perspective. *Geomorphology*,
1488 318, p.26–57.

1489 Conway, S.J. et al., 2017. New Slope-Normalised Global Gully Density and Orientation Maps for Mars.
1490 *Geological Society, London, Special Publications*, 467.

1491 Conway, S.J. et al., 2015. The comparison of topographic long profiles of gullies on Earth to gullies on
1492 Mars: A signal of water on Mars. *Icarus*, 253(0), p.189–204.

1493 Conway, S.J. et al., 2011b. The indication of Martian gully formation processes by slope–area analysis.
1494 *Geological Society, London, Special Publications*, 356(1), p.171–201.

1495 Conway, S.J. & Balme, M.R., 2016. A novel topographic parameterization scheme indicates that martian
1496 gullies display the signature of liquid water. *Earth and Planetary Science Letters*, 454, p.36–45.

1497 Conway, S.J. & Balme, M.R., 2014. Decametre-thick remnant glacial ice deposits on Mars. *Geophysical*
1498 *Research Letters*, 41(15), p.5402–5409.

1499 Conway, S.J., de Haas, T. & Harrison, T.N., 2019b. Martian gullies: a comprehensive review of
1500 observations, mechanisms and the insights from Earth analogues. *Geological Society, London,*
1501 *Special Publications*, 467.

1502 Conway, S.J., Harrison, T.N. & Lewis, S.R., 2018b. Chapter 3: Martian gullies and their connection with the
1503 martian climate. In R. J. Soare, S. J. Conway, & S. M. Clifford, eds. *Dynamic Mars: Recent and*
1504 *Current Landscape Evolution of the Red Planet*. Elsevier.

1505 Corbel, J. & Gallo, G., 1970. Cryokarsts et chimie des neiges en zone polaire. *Revue géographique des*
1506 *Pyrénées et du Sud-Ouest. Sud-Ouest Européen*, 41(2), p.123–138.

1507 Costard, F. et al., 2007. Debris flows in Greenland and on Mars. In M. Chapman, ed. *The Geology of Mars:*
1508 *Evidence from Earth-based Analogs*. Cambridge: Cambridge University Press, pp. 265–278.

1509 Costard, F. et al., 2002. Formation of recent Martian debris flows by melting of near-surface ground ice
1510 at high obliquity. *Science*, 295(5552), p.110–113.

1511 Costard, F. et al., 2016. Modeling and observational occurrences of near-surface drainage in Utopia
1512 Planitia, Mars. *Geomorphology*, 275, p.80–89.

1513 Costard, F. et al., 2017. Modeling tsunami propagation and the emplacement of thumbprint terrain in an
1514 early Mars ocean: TSUNAMIS ON MARS. *Journal of Geophysical Research: Planets*, 122(3), p.633–
1515 649.

1516 Costard, F., 2007. Vallées de débâcle et processus cryokarstiques sur Mars et en Sibérie. *Géographie*
1517 *physique et Quaternaire*, 44(1), p.97–104.

1518 Costard, FrançoisM., 1989. The spatial distribution of volatiles in the Martian hydrolithosphere. *Earth,*
1519 *Moon, and Planets*, 45(3), p.265–290.

1520 Craddock, R.A. & Howard, A.D., 2002. The case for rainfall on a warm, wet early Mars. *J. Geophys. Res.*,
1521 107(E11), p.5111.

1522 Cull, S., Kennedy, E. & Clark, A., 2014. Aqueous and non-aqueous soil processes on the northern plains of
1523 Mars: Insights from the distribution of perchlorate salts at the Phoenix landing site and in Earth
1524 analog environments. *Planetary and Space Science*, 96(0), p.29–34.

1525 David, R.O. et al., 2019. Pore condensation and freezing is responsible for ice formation below water
1526 saturation for porous particles. *Proceedings of the National Academy of Sciences*, 116(17),
1527 p.8184–8189.

1528 De Toffoli, B. et al., 2018. Estimate of depths of source fluids related to mound fields on Mars. *Planetary*
1529 *and Space Science*. Available at:
1530 http://www.sciencedirect.com/science/article/pii/S0032063318301387.

1531 De Toffoli, B. et al., 2019. Surface Expressions of Subsurface Sediment Mobilization Rooted into a Gas
1532 Hydrate-Rich Cryosphere on Mars. *Scientific Reports*, 9(1), p.8603.

1533 de Haas, T. et al., 2019. Initiation and Flow Conditions of Contemporary Flows in Martian Gullies. *Journal*
1534 *of Geophysical Research: Planets*, 124(8), p.2018JE005899.

1535 Dickson, J.L. et al., 2013. Don Juan Pond, Antarctica: Near-surface CaCl2-brine feeding Earth's most saline
1536 lake and implications for Mars. *Scientific Reports*, 3(1), p.1166.

1537 Dickson, J.L. et al., 2018. Gully Formation in the McMurdo Dry Valleys, Antarctica: Multiple Sources of
1538 Water, Temporal Sequence and Relative Importance in Gully Erosion and Deposition Processes.
1539 *Geological Society, London, Special Publications*, accepted.

1540 Dickson, J.L. et al., 2015. Recent climate cycles on Mars: Stratigraphic relationships between multiple
1541 generations of gullies and the latitude dependent mantle. *Icarus*, 252, p.83–94.

1542 Dickson, J.L., Fassett, C.I. & Head, J.W., 2009. Amazonian-aged fluvial valley systems in a climatic
1543 microenvironment on Mars: Melting of ice deposits on the interior of Lyot Crater. *Geophysical*
1544 *Research Letters*, 36, p.08201.

1545 Dickson, J.L., Head, J.W. & Kreslavsky, M., 2007. Martian gullies in the southern mid-latitudes of Mars:
1546 Evidence for climate-controlled formation of young fluvial features based upon local and global
1547 topography. *Icarus*, 188, p.315–323.

1548 Diniega, S. et al., 2013. A new dry hypothesis for the formation of martian linear gullies. *Icarus*, 225(1),
1549 p.526–537.

1550 Diniega, S., 2021. Linear Gullies (Mars). In H. Hargitai & Á. Kereszturi, eds. *Encyclopedia of Planetary*
1551 *Landforms*. New York, NY: Springer New York, pp. 1–5. Available at:
1552 http://dx.doi.org/10.1007/978-1-4614-9213-9_582-1.

1553 Diniega, S. et al., 2010. Seasonality of present-day Martian dune-gully activity. *Geology*, 38(11), p.1047–
1554 1050.

1555 Dohm, J.M. et al., 2001. Latent outflow activity for western Tharsis, Mars: Significant flood record
1556 exposed. *Journal of Geophysical Research: Planets*, 106(E6), p.12301–12314.

1557 Dundas, C.M. et al., 2019a. Active Boulder Movement at High Martian Latitudes. *Geophysical Research*
1558 *Letters*, p.2019GL082293.

1559 Dundas, C.M. et al., 2020. Distribution and Properties of Ice-Exposing Scarps and Craters on Mars. *Icarus*,
1560 submitted.

1561 Dundas, C.M. et al., 2018. Exposed subsurface ice sheets in the Martian mid-latitudes. *Science*,
1562 359(6372), p.199–201.

1563 Dundas, C.M., 2020. Geomorphological evidence for a dry dust avalanche origin of slope streaks on Mars.
1564 *Nature Geoscience*, 13(7), p.473–476.

1565 Dundas, C.M. et al., 2017. Granular flows at recurring slope lineae on Mars indicate a limited role for
1566 liquid water. *Nature Geoscience*, 10, p.903–907.

1567 Dundas, C.M. et al., 2008. HiRISE observations of fractured mounds: Possible Martian pingos.
1568 *Geophysical Research Letters*, 35(4), p.L04201.

1569 Dundas, C.M. et al., 2014. HiRISE observations of new impact craters exposing Martian ground ice.
1570 *Journal of Geophysical Research: Planets*, 119(1), p.2013JE004482.

1571 Dundas, C.M. et al., 2012. Seasonal activity and morphological changes in martian gullies. *Icarus*, 220(1),
1572 p.124–143.

1573 Dundas, C.M. et al., 2019b. The Formation of Gullies on Mars Today. *Geological Society, London, Special*
1574 *Publications*, Martian Gullies and their Earth Analogues(467).

1575 Dundas, C.M., Byrne, S. & McEwen, A.S., 2015a. Modeling the development of martian sublimation
1576 thermokarst landforms. *Icarus*, 262, p.154–169.

1577 Dundas, C.M., Diniega, S. & McEwen, A.S., 2015b. Long-Term Monitoring of Martian Gully Formation and
1578 Evolution with MRO/HiRISE. *Icarus*, 251, p.244–263.

1579 Dundas, C.M. & McEwen, A.S., 2010. An assessment of evidence for pingos on Mars using HiRISE. *Icarus*,
1580 205(1), p.244–258.

1581 Ehlmann, B.L. et al., 2011a. Evidence for low-grade metamorphism, hydrothermal alteration, and
1582 diagenesis on Mars from phyllosilicate mineral assemblages. *Clays and Clay Minerals*, 59(4),
1583 p.359–377.

1584 Ehlmann, B.L. et al., 2011b. Subsurface water and clay mineral formation during the early history of
1585 Mars. *Nature*, 479(7371), p.53–60.

El-Maarry, M.R. et al., 2013. Morphology and evolution of the ejecta of Hale crater in Argyre basin, Mars: Results from high resolution mapping. *Icarus*, 226(1), p.905–922.

Fagents, S.A., Lanagan, P. & Greeley, R., 2002. Rootless cones on Mars: a consequence of lava-ground ice interaction. *Geological Society, London, Special Publications*, 202(1), p.295–317.

Farrell, W.M. et al., 2009. Is the Martian water table hidden from radar view?: MARTIAN WATER TABLE. *Geophysical Research Letters*, 36(15), p.n/a-n/a.

Fassett, C.I. et al., 2010. Supraglacial and proglacial valleys on Amazonian Mars. *Icarus*, 208(1), p.86–100.

Fassett, C.I. & Head III, J.W., 2008. The timing of martian valley network activity: Constraints from buffered crater counting. *Icarus*, 195(1), p.61–89.

Fastook, J.L. et al., 2012. Early Mars climate near the Noachian–Hesperian boundary: Independent evidence for cold conditions from basal melting of the south polar ice sheet (Dorsa Argentea Formation) and implications for valley network formation. *Icarus*, 219(1), p.25–40.

Fastook, J.L. & Head, J.W., 2014. Amazonian mid- to high-latitude glaciation on Mars: Supply-limited ice sources, ice accumulation patterns, and concentric crater fill glacial flow and ice sequestration. *Planetary and Space Science*, 91(0), p.60–76.

Fastook, J.L. & Head, J.W., 2015. Glaciation in the Late Noachian Icy Highlands: Ice accumulation, distribution, flow rates, basal melting, and top-down melting rates and patterns. *Planetary and Space Science*, 106, p.82–98.

Feldman, W.C. et al., 2004. Global distribution of near-surface hydrogen on Mars. *J. Geophys. Res.*, 109(E9). Available at: http://dx.doi.org/10.1029/2003JE002160.

Feldman, W.C. et al., 2011. Mars Odyssey neutron data: 2. Search for buried excess water ice deposits at nonpolar latitudes on Mars. *J. Geophys. Res.*, 116(E11), p.E11009.

Feldman, W.C. et al., 2008. North to south asymmetries in the water-equivalent hydrogen distribution at high latitudes on Mars. *Journal of Geophysical Research*, 113(E8), p.E08006.

Feldman, W.C. et al., 2007. Vertical distribution of hydrogen at high northern latitudes on Mars: The Mars Odyssey Neutron Spectrometer: MARS ODYSSEY NEUTRON SPECTROMETER. *Geophysical Research Letters*, 34(5). Available at: http://doi.wiley.com/10.1029/2006GL028936 [Accessed March 3, 2020].

Fishbaugh, K.E. & Hvidberg, C.S., 2006. Martian north polar layered deposits stratigraphy: Implications for accumulation rates and flow. *J. Geophys. Res.*, 111(E6), p.doi:10.1029/2005je002571.

Fisher, D.A., 2005. A process to make massive ice in the martian regolith using long-term diffusion and thermal cracking. *Icarus*, 179(2), p.387–397.

Fitzsimons, S. & Howarth, J., 2020. Development of push moraines in deeply frozen sediment adjacent to a cold-based glacier in the McMurdo Dry Valleys, Antarctica. *Earth Surface Processes and Landforms*, 45(3), p.622–637.

1621 Flemal, R.C., 1976. Pingos and Pingo Scars: Their Characteristics, Distribution, and Utility in
1622 Reconstructing Former Permafrost Environments. *Quaternary Research*, 6(1), p.37–53.

1623 French, H.M., 2013. *The periglacial environment* 3rd ed., Chichester, England: John Wiley & Sons.

1624 Frey, H. & Jarosewich, M., 1982. Subkilometer Martian volcanoes: Properties and possible terrestrial
1625 analogs. *Journal of Geophysical Research*, 87(B12), p.9867.

1626 Gaidos, E.J., 2001. Cryovolcanism and the recent flow of liquid water on Mars. *Icarus*, 153(1), p.218–223.

1627 Gallagher, C. et al., 2018. Formation and degradation of chaotic terrain in the Galaxias regions of Mars;
1628 implications for near-surface storage of ice. *Icarus*. Available at:
1629 https://www.sciencedirect.com/science/article/pii/S0019103517305882.

1630 Gallagher, C. et al., 2011. Sorted clastic stripes, lobes and associated gullies in high-latitude craters on
1631 Mars: Landforms indicative of very recent, polycyclic ground-ice thaw and liquid flows. *Icarus*,
1632 211(1), p.458–471.

1633 Gallagher, C. & Balme, M., 2015. Eskers in a complete, wet-based glacial system in the Phlegra Montes
1634 region, Mars. *Earth and Planetary Science Letters*, 431, p.96–109.

1635 Gallagher, C.J. & Balme, M.R., 2011. Landforms indicative of ground-ice thaw in the northern high
1636 latitudes of Mars. *Geological Society, London, Special Publications*, 356(1), p.87–110.

1637 Gardin, E. et al., 2010. Defrosting, dark flow features, and dune activity on Mars: Example in Russell
1638 crater. *J. Geophys. Res.*, 115(E6), p.doi:10.1029/2009JE003515.

1639 Gastineau, R. et al., 2020. Small-scale lobate hillslope features on Mars: A comparative 3D morphological
1640 study with terrestrial solifluction lobes and zebra stripe lobes. *Icarus*, accepted.

1641 Gellert, R., 2004. Chemistry of Rocks and Soils in Gusev Crater from the Alpha Particle X-ray
1642 Spectrometer. *Science*, 305(5685), p.829–832.

1643 Ghatan, G.J. & Head III, J.W., 2002. Candidate subglacial volcanoes in the south polar region of Mars:
1644 Morphology, morphometry, and eruption conditions. *Journal of Geophysical Research*, 107(E7).
1645 Available at: http://doi.wiley.com/10.1029/2001JE001519 [Accessed September 11, 2017].

1646 Ghent, R.R., Anderson, S.W. & Pithawala, T.M., 2012. The formation of small cones in Isidis Planitia, Mars
1647 through mobilization of pyroclastic surge deposits. *Icarus*, 217(1), p.169–183.

1648 Gillet, Ph. et al., 2002. Aqueous alteration in the Northwest Africa 817 (NWA 817) Martian meteorite.
1649 *Earth and Planetary Science Letters*, 203(1), p.431–444.

1650 Giuranna, M. et al., 2008. PFS/MEX observations of the condensing CO2 south polar cap of Mars. *Icarus*,
1651 197(2), p.386–402.

1652 Glavin, D.P. et al., 2013a. Evidence for perchlorates and the origin of chlorinated hydrocarbons detected
1653 by SAM at the Rocknest aeolian deposit in Gale Crater: EVIDENCE FOR PERCHLORATES AT
1654 ROCKNEST. *Journal of Geophysical Research: Planets*, 118(10), p.1955–1973.

Glavin, D.P. et al., 2013b. Evidence for perchlorates and the origin of chlorinated hydrocarbons detected by SAM at the Rocknest aeolian deposit in Gale Crater: EVIDENCE FOR PERCHLORATES AT ROCKNEST. *Journal of Geophysical Research: Planets*, 118(10), p.1955–1973.

Goddard, K. et al., 2014. Mechanisms and Timescales of Fluvial Activity at Mojave and other Young Martian Craters. *Journal of Geophysical Research: Planets*, p.2013JE004564.

Goldspiel, J.M. & Squyres, S.W., 2011. Groundwater discharge and gully formation on martian slopes. *Icarus*, 211(1), p.238–258.

Gosse, G. & Jones, B.M., 2011. Spatial distribution of pingos in northern Asia. *The Cryosphere*, 5, p.13–33.

Gough, R.V. et al., 2011. Laboratory studies of perchlorate phase transitions: Support for metastable aqueous perchlorate solutions on Mars. *Earth and Planetary Science Letters*, 312(3–4), p.371–377.

Gough, R.V., Chevrier, V.F. & Tolbert, M.A., 2016. Formation of liquid water at low temperatures via the deliquescence of calcium chloride: Implications for Antarctica and Mars. *Planetary and Space Science*, 131, p.79–87.

Grant, J.A. & Wilson, S.A., 2011. Late alluvial fan formation in southern Margaritifer Terra, Mars. *Geophys. Res. Lett.*, 38(8), p.L08201.

Grasby, S.E., Proemse, B.C. & Beauchamp, B., 2014. Deep groundwater circulation through the High Arctic cryosphere forms Mars-like gullies. *Geology*, 42(8), p.651–654.

Grau Galofre, A., Jellinek, A.M. & Osinski, G.R., 2020. Valley formation on early Mars by subglacial and fluvial erosion. *Nature Geoscience*. Available at: http://www.nature.com/articles/s41561-020-0618-x [Accessed September 28, 2020].

Grimm, R.E. et al., 2020. A Magnetotelluric Sounder to Probe Terrestrial Planet and Satellite Interiors. In *Lunar and Planetary Science Conference*. p. 1568. Available at: https://ui.adsabs.harvard.edu/abs/2020LPI....51.1568G.

Grimm, R.E., 2002. Low-frequency electromagnetic exploration for groundwater on Mars. *Journal of Geophysical Research*, 107(E2). Available at: http://doi.wiley.com/10.1029/2001JE001504 [Accessed April 7, 2020].

Grimm, R.E. et al., 2017. On the secular retention of ground water and ice on Mars. *Journal of Geophysical Research: Planets*, 122(1), p.94–109.

Grimm, R.E., Harrison, K.P. & Stillman, D.E., 2014. Water budgets of martian recurring slope lineae. *Icarus*, 233(0), p.316–327.

Grimm, R.E. & Stillman, D.E., 2015. Field Test of Detection and Characterisation of Subsurface Ice using Broadband Spectral-Induced Polarisation: Subsurface Ice Characterisation using Spectral-Induced Polarisation. *Permafrost and Periglacial Processes*, 26(1), p.28–38.

1689 Guidat, T. et al., 2015. Landform assemblage in Isidis Planitia, Mars: Evidence for a 3 Ga old polythermal
1690 ice sheet. *Earth and Planetary Science Letters*, 411, p.253–267.

1691 de Haas, T. et al., 2016. Autogenic avulsion, channelization and backfilling dynamics of debris-flow fans
1692 D. Mohrig, ed. *Sedimentology*, 63(6), p.1596–1619.

1693 de Haas, T. et al., 2015a. Earth-like aqueous debris-flow activity on Mars at high orbital obliquity in the
1694 last million years. *Nature Communications*, 6. Available at:
1695 http://dx.doi.org/10.1038/ncomms8543.

1696 de Haas, T. et al., 2015b. Sedimentological analyses of martian gullies: The subsurface as the key to the
1697 surface. *Icarus*, 258(0), p.92–108.

1698 de Haas, T. et al., 2015c. Surface morphology of fans in the high-arctic periglacial environment of
1699 Svalbard: Controls and processes. *Earth-Science Reviews*, (0). Available at:
1700 http://www.sciencedirect.com/science/article/pii/S0012825215000641.

1701 de Haas, T. et al., 2018a. Time will tell: temporal evolution of Martian gullies and paleoclimatic
1702 implications. *Geological Society, London, Special Publications*, 467.

1703 de Haas, T., Kruijt, A. & Densmore, A.L., 2018b. Effects of debris-flow magnitude-frequency distribution
1704 on avulsions and fan development: Effects of debris-flow magnitude-frequency distribution on
1705 avulsions and fan development. *Earth Surface Processes and Landforms*, 43(13), p.2779–2793.

1706 Haberle, R.M. et al. eds., 2017. *The Atmosphere and Climate of Mars*, Cambridge: Cambridge University
1707 Press. Available at: http://ebooks.cambridge.org/ref/id/CBO9781139060172 [Accessed March 2,
1708 2020].

1709 Hallet, B., 1990. Self-organization in freezing soils: from microscopic ice lenses to patterned ground.
1710 *Canadian Journal of Physics*, 68(9), p.842–852.

1711 Hanna, J.C. & Phillips, R.J., 2006. Tectonic pressurization of aquifers in the formation of Mangala and
1712 Athabasca Valles, Mars. *Journal of Geophysical Research*, 111(E3). Available at:
1713 http://doi.wiley.com/10.1029/2005JE002546 [Accessed March 24, 2020].

1714 Hansen, C.J. et al., 2013. Observations of the northern seasonal polar cap on Mars: I. Spring sublimation
1715 activity and processes. *Mars Polar Science V*, 225(2), p.881–897.

1716 Hansen, G. et al., 2005. PFS-MEX observation of ices in the residual south polar cap of Mars. *Planetary
1717 and Space Science*, 53(10), p.1089–1095.

1718 Harrison, K.P. & Grimm, R.E., 2008. Multiple flooding events in Martian outflow channels. *Journal of
1719 Geophysical Research*, 113(E2), p.E02002.

1720 Harrison, T.N. et al., 2015. Global Documentation of Gullies with the Mars Reconnaissance Orbiter
1721 Context Camera and Implications for Their Formation. *Icarus*, 252, p.236–254.

1722 Harrison, T.N. et al., 2010. Impact-induced overland fluid flow and channelized erosion at Lyot Crater,
1723 Mars. *Geophysical Research Letters*, 37(21). Available at:
1724 http://dx.doi.org/10.1029/2010GL045074.

1725 Hartmann, W.K., Thorsteinsson, T. & Sigurdsson, F., 2003. Martian hillside gullies and Icelandic analogs.
1726 *Icarus*, 162(2), p.259–277.

1727 Hartmann, W.K. & Werner, S.C., 2010. Martian Cratering 10. Progress in use of crater counts to interpret
1728 geological processes: Examples from two debris aprons. *Earth and Planetary Science Letters*,
1729 294(3–4), p.230–237.

1730 Hauber, E. et al., 2013. Asynchronous formation of Hesperian and Amazonian-aged deltas on Mars and
1731 implications for climate. *Journal of Geophysical Research: Planets*, 118(7), p.1529–1544.

1732 Hauber, E. et al., 2018. Debris Flows and Water Tracks in Northern Victoria Land, Continental East
1733 Antarctica: A New Terrestrial Analogue Site for Gullies and Recurrent Slope Lineae on Mars.
1734 *Geological Society, London, Special Publications*, in review.

1735 Hauber, E. et al., 2011a. Landscape evolution in Martian mid-latitude regions: insights from analogous
1736 periglacial landforms in Svalbard. *Geological Society, London, Special Publications*, 356(1), p.111–
1737 131.

1738 Hauber, E. et al., 2011b. Periglacial landscapes on Svalbard: Terrestrial analogs for cold-climate
1739 landforms on Mars. *Geological Society of America Special Papers*, 483, p.177–201.

1740 Hayne, P.O., Paige, D.A. & Heavens, N.G., 2014. The role of snowfall in forming the seasonal ice caps of
1741 Mars: Models and constraints from the Mars Climate Sounder. *Icarus*, 231, p.122–130.

1742 Head, J.W. et al., 2010. Northern mid-latitude glaciation in the Late Amazonian period of Mars: Criteria
1743 for the recognition of debris-covered glacier and valley glacier landsystem deposits. *Earth and*
1744 *Planetary Science Letters*, 294(3–4), p.306–320.

1745 Head, J.W. et al., 2003. Recent ice ages on Mars. *Nature*, 426(6968), p.797–802.

1746 Head, J.W., Marchant, D.R. & Kreslavsky, M.A., 2008. Formation of gullies on Mars: Link to recent climate
1747 history and insolation microenvironments implicate surface water flow origin. *Proceedings of the*
1748 *National Academy of Sciences of the United States of America*, 105(36), p.13258–13263.

1749 Head, J.W. & Pratt, S., 2001. Extensive Hesperian-aged south polar ice sheet on Mars: Evidence for
1750 massive melting and retreat, and lateral flow and ponding of meltwater. *Journal of Geophysical*
1751 *Research: Planets*, 106(E6), p.12275–12299.

1752 Hecht, M.H. et al., 2009. Detection of Perchlorate and the Soluble Chemistry of Martian Soil at the
1753 Phoenix Lander Site. *Science*, 325(5936), p.64.

1754 Hecht, M.H., 2002. Metastability of liquid water on Mars. *Icarus*, 156(2), p.373–386.

1755 Heckmann, T. & Schwanghart, W., 2013. Geomorphic coupling and sediment connectivity in an alpine
1756 catchment — Exploring sediment cascades using graph theory. *Geomorphology*, 182, p.89–103.

1757 Heinz, J., Schulze-Makuch, D. & Kounaves, S.P., 2016. Deliquescence-induced wetting and RSL-like
1758 darkening of a Mars analogue soil containing various perchlorate and chloride salts. *Geophysical*
1759 *Research Letters*, 43(10), p.4880–4884.

1760 Heldmann, J.L. et al., 2005. Formation of Martian gullies by the action of liquid water flowing under
1761 current Martian environmental conditions. *J. Geophys. Res.-Planets*, 110(E5),
1762 p.doi:10.1029/2004JE002261.

1763 Heldmann, J.L. et al., 2014. Midlatitude Ice-Rich Ground on Mars as a Target in the Search for Evidence of
1764 Life and for in situ Resource Utilization on Human Missions. *Astrobiology*, (2), p.102–118.

1765 Heldmann, J.L. et al., 2007. Observations of martian gullies and constraints on potential formation
1766 mechanisms II. The northern hemisphere. *Icarus*, 188, p.324–344.

1767 Heldmann, J.L. et al., 2010. Possible Liquid Water Origin for Atacama Desert Mudflow and Recent Gully
1768 Deposits on Mars. *Icarus*, 206(2), p.685–690.

1769 Heldmann, J.L. & Mellon, M.T., 2004. Observations of martian gullies and constraints on potential
1770 formation mechanisms. *Icarus*, 168(2), p.285–304.

1771 Hemmi, R. & Miyamoto, H., 2017. Distribution, morphology, and morphometry of circular mounds in the
1772 elongated basin of northern Terra Sirenum, Mars. *Progress in Earth and Planetary Science*, 4(1).
1773 Available at: http://progearthplanetsci.springeropen.com/articles/10.1186/s40645-017-0141-x
1774 [Accessed March 23, 2020].

1775 Hemmi, R. & Miyamoto, H., 2018. High-Resolution Topographic Analyses of Mounds in Southern Acidalia
1776 Planitia, Mars: Implications for Possible Mud Volcanism in Submarine and Subaerial
1777 Environments. *Geosciences*, 8(5), p.152.

1778 Hepburn, A.J. et al., 2019. Polyphase mid-latitude glaciation on Mars: chronology of the formation of
1779 superposed glacier-like forms from crater-count dating. *Journal of Geophysical Research: Planets*,
1780 p.2019JE006102.

1781 Herkenhoff, K., 2001. *Geologic map of the MTM-85000 Quadrangle, Planum Australe region of Mars*, The
1782 US Geological Survey. Available at: https://pubs.usgs.gov/imap/i2686/.

1783 Herkenhoff, K.E. & Plaut, J.J., 2000. Surface Ages and Resurfacing Rates of the Polar Layered Deposits on
1784 Mars. *Icarus*, 144(2), p.243–253.

1785 Herny, C. et al., 2019. Unstable liquid water as a geomorphological agent in martian gullies: experimental
1786 investigation of the effect of boiling intensity on downslope sediment transport. *Geological*
1787 *Society, London, Special Publications*, 467.

1788 Herschel, W., 1784. On the Remarkable Appearances at the Polar Regions of the Planet Mars, the
1789 Inclination of Its Axis, the Position of Its Poles, and Its Spheroidical Figure; With a Few Hints
1790 Relating to Its Real Diameter and Atmosphere. By William Herschel, Esq. F. R. S. *Philosophical*
1791 *Transactions of the Royal Society of London*, 74, p.233–273.

1792 Hess, S.L. et al., 1980. The annual cycle of pressure on Mars measured by Viking Landers 1 and 2.
1793 *Geophysical Research Letters*, 7(3), p.197–200.

1794 Heyer, T. et al., 2019. Seasonal formation rates of martian slope streaks. *Icarus*, 323, p.76–86.

1795 Hobbs, S.W., Paull, D.J. & Clarke, J.D.A., 2017. Testing the water hypothesis: Quantitative morphological
1796 analysis of terrestrial and martian mid-latitude gullies. *Geomorphology*, 295, p.705–721.

1797 Holt, J.W. et al., 2008. Radar Sounding Evidence for Buried Glaciers in the Southern Mid-Latitudes of
1798 Mars. *Science*, 322, p.1235–1238.

1799 Horvath, A. et al., 2009. Analysis of Dark Albedo Features on a Southern Polar Dune Field of Mars.
1800 *Astrobiology*, 9(1), p.90–103.

1801 Hovius, N., Lea-Cox, A. & Turowski, J.M., 2008. Recent volcano-ice interaction and outburst flooding in a
1802 Mars polar cap re-entrant. *Icarus*, 197(1), p.24–38.

1803 Howard, A.D. & Moore, J.M., 2011. Late Hesperian to early Amazonian midlatitude Martian valleys:
1804 Evidence from Newton and Gorgonum basins. *J. Geophys. Res.*, 116(E5), p.E05003.

1805 Hubbard, G.S., Naderi, F.M. & Garvin, J.B., 2002. Following the water, the new program for Mars
1806 exploration. *Acta Astronautica*, 51(1–9), p.337–350.

1807 Huber, C. et al., 2020. Physical models and predictions for recurring slope lineae formed by wet and dry
1808 processes. *Icarus*, 335, p.113385.

1809 Hynek, B.M., Beach, M. & Hoke, M.R.T., 2010. Updated global map of Martian valley networks and
1810 implications for climate and hydrologic processes. *J. Geophys. Res.*, 115(E9),
1811 p.doi:10.1029/2009JE003548.

1812 Hynek, B.M. & Phillips, R.J., 2003. New data reveal mature, integrated drainage systems on Mars
1813 indicative of past precipitation. *Geology*, 31(9), p.757.

1814 Ivanov, M.A. et al., 2014. Mud volcanism and morphology of impact craters in Utopia Planitia on Mars:
1815 Evidence for the ancient ocean. *Icarus*, 228(0), p.121–140.

1816 Jakosky, B.M., 1983. The role of seasonal reservoirs in the Mars water cycle. *Icarus*, 55(1), p.1–18.

1817 Jakosky, B.M. & Carr, M.H., 1985. Possible precipitation of ice at low latitudes of Mars during periods of
1818 high obliquity. *Nature*, 315(6020), p.559–561.

1819 Jakosky, B.M., Henderson, B.G. & Mellon, M.T., 1995. Chaotic obliquity and the nature of the Martian
1820 climate. *Journal of Geophysical Research*, 100(E1), p.1579.

1821 Jakosky, B.M. & Phillips, R.J., 2001. Mars' volatile and climate history. *Nature*, 412, p.237–244.

1822 Jawin, E.R., Head, J.W. & Marchant, D.R., 2018. Transient post-glacial processes on Mars:
1823 Geomorphologic evidence for a paraglacial period. *Icarus*, 309, p.187–206.

1824 Johnsson, A. et al., 2014. Evidence for very recent melt-water and debris flow activity in gullies in a
1825 young mid-latitude crater on Mars. *Icarus*, 235, p.37–54.

1826 Johnsson, A. et al., 2012. Periglacial mass-wasting landforms on Mars suggestive of transient liquid water
1827 in the recent past: Insights from solifluction lobes on Svalbard. *Icarus*, 218(1), p.489–505.

1828 Johnsson, A. et al., 2018. Slow periglacial mass wasting (solifluction) on Mars. In R. J. Soare, S. J. Conway,
1829 & S. M. Clifford, eds. *Dynamic Mars*. Elsevier.

1830 Jones, A.P. et al., 2011. A geomorphic analysis of Hale crater, Mars: The effects of impact into ice-rich
1831 crust. *Icarus*, 211(1), p.259–272.

1832 Jones, B.M. et al., 2012. Assessment of pingo distribution and morphometry using an IfSAR derived
1833 digital surface model, western Arctic Coastal Plain, Northern Alaska. *Geomorphology*, 138(1),
1834 p.1–14.

1835 Jones, E.G. & Lineweaver, C.H., 2012. Using the phase diagram of liquid water to search for life.
1836 *Australian Journal of Earth Sciences*, 59(2), p.253–262.

1837 Jouannic, G. et al., 2018. Morphological characterization of landforms produced by springtime seasonal
1838 activity on Russell dune (Mars). *Geological Society, London, Special Publications*, 467.

1839 Jouglet, D. et al., 2007. Hydration state of the Martian surface as seen by Mars Express OMEGA: 1.
1840 Analysis of the 3 μ m hydration feature: HYDRATION STATE OF THE MARTIAN SURFACE, 1.
1841 *Journal of Geophysical Research: Planets*, 112(E8). Available at:
1842 http://doi.wiley.com/10.1029/2006JE002846 [Accessed September 28, 2020].

1843 Karatekin, Ö., Van Hoolst, T. & Dehant, V., 2006. Martian global-scale CO_2 exchange from time-variable
1844 gravity measurements. *Journal of Geophysical Research*, 111(E6), p.E06003.

1845 Kargel, J.S. et al., 1995. Evidence of ancient continental glaciation in the Martian northern plains. *Journal*
1846 *of Geophysical Research*, 100(E3), p.5351.

1847 Karlsson, N.B., Schmidt, L.S. & Hvidberg, C.S., 2015. Volume of Martian midlatitude glaciers from radar
1848 observations and ice flow modeling. *Geophysical Research Letters*, 42(8), p.2627–2633.

1849 Keller, J.M. et al., 2007. Equatorial and midlatitude distribution of chlorine measured by Mars Odyssey
1850 GRS. *Journal of Geophysical Research*, 112(E3), p.E03S08.

1851 Kereszturi, A. et al., 2010. Indications of brine related local seepage phenomena on the northern
1852 hemisphere of Mars. *Icarus*, 207(1), p.149–164.

1853 Kereszturi, A. et al., 2016. Indicators and Methods to Understand Past Environments from ExoMars
1854 Rover Drills. *Origins of Life and Evolution of Biospheres*, 46(4), p.435–454.

1855 Kereszturi, A. et al., 2011a. Possible role of brines in the darkening and flow-like features on the Martian
1856 polar dunes based on HiRISE images. *Planetary and Space Science*, 59(13), p.1413–1427.

1857 Kereszturi, A. et al., 2009. Recent rheologic processes on dark polar dunes of Mars: Driven by interfacial
1858 water? *Icarus*, 201(2), p.492–503.

1859 Kereszturi, A. & Appéré, T., 2014. Searching for springtime zonal liquid interfacial water on Mars. *Icarus*,
1860 238, p.66–76.

1861 Kereszturi, A. & Petrik, A., 2020. Age determination for valley networks on Mars using tectonic-fluvial
1862 interaction. *Planetary and Space Science*, 180, p.104754.

1863 Kereszturi, A. & Rivera-Valentin, E.G., 2012. Locations of thin liquid water layers on present-day Mars.
1864 *Icarus*, 221(1), p.289–295.

1865 Kereszturi, A. & Rivera-Valentin, E.G., 2016. Possible water lubricated grain movement in the circumpolar
1866 region of Mars. *Planetary and Space Science*, 125, p.130–146.

1867 Kereszturi, A., Vincendon, M. & Schmidt, F., 2011b. Water ice in the dark dune spots of Richardson crater
1868 on Mars. *Planetary and Space Science*, 59(1), p.26–42.

1869 Kessler, M.A. & Werner, B.T., 2003. Self-Organization of Sorted Patterned Ground. *Science*, 299(5605),
1870 p.380–383.

1871 Kieffer, H.H., Christensen, P.R. & Titus, T.N., 2006. CO2 jets formed by sublimation beneath translucent
1872 slab ice in Mars' seasonal south polar ice cap. *Nature*, 442(7104), p.793–796.

1873 Kite, E.S. et al., 2011. Localized precipitation and runoff on Mars. *J. Geophys. Res.*, 116(E7), p.E07002.

1874 Kite, E.S. et al., 2019. Persistence of intense, climate-driven runoff late in Mars history. *Science Advances*,
1875 5(3), p.eaav7710.

1876 Kite, E.S. et al., 2017. Persistent or repeated surface habitability on Mars during the late Hesperian -
1877 Amazonian: Mars Alluvial Fan Aggradation Took >20 Ma. *Geophysical Research Letters*, 44(9),
1878 p.3991–3999.

1879 Kminek, G. et al., 2010. Report of the COSPAR mars special regions colloquium. *Life Sciences in Space*,
1880 46(6), p.811–829.

1881 Kneissl, T. et al., 2010. Distribution and orientation of northern-hemisphere gullies on Mars from the
1882 evaluation of HRSC and MOC-NA data. *Earth and Planetary Science Letters*, 294(3–4), p.357–367.

1883 Kokelj, S.V. & Jorgenson, M.T., 2013. Advances in Thermokarst Research: Recent Advances in Research
1884 Investigating Thermokarst Processes. *Permafrost and Periglacial Processes*, 24(2), p.108–119.

1885 Kolb, K.J., Pelletier, J.D. & McEwen, A.S., 2010. Modeling the formation of bright slope deposits
1886 associated with gullies in Hale Crater, Mars: Implications for recent liquid water. *Icarus*, 205(1),
1887 p.113–137.

1888 Komar, P.D., 1979. Comparisons of the hydraulics of water flows in Martian outflow channels with flows
1889 of similar scale on earth. *Icarus*, 37(1), p.156–181.

1890 Komatsu, G. et al., 2016. Small edifice features in Chryse Planitia, Mars: Assessment of a mud volcano
1891 hypothesis. *Icarus*, 268, p.56–75.

1892 Kossacki, K.J. & Markiewicz, W.J., 2010. Interfacial liquid water on Mars and its potential role in
1893 formation of hill and dune gullies. *Icarus*, 210(1), p.83–91.

1894 Kossacki, K.J. & Markiewicz, W.J., 2004. Seasonal melting of surface water ice condensing in martian
1895 gullies. *Icarus*, 171(2), p.272–283.

1896 Kounaves, S.P. et al., 2010. Soluble sulfate in the martian soil at the Phoenix landing site: SULFATE AT
1897 THE PHOENIX LANDING SITE. *Geophysical Research Letters*, 37(9), p.n/a-n/a.

1898 Kreslavsky, M.A. & Head, J.W., 2000. Kilometer-scale roughness of Mars: Results from MOLA data
1899 analysis. *Journal of Geophysical Research*, 105, p.26695–26712.

1900 Kreslavsky, M.A. & Head, J.W., 2002. Mars: Nature and evolution of young latitude-dependent water-ice-
1901 rich mantle. *Geophysical Research Letters*, 29, p.14–1.

1902 Kreslavsky, M.A. & Head, J.W., 2003. North-south topographic slope asymmetry on Mars: Evidence for
1903 insolation-related erosion at high obliquity. *Geophys. Res. Lett.*, 30(15),
1904 p.doi:10.1029/2003GL017795.

1905 Kreslavsky, M.A. & Head, J.W., 2009. Slope streaks on Mars: A new 'wet' mechanism. *Icarus*, 201, p.517–
1906 527.

1907 Kress, A.M. & Head, J.W., 2015. Late Noachian and early Hesperian ridge systems in the south
1908 circumpolar Dorsa Argentea Formation, Mars: Evidence for two stages of melting of an extensive
1909 late Noachian ice sheet. *Planetary and Space Science*, 109–110, p.1–20.

1910 Landis, M.E. et al., 2016. A revised surface age for the North Polar Layered Deposits of Mars. *Geophysical*
1911 *Research Letters*, 43(7), p.3060–3068.

1912 Lanza, N.L. et al., 2010. Evidence for debris flow gully formation initiated by shallow subsurface water on
1913 Mars. *Icarus*, 205(1), p.103–112.

1914 Laskar, J. et al., 2004. Long term evolution and chaotic diffusion of the insolation quantities of Mars.
1915 *Icarus*, 170(2), p.343–364.

1916 Laskar, J., Levrard, B. & Mustard, J.F., 2002. Orbital forcing of the martian polar layered deposits. *Nature*,
1917 419(6905), p.375–377.

1918 Lasue, J. et al., 2019. The Hydrology of Mars Including a Potential Cryosphere. In *Volatiles in the Martian*
1919 *Crust*. Elsevier, pp. 185–246. Available at:
1920 https://linkinghub.elsevier.com/retrieve/pii/B9780128041918000076 [Accessed March 4, 2020].

1921 Lauro, S.E. et al., 2020. Multiple subglacial water bodies below the south pole of Mars unveiled by new
1922 MARSIS data. *Nature Astronomy*. Available at: http://www.nature.com/articles/s41550-020-
1923 1200-6 [Accessed October 1, 2020].

1924 Leask, E.K. et al., 2018. Challenges in the Search for Perchlorate and Other Hydrated Minerals With 2.1-
1925 µm Absorptions on Mars. *Geophysical Research Letters*, 45(22). Available at:
1926 https://onlinelibrary.wiley.com/doi/abs/10.1029/2018GL080077 [Accessed February 24, 2020].

1927 Leask, H.J., Wilson, L. & Mitchell, K.L., 2007. Formation of Mangala Valles outflow channel, Mars:
1928 Morphological development and water discharge and duration estimates. *Journal of Geophysical*
1929 *Research (Planets)*, 112, p.doi: 10.1029/2006JE002851.

1930 Lefort, A., Russell, P.S. & Thomas, N., 2010. Scalloped terrains in the Peneus and Amphitrites Paterae
1931 region of Mars as observed by HiRISE. *Icarus*, 205(1), p.259–268.

1932 Leung, C.W.S. et al., 2020. Atmospheric Water Budgets for Recurring Slope Lineae Activity. *Journal of*
1933 *Geophysical Research*, in review.

1934 Leverington, D.W., 2011. A volcanic origin for the outflow channels of Mars: Key evidence and major
1935 implications. *Geomorphology*, 132(3–4), p.51–75.

1936 Leverington, D.W., 2009. Reconciling channel formation processes with the nature of elevated outflow
1937 systems at Ophir and Aurorae Plana, Mars. *Journal of Geophysical Research (Planets)*, 114,
1938 p.10005.

1939 Levrard, B. et al., 2007. Recent formation and evolution of northern Martian polar layered deposits as
1940 inferred from a Global Climate Model. *Journal of Geophysical Research: Planets*, 112(E6).
1941 Available at: http://dx.doi.org/10.1029/2006JE002772.

1942 Levy, J.S. et al., 2009a. Geologically recent gully-polygon relationships on Mars: Insights from the
1943 Antarctic dry valleys on the roles of permafrost, microclimates, and water sources for surface
1944 flow. *Icarus*, 201(1), p.113–126.

1945 Levy, J.S. et al., 2010a. Identification of gully debris flow deposits in Protonilus Mensae, Mars:
1946 Characterization of a water-bearing, energetic gully-forming process. *Earth and Planetary Science*
1947 *Letters*, 294(3–4), p.368–377.

1948 Levy, J.S. et al., 2014. Sequestered glacial ice contribution to the global Martian water budget: Geometric
1949 constraints on the volume of remnant, midlatitude debris-covered glaciers. *Journal of*
1950 *Geophysical Research: Planets*, 119(10), p.2014JE004685.

1951 Levy, J.S., Head, J. & Marchant, D., 2009b. Thermal contraction crack polygons on Mars: Classification,
1952 distribution, and climate implications from HiRISE observations. *Journal of Geophysical Research*
1953 *(Planets)*, 114, p.01007.

1954 Levy, J.S., Head, J.W. & Marchant, D.R., 2009c. Concentric crater fill in Utopia Planitia: History and
1955 interaction between glacial 'brain terrain' and periglacial mantle processes. *Icarus*, 202(2),
1956 p.462–476.

1957 Levy, J.S., Marchant, D.R. & Head, J.W., 2010b. Thermal contraction crack polygons on Mars: A synthesis
1958 from HiRISE, Phoenix, and terrestrial analog studies. *Solar Wind Interactions with Mars*, 206(1),
1959 p.229–252.

1960 L'Haridon, J. et al., 2018. Chemical variability in mineralized veins observed by ChemCam on the lower
1961 slopes of Mount Sharp in Gale crater, Mars. *Icarus*, 311, p.69–86.

Lillis, R.J., Frey, H.V. & Manga, M., 2008. Rapid decrease in Martian crustal magnetization in the Noachian era: Implications for the dynamo and climate of early Mars. *Geophys. Res. Lett.*, 35(14), p.L14203.

Loizeau, D. et al., 2007. Phyllosilicates in the Mawrth Vallis region of Mars. *J. Geophys. Res.*, 112(E8), p.E08S08.

Lowe, D.R. et al., 2020. Deposition of >3.7 Ga clay-rich strata of the Mawrth Vallis Group, Mars, in lacustrine, alluvial, and aeolian environments. *GSA Bulletin*, 132(1–2), p.17–30.

Lucchitta, B.K., 1987. Valles Marineris, Mars: Wet debris flows and ground ice. *Icarus*, 72(2), p.411–429.

Luo, W., Cang, X. & Howard, A.D., 2017. New Martian valley network volume estimate consistent with ancient ocean and warm and wet climate. *Nature Communications*, 8(1), p.15766.

Mackay, J.R., 2002. Pingo Growth and collapse, Tuktoyaktuk Peninsula Area, Western Arctic Coast, Canada: a long-term field study. *Géographie physique et Quaternaire*, 52(3), p.271–323.

Mackay, J.R., 1987. Some mechanical aspects of pingo growth and failure, western Arctic coast, Canada. *Canadian Journal of Earth Sciences*, 24(6), p.1108–1119.

MacKay, J.R., 2002. Thermally induced movements in ice-wedge polygons, western arctic coast: a long-term study. *Géographie physique et Quaternaire*, 54(1), p.41–68.

Madeleine, J.B. et al., 2009. Amazonian northern mid-latitude glaciation on Mars: A proposed climate scenario. *Icarus*, 203, p.390–405.

Madeleine, J.-B. et al., 2014. Recent Ice Ages on Mars: The role of radiatively active clouds and cloud microphysics. *Geophysical Research Letters*. Available at: http://dx.doi.org/10.1002/2014GL059861.

Malin, M.C. et al., 2006. Present-day impact cratering rate and contemporary gully activity on Mars. *Science*, 314(5805), p.1573–1577.

Malin, M.C. & Edgett, K.S., 2000. Evidence for recent groundwater seepage and surface runoff on Mars. *Science*, 288(5475), p.2330–2335.

Maltagliati, L. et al., 2011. Evidence of Water Vapor in Excess of Saturation in the Atmosphere of Mars. *Science*, 333(6051), p.1868–1871.

Mangold, N. et al., 2012. A chronology of early Mars climatic evolution from impact crater degradation. *Journal of Geophysical Research (Planets)*, 117(E4), p.E04003.

Mangold, N., 2012. Fluvial landforms on fresh impact ejecta on Mars. *Planetary and Space Science*, 62(1), p.69–85.

Mangold, N., 2003. Geomorphic analysis of lobate debris aprons on Mars at Mars Orbiter Camera scale: Evidence for ice sublimation initiated by fractures. *J. Geophys. Res.*, 108(E4), p.8021.

Mangold, N., 2005. High latitude patterned grounds on Mars: Classification, distribution and climatic control. *Mars Polar Science III*, 174(2), p.336–359.

Manning, C., Mckay, C. & Zahnle, K., 2006. Thick and thin models of the evolution of carbon dioxide on Mars. *Icarus*, 180(1), p.38–59.

Manning, C.V. et al., 2019. The formation and stability of buried polar CO2 deposits on Mars. *Icarus*, 317, p.509–517.

Marchant, D.R. et al., 2002. Formation of patterned ground and sublimation till over Miocene glacier ice in Beacon Valley, southern Victoria Land, Antarctica. *Geological Society of America Bulletin*, 114(6), p.718–730.

Marquez, A. et al., 2005. Evidence of gully formation by regional groundwater flow in the Gorgonum-Newton region (Mars). *Icarus*, 179(2), p.398–414.

Marra, W.A. et al., 2015. Pressurized groundwater systems in Lunae and Ophir Plana (Mars): Insights from small-scale morphology and experiments. *GeoResJ*, 8, p.1–13.

Marra, W.A. et al., 2014. Valley formation by groundwater seepage, pressurized groundwater outbursts and crater-lake overflow in flume experiments with implications for Mars. *Icarus*, 232, p.97–117.

Martínez-Alonso, S. et al., 2011. Evidence of volcanic and glacial activity in Chryse and Acidalia Planitiae, Mars. *Icarus*, 212(2), p.597–621.

Martín-Torres, F.J. et al., 2015. Transient liquid water and water activity at Gale crater on Mars. *Nature Geoscience*, 8(5), p.357–361.

Massé, M. et al., 2014. Spectroscopy and detectability of liquid brines on mars. *Planetary and Space Science*, 92, p.136–149.

Massé, M. et al., 2016. Transport processes induced by metastable boiling water under Martian surface conditions. *Nature Geoscience*, 9, p.425–428.

Matsuoka, N., 2001. Solifluction rates, processes and landforms: a global review. *Earth-Science Reviews*, 55(1–2), p.107–134.

Maurice, S. et al., 2011. Mars Odyssey neutron data: 1. Data processing and models of water-equivalent-hydrogen distribution. *J. Geophys. Res.*, 116(E11), p.E11008.

Max, M.D. & Clifford, S.M., 2001. Initiation of Martian outflow channels: Related to the dissociation of gas hydrate? *Geophysical Research Letters*, 28(9), p.1787–1790.

May, C.L. & Gresswell, R.E., 2004. Spatial and temporal patterns of debris-flow deposition in the Oregon Coast Range, USA. *Geomorphology*, 57(3–4), p.135–149.

McColl, S.T. et al., 2019. Origin and age of The Hillocks and implications for post-glacial landscape development in the upper Lake Wakatipu catchment, New Zealand. *Journal of Quaternary Science*, 34(8), p.685–696.

McColl, S.T. & Davies, T.R., 2011. Evidence for a rock-avalanche origin for 'The Hillocks' "moraine", Otago, New Zealand. *Geomorphology*, 127(3–4), p.216–224.

McEwen, A. et al., 2012. Future Orbital Measurements Needed to Understand Present-Day Liquid H2O on Mars. In *Concepts and Approaches for Mars Exploration*. p. 4284. Available at: https://ui.adsabs.harvard.edu/abs/2012LPICo1679.4284M.

McEwen, A.S. et al., 2007. A Closer Look at Water-Related Geologic Activity on Mars. *Science*, 317(5845), p.1706–1709.

McEwen, A.S. et al., 2019. Abundant Recurring Slope Lineae (RSL) Following the 2018 Planet-Encircling Dust Event (PEDE). In p. 1376. Available at: https://ui.adsabs.harvard.edu/abs/2019LPI....50.1376M.

McEwen, A.S. et al., 2014. Recurring slope lineae in equatorial regions of Mars. *Nature Geosci*, 7(1), p.53–58.

McEwen, A.S. et al., 2011. Seasonal Flows on Warm Martian Slopes. *Science*, 333(6043), p.740–743.

McGill, G.E., 1986. The giant polygons of Utopia, northern Martian Plains. *Geophysical Research Letters*, 13(8), p.705–708.

McGowan, E.M., 2011. The Utopia/Isidis overlap: Possible conduit for mud volcanism on Mars. *Icarus*, 212(2), p.622–628.

McSween, H.Y. & Keil, K., 2000. Mixing relationships in the Martian regolith and the composition of globally homogeneous dust. *Geochimica et Cosmochimica Acta*, 64(12), p.2155–2166.

Mellon, M.T. et al., 2009. Ground ice at the Phoenix Landing Site: Stability state and origin. *Journal of Geophysical Research: Planets*, 114(E1), p.E00E07.

Mellon, M.T., 1997. Small-scale polygonal features on Mars: Seasonal thermal contraction cracks in permafrost. *Journal of Geophysical Research: Planets*, 102(E11), p.25617–25628.

Mellon, M.T. & Jakosky, B.M., 1993. Geographic variations in the thermal and diffusive stability of ground ice on Mars. *Journal of Geophysical Research*, 98(E2), p.3345.

Mellon, M.T. & Jakosky, B.M., 1995. The distribution and behavior of Martian ground ice during past and present epochs. *Journal of Geophysical Research*, 100, p.3367.

Mellon, M.T. & Phillips, R.J., 2001. Recent gullies on Mars and the source of liquid water. *J. Geophys. Res.-Planets*, 106(E10), p.23165–23179.

Melosh, H.J., 1989. *Impact cratering: a geologic process*, Oxford University Press.

Milbury, C. et al., 2012. The history of Mars' dynamo as revealed by modeling magnetic anomalies near Tyrrhenus Mons and Syrtis Major: MARS' DYNAMO HISTORY. *Journal of Geophysical Research: Planets*, 117(E10). Available at: http://doi.wiley.com/10.1029/2012JE004099 [Accessed March 1, 2020].

Milliken, R.E. et al., 2007. Hydration state of the Martian surface as seen by Mars Express OMEGA: 2. H_2O content of the surface: HYDRATION STATE OF THE MARTIAN SURFACE. *Journal of Geophysical Research: Planets*, 112(E8). Available at: http://doi.wiley.com/10.1029/2006JE002853 [Accessed September 28, 2020].

Milliken, R.E. & Bish, D.L., 2010. Sources and sinks of clay minerals on Mars. *Philosophical Magazine*, 90(17–18), p.2293–2308.

Milliken, R.E., Mustard, J.F. & Goldsby, D.L., 2003. Viscous flow features on the surface of Mars: Observations from high-resolution Mars Orbiter Camera (MOC) images. *Journal of Geophysical Research-Planets*, 108(E6), p.5057.

Mitchell, J.L. & Christensen, P.R., 2016. Recurring slope lineae and chlorides on the surface of Mars: RSL and Chlorides on Mars Surface. *Journal of Geophysical Research: Planets*, 121(8), p.1411–1428.

Miyamoto, H., 2004. Fluid dynamical implications of anastomosing slope streaks on Mars. *Journal of Geophysical Research*, 109(E6). Available at: http://doi.wiley.com/10.1029/2003JE002234 [Accessed September 28, 2020].

Möhlmann, D. & Kereszturi, A., 2010. Viscous liquid film flow on dune slopes of Mars. *Icarus*, 207(2), p.654–658.

Möhlmann, D.T.F., 2010. Temporary liquid water in upper snow/ice sub-surfaces on Mars? *Icarus*, 207(1), p.140–148.

Möhlmann, D.T.F., 2008. The influence of van der Waals forces on the state of water in the shallow subsurface of Mars. *Icarus*, 195(1), p.131–139.

Möhlmann, D.T.F., 2004. Water in the upper martian surface at mid- and low-latitudes: presence, state, and consequences. *Icarus*, 168(2), p.318–323.

Montgomery, D.R. & Gillespie, A., 2005. Formation of Martian outflow channels by catastrophic dewatering of evaporite deposits. *Geology*, 33(8), p.625–628.

Morgan, G.A., Head, J.W. & Marchant, D.R., 2009. Lineated valley fill (LVF) and lobate debris aprons (LDA) in the Deuteronilus Mensae northern dichotomy boundary region, Mars: Constraints on the extent, age and episodicity of Amazonian glacial events. *Icarus*, 202(1), p.22–38.

Morris, A.R., Mouginis-Mark, P.J. & Garbeil, H., 2010. Possible impact melt and debris flows at Tooting Crater, Mars. *Icarus*, 209(2), p.369–389.

Mouginis-Mark, P., 1981. Ejecta emplacement and modes of formation of martian fluidized ejecta craters. *Icarus*, 45(1), p.60–76.

Mouginis-Mark, P., 1979. Martian fluidized crater morphology: Variations with crater size, latitude, altitude, and target material. *Journal of Geophysical Research*, 84(B14), p.8011.

Mouginis-Mark, P.J. & Boyce, J.M., 2012. Tooting crater: Geology and geomorphology of the archetype large, fresh, impact crater on Mars. *Chemie der Erde - Geochemistry*, 72(1), p.1–23.

Munaretto, G. et al., 2020. Implications for the origin and evolution of Martian recurring slope lineae at Hale crater from CaSSIS observations. *Planetary and Space Science*, in review.

Murton, J.B., Worsley, P. & Gozdzik, J., 2000. Sand veins and wedges in cold aeolian environments. *Quaternary Science Reviews*, 19(9), p.899–922.

Mustard, J.F., Cooper, C.D. & Rifkin, M.K., 2001. Evidence for recent climate change on Mars from the identification of youthful near-surface ground ice. *Nature*, 412(6845), p.411–414.

National Aeronautics and Space Administration, 2005. *Planetary Protection Provisions for Roboti c Extraterrestrial Missions.*, Washington, D.C.

Navarro-González, R. et al., 2010. Reanalysis of the Viking results suggests perchlorate and organics at midlatitudes on Mars. *Journal of Geophysical Research*, 115(E12). Available at: http://doi.wiley.com/10.1029/2010JE003599 [Accessed September 28, 2020].

Newsom, H.E., 1980. Hydrothermal alteration of impact melt sheets with implications for Mars. *Icarus*, 44(1), p.207–216.

Nuding, D.L. et al., 2015. The aqueous stability of a Mars salt analog: Instant Mars. *Journal of Geophysical Research: Planets*, 120(3), p.588–598.

Nunes, D.C. et al., 2010. Examination of gully sites on Mars with the shallow radar. *J. Geophys. Res.*, 115(E10), p.doi:10.1029/2009JE003509.

Oberbeck, V.R., 2009. Layered ejecta craters and the early water/ice aquifer on Mars. *Meteoritics & Planetary Science*, 44(1), p.43–54.

Oehler, D.Z. & Allen, C.C., 2010. Evidence for pervasive mud volcanism in Acidalia Planitia, Mars. *Icarus*, 208(2), p.636–657.

Ojha, L. et al., 2014. HiRISE observations of Recurring Slope Lineae (RSL) during southern summer on Mars. *Icarus*, 231(Supplement C), p.365–376.

Ojha, L. et al., 2017. Seasonal Slumps in Juventae Chasma, Mars: Seasonal Slumps in Juventae Chasma, Mars. *Journal of Geophysical Research: Planets*. Available at: http://doi.wiley.com/10.1002/2017JE005375 [Accessed October 18, 2017].

Ojha, L. et al., 2015. Spectral evidence for hydrated salts in recurring slope lineae on Mars. *Nature Geosci*, 8(11), p.829–832.

Okubo, C.H., 2016. Morphologic evidence of subsurface sediment mobilization and mud volcanism in Candor and Coprates Chasmata, Valles Marineris, Mars. *Icarus*, 269, p.23–37.

Ordonez-Etxeberria, I. et al., 2019. Meteorological pressure at Gale crater from a comparison of REMS/MSL data and MCD modelling: Effect of dust storms. *Icarus*, 317, p.591–609.

Orgel, C. et al., 2018. Gridmapping the Northern Plains of Mars: A New Overview of Recent Water- and Ice-Related Landforms in Acidalia Planitia. *Journal of Geophysical Research: Planets*. Available at: http://doi.wiley.com/10.1029/2018JE005664 [Accessed October 16, 2018].

Orloff, T. et al., 2011. Boulder movement at high northern latitudes of Mars. *Journal of Geophysical Research*, 116(E11). Available at: http://doi.wiley.com/10.1029/2011JE003811 [Accessed March 23, 2020].

Orloff, T.C., Kreslavsky, M.A. & Asphaug, E.I., 2013. Possible mechanism of boulder clustering on Mars. *Icarus*, 225(2), p.992–999.

Orosei, R. et al., 2018. Radar evidence of subglacial liquid water on Mars. *Science*, p.eaar7268.

Osinski, G.R. et al., 2013. Impact-generated hydrothermal systems on Earth and Mars. *Icarus*, 224(2), p.347–363.

Pál, B. & Kereszturi, Á., 2017. Possibility of microscopic liquid water formation at landing sites on Mars and their observational potential. *Icarus*, 282, p.84–92.

Palumbo, A.M. & Head, J.W., 2019. Oceans on Mars: The possibility of a Noachian groundwater-fed ocean in a sub-freezing martian climate. *Icarus*, 331, p.209–225.

Pankine, A.A. & Tamppari, L.K., 2019. MGS TES observations of the water vapor in the martian southern polar atmosphere during spring and summer. *Icarus*, 331, p.26–48.

Pankine, A.A., Tamppari, L.K. & Smith, M.D., 2010. MGS TES observations of the water vapor above the seasonal and perennial ice caps during northern spring and summer. *Icarus*, 210(1), p.58–71.

Paola, C. et al., 2009. The “unreasonable effectiveness” of stratigraphic and geomorphic experiments. *Earth-Science Reviews*, 97(1), p.1–43.

Parsons, R.A. & Nimmo, F., 2010. Numerical modeling of Martian gully sediment transport: Testing the fluvial hypothesis. *J. Geophys. Res.*, 115(E6), p.doi:10.1029/2009JE003517.

Parsons, R.A., Nimmo, F. & Miyamoto, H., 2011. Constraints on martian lobate debris apron evolution and rheology from numerical modeling of ice flow. *Icarus*, 214(1), p.246–257.

Pasquon, K. et al., 2018. Are different Martian gully morphologies due to different processes on the Kaiser dune field? *Geological Society, London, Special Publications*, 467.

Pasquon, K. et al., 2019. Present-day development of gully-channel sinuosity by carbon dioxide gas supported flows on Mars. *Icarus*, 329, p.296–313.

Pasquon, K. et al., 2016. Present-day formation and seasonal evolution of linear dune gullies on Mars. *Icarus*, 274, p.195–210.

Pathare, A.V. et al., 2018. Driven by excess? Climatic implications of new global mapping of near-surface water-equivalent hydrogen on Mars. *Icarus*, 301, p.97–116.

Peel, S.E. & Fassett, C.I., 2013. Valleys in pit craters on Mars: Characteristics, distribution, and formation mechanisms. *Icarus*, 225(1), p.272–282.

Pelletier, J.D. et al., 2008. Recent bright gully deposits on Mars: Wet or dry flow? *Geology*, 36(3), p.211–214.

2167 Penido, J.C., Fassett, C.I. & Som, S.M., 2013. Scaling relationships and concavity of small valley networks
2168 on Mars. *Planetary and Space Science*, 75, p.105–116.

2169 Perry, M.R. et al., 2019. Mars Subsurface Water Ice Mapping (SWIM): The SWIM Equation and Project
2170 Infrastructure. In p. 3083. Available at: https://ui.adsabs.harvard.edu/abs/2019LPI....50.3083P.

2171 Petersen, E.I., Holt, J.W. & Levy, J.S., 2018. High Ice Purity of Martian Lobate Debris Aprons at the
2172 Regional Scale: Evidence From an Orbital Radar Sounding Survey in Deuteronilus and Protonilus
2173 Mensae. *Geophysical Research Letters*, 45(21), p.11,595-11,604.

2174 Pewe, T.L., 1959. Sand-wedge polygons (tesselations) in the McMurdo Sound region, Antarctica; a
2175 progress report. *American Journal of Science*, 257(8), p.545–552.

2176 Phillips, C.B., Burr, D.M. & Beyer, R.A., 2007. Mass movement within a slope streak on Mars. *Geophysical*
2177 *Research Letters*, 34(21), p.doi:10.1029/2007GL031577.

2178 Phillips, R.J. et al., 2011. Massive CO2 Ice Deposits Sequestered in the South Polar Layered Deposits of
2179 Mars. *Science*, 332(6031), p.838–841.

2180 Piqueux, S. et al., 2015. Variability of the martian seasonal CO2 cap extent over eight Mars Years.
2181 *Dynamic Mars*, 251, p.164–180.

2182 Piqueux, S. et al., 2019. Widespread Shallow Water Ice on Mars at High Latitudesand Midlatitudes.
2183 *Geophysical Research Letters*, p.2019GL083947.

2184 Plaut, J.J. et al., 2009. Radar evidence for ice in lobate debris aprons in the mid-northern latitudes of
2185 Mars. *Geophysical Research Letters*, 36, p.02203.

2186 Plaut, J.J. et al., 2007. Subsurface Radar Sounding of the South Polar Layered Deposits of Mars. *Science*,
2187 316(5821), p.92.

2188 Poulet, F. et al., 2005. Phyllosilicates on Mars and implications for early martian climate. *Nature*,
2189 438(7068), p.623–627.

2190 Primm, K.M., 2018. *Exploring the water uptake and release of Mars-relevant salt and surface analogs*
2191 *through Raman microscopy*. University of Colorado at Boulder.

2192 Primm, K.M. et al., 2017. Freezing of perchlorate and chloride brines under Mars-relevant conditions.
2193 *Geochimica et Cosmochimica Acta*, 212, p.211–220.

2194 Primm, K.M. et al., 2018. The Effect of Mars-Relevant Soil Analogs on the Water Uptake of Magnesium
2195 Perchlorate and Implications for the Near-Surface of Mars. *Journal of Geophysical Research:*
2196 *Planets*, 123(8), p.2076–2088.

2197 Primm, K.M., Stillman, D.E. & Michaels, T.I., 2019. Investigating the hysteretic behavior of Mars-relevant
2198 chlorides. *Icarus*. Available at: https://linkinghub.elsevier.com/retrieve/pii/S0019103519301794
2199 [Accessed March 19, 2020].

2200 Raack, J. et al., 2020. Present-day gully activity in Sisyphi Cavi, Mars – Flow-like features and block
2201 movements. *Icarus*, 350, p.113899.

Raack, J. et al., 2015. Present-Day Seasonal Gully Activity in a South Polar Pit (Sisyphi Cavi) on Mars. *Icarus*, 251, p.226–243.

Raack, J. et al., 2017. Water induced sediment levitation enhances down-slope transport on Mars. *Nature Communications*, 8, p.1151.

Rager, A.H. et al., 2014. The effects of water vaporization on rock fragmentation during rapid decompression: Implications for the formation of fluidized ejecta on Mars. *Earth and Planetary Science Letters*, 385, p.68–78.

Ramsdale, J.D. et al., 2018. Gridmapping the northern plains of Mars: Geomorphological, Radar and Water-Equivalent Hydrogen results from Arcadia Plantia. *Journal of Geophysical Research: Planets*. Available at: http://doi.wiley.com/10.1029/2018JE005663 [Accessed October 16, 2018].

Rathbun, J.A. & Squyres, S.W., 2002. Hydrothermal Systems Associated with Martian Impact Craters. *Icarus*, 157, p.362–372.

Reiss, D. et al., 2004. Absolute dune ages and implications for the time of formation of gullies in Nirgal Vallis, Mars. *J. Geophys. Res.-Planets*, 109(E6), p.doi:10.1029/2004JE002251.

Reiss, D. & Jaumann, R., 2003. Recent debris flows on Mars: Seasonal observations of the Russell Crater dune field. *Geophys. Res. Lett.*, 30(6), p.doi:10.1029/2002GL016704.

Rempel, A.W., 2007. Formation of ice lenses and frost heave. *Journal of Geophysical Research*, 112(F2). Available at: http://doi.wiley.com/10.1029/2006JF000525 [Accessed March 1, 2020].

Rempel, A.W., 2012. Hydromechanical Processes in Freezing Soils. *Vadose Zone Journal*, 11(4), p.vzj2012.0045.

Richardson, M.I. & Mischna, M.A., 2005. Long-term evolution of transient liquid water on Mars. *Journal of Geophysical Research (Planets)*, 110, p.03003.

Rodriguez, J.A.P. et al., 2015. Did the martian outflow channels mostly form during the Amazonian Period? *Icarus*, 257, p.387–395.

Rossbacher, L.A. & Judson, S., 1981. Ground ice on Mars: Inventory, distribution, and resulting landforms. *Icarus*, 45(1), p.39–59.

Rummel, J.D. et al., 2014. A New Analysis of Mars “Special Regions”: Findings of the Second MEPAG Special Regions Science Analysis Group (SR-SAG2). *Astrobiology*, 14(11), p.887–968.

Salese, F. et al., 2019. Geological Evidence of Planet-Wide Groundwater System on Mars. *Journal of Geophysical Research: Planets*, 124(2), p.374–395.

Salvatore, M.R. & Christensen, P.R., 2014. On the origin of the Vastitas Borealis Formation in Chryse and Acidalia Planitiae, Mars: Vastitas Borealis Formation, Mars. *Journal of Geophysical Research: Planets*, 119(12), p.2437–2456.

Scanlon, K.E. et al., 2018. The Dorsa Argentea Formation and the Noachian-Hesperian climate transition. *Icarus*, 299, p.339–363.

Scanlon, K.E., Head, J.W. & Marchant, D.R., 2015. Volcanism-induced, local wet-based glacial conditions recorded in the Late Amazonian Arsia Mons tropical mountain glacier deposits. *Icarus*, 250, p.18–31.

Schaefer, E.I., McEwen, A.S. & Sutton, S.S., 2019. A case study of recurring slope lineae (RSL) at Tivat crater: Implications for RSL origins. *Icarus*, 317, p.621–648.

Schmidt, F. et al., 2017. Formation of recurring slope lineae on Mars by rarefied gas-triggered granular flows. *Nature Geosci*, 10, p.270–273.

Schon, S.C., Head, J.W. & Fassett, C.I., 2009a. Unique chronostratigraphic marker in depositional fan stratigraphy on Mars: Evidence for ca. 1.25 Ma gully activity and surficial meltwater origin. *Geology*, 37(3), p.207–210.

Schon, S.C., Head, J.W. & Milliken, R.E., 2009b. A recent ice age on Mars: Evidence for climate oscillations from regional layering in mid-latitude mantling deposits. *Geophys. Res. Lett.*, 36(15). Available at: http://dx.doi.org/10.1029/2009GL038554.

Schorghofer, N. et al., 2007. Three decades of slope streak activity on Mars. *Icarus*, 191(1), p.132–140.

Schorghofer, N. & Aharonson, O., 2005. Stability and exchange of subsurface ice on Mars. *J. Geophys. Res.-Planets*, 110(E5), p.doi:10.1029/2004JE002350.

Schorghofer, N., Aharonson, O. & Khatiwala, S., 2002. Slope streaks on Mars: Correlations with surface properties and the potential role of water. *Geophysical Research Letters*, 29(23), p.2126.

Schwenzer, S.P. et al., 2016. Fluids during diagenesis and sulfate vein formation in sediments at Gale crater, Mars. *Meteoritics & Planetary Science*, 51(11), p.2175–2202.

Scott, D.H. & Tanaka, K.L., 1987. *Geologic map of the polar regions of Mars*, U.S. Geological Survey.

Segura, T.L., 2002. Environmental Effects of Large Impacts on Mars. *Science*, 298(5600), p.1977–1980.

Segura, T.L., Toon, O.B. & Colaprete, A., 2008. Modeling the environmental effects of moderate-sized impacts on Mars. *Journal of Geophysical Research*, 113(E11). Available at: http://doi.wiley.com/10.1029/2008JE003147 [Accessed April 19, 2018].

Séjourné, A. et al., 2018. Grid-mapping the northern plains of Mars: using morphotype and distribution of ice-related landforms to understand multiple ice-rich deposits in Utopia Planitia. *Journal of Geophysical Research: Planets*. Available at: http://doi.wiley.com/10.1029/2018JE005665 [Accessed October 16, 2018].

Selvans, M.M. et al., 2010. Internal structure of Planum Boreum, from Mars advanced radar for subsurface and ionospheric sounding data. *J. Geophys. Res.*, 115(E9), p.doi:10.1029/2009JE003537.

Senthil Kumar, P. et al., 2019. Recent seismicity in Valles Marineris, Mars: Insights from young faults, landslides, boulder falls and possible mud volcanoes. *Earth and Planetary Science Letters*, 505, p.51–64.

Shoji, D. et al., 2019. *Angle of repose of Martian wet sand using discrete element method: Implication for the seasonal cycle of recurring slope lineae(RSL) by relative humidity*, https://arxiv.org/abs/1909.06144. Available at: https://arxiv.org/abs/1909.06144.

Sinha, R.K. et al., 2020. Global documentation of overlapping lobate deposits in Martian gullies. *Icarus*, in review.

Sinha, R.K. et al., 2018. Gullies and Debris-flows in Ladakh Himalaya, India: a potential Martian analogue. *Geological Society, London, Special Publications*, accepted.

Sizemore, H.G., Zent, A.P. & Rempel, A.W., 2015. Initiation and Growth of Martian Ice Lenses. *Icarus*, 251(1), p.191–210.

Skinner, J.A. & Mazzini, A., 2009. Martian mud volcanism: Terrestrial analogs and implications for formational scenarios. *Marine and Petroleum Geology*, 26(9), p.1866–1878.

Skinner, J.A. & Tanaka, K.L., 2007. Evidence for and implications of sedimentary diapirism and mud volcanism in the southern Utopia highland–lowland boundary plain, Mars. *Icarus*, 186(1), p.41–59.

Smith, D.E., Zuber, M.T. & Neumann, G.A., 2001. Seasonal Variations of Snow Depth on Mars. *Science*, 294(5549), p.2141–2146.

Smith, I.B. et al., 2013. The spiral troughs of Mars as cyclic steps: THE SPIRAL TROUGHS OF MARS. *Journal of Geophysical Research: Planets*, 118(9), p.1835–1857.

Smith, I.B. & Holt, J.W., 2010. Onset and migration of spiral troughs on Mars revealed by orbital radar. *Nature*, 465(7297), p.450–453.

Smith, M.D., 2002. The annual cycle of water vapor on Mars as observed by the Thermal Emission Spectrometer. *J. Geophys. Res.*, 107(E11), p.5115.

Smith, M.L. et al., 2014. The formation of sulfate, nitrate and perchlorate salts in the martian atmosphere. *Icarus*, 231, p.51–64.

Soare, R.J. et al., 2012. A re-interpretation of the recent stratigraphical history of Utopia Planitia, Mars: Implications for late-Amazonian periglacial and ice-rich terrain. *Planetary and Space Science*, 60(1), p.131–139.

Soare, R.J. et al., 2018a. Paleo-Periglacial and “Ice-Rich” Complexes in Utopia Planitia. In *Dynamic Mars*. Elsevier, pp. 209–237. Available at: https://linkinghub.elsevier.com/retrieve/pii/B9780128130186000078 [Accessed March 1, 2020].

Soare, R.J. et al., 2018b. Periglacial complexes and the deductive evidence of “wet”-flows at the Hale impact-crater, Mars. *Geological Society, London, Special Publications*, 467.

Soare, R.J. et al., 2013a. Possible crater-based pingos, paleolakes and periglacial landscapes at the high latitudes of Utopia Planitia, Mars. *Mars Polar Science V*, 225(2), p.971–981.

2306 Soare, R.J. et al., 2014a. Possible open-system (hydraulic) pingos in and around the Argyre impact region
2307 of Mars. *Earth and Planetary Science Letters*, 398(0), p.25–36.

2308 Soare, R.J. et al., 2016. Sorted (clastic) polygons in the Argyre region, Mars, and possible evidence of pre-
2309 and post-glacial periglaciation in the Late Amazonian Epoch. *Icarus*, 264, p.184–197.

2310 Soare, R.J. et al., 2013b. Sub-kilometre (intra-crater) mounds in Utopia Planitia, Mars: character,
2311 occurrence and possible formation hypotheses. *Mars Polar Science V*, 225(2), p.982–991.

2312 Soare, R.J. et al., 2011. The Tuktoyaktuk Coastlands of northern Canada: A possible "wet" periglacial
2313 analog of Utopia Planitia, Mars. *Geological Society of America Special Papers*, 483, p.203–218.

2314 Soare, R.J. et al., 2015. Volcanic terrain and the possible periglacial formation of "excess ice" at the mid-
2315 latitudes of Utopia Planitia, Mars. *Earth and Planetary Science Letters*, 423, p.182–192.

2316 Soare, R.J., Burr, D.M. & Wan Bun Tseung, J.M., 2005. Possible pingos and a periglacial landscape in
2317 northwest Utopia Planitia. *Icarus*, 174(2), p.373–382.

2318 Soare, R.J., Conway, S.J. & Dohm, J.M., 2014b. Possible ice-wedge polygons and recent landscape
2319 modification by "wet" periglacial processes in and around the Argyre impact basin, Mars. *Icarus*,
2320 233(0), p.214–228.

2321 Soare, R.J., Osinski, G.R. & Roehm, C.L., 2008. Thermokarst lakes and ponds on Mars in the very recent
2322 (late Amazonian) past. *Earth and Planetary Science Letters*, 272(1–2), p.382–393.

2323 Sori, M.M. et al., 2019. Islands of ice on Mars and Pluto. *Journal of Geophysical Research: Planets*,
2324 124(10), p.2522–2542.

2325 Stack, K.M. et al., 2014. Diagenetic origin of nodules in the Sheepbed member, Yellowknife Bay
2326 formation, Gale crater, Mars: Diagenetic Nodules in Gale Crater. *Journal of Geophysical*
2327 *Research: Planets*, 119(7), p.1637–1664.

2328 Stamenkovic, V. et al., 2020. Probing the Modern-Day Martian Subsurface Habitability with VALKYRIE. In
2329 *Lunar and Planetary Science Conference*. p. 1812. Available at:
2330 https://ui.adsabs.harvard.edu/abs/2020LPI....51.1812S.

2331 Steakley, K. et al., 2019. Testing the impact heating hypothesis for early Mars with a 3-D global climate
2332 model. *Icarus*, 330, p.169–188.

2333 Stillman, D.E. et al., 2020. Evaluation of wet and dry recurring slope lineae (RSL) formation mechanisms
2334 based on quantitative mapping of RSL in Garni Crater, Valles Marineris, Mars. *Icarus*, 335,
2335 p.113420.

2336 Stillman, D.E. et al., 2014. New observations of martian southern mid-latitude recurring slope lineae
2337 (RSL) imply formation by freshwater subsurface flows. *Icarus*, 233(0), p.328–341.

2338 Stillman, D.E. et al., 2016. Observations and modeling of northern mid-latitude recurring slope lineae
2339 (RSL) suggest recharge by a present-day martian briny aquifer. *Icarus*, 265, p.125–138.

2340 Stillman, D.E. & Grimm, R.E., 2011. Radar penetrates only the youngest geological units on Mars. *Journal*
2341 *of Geophysical Research*, 116(E3). Available at: http://doi.wiley.com/10.1029/2010JE003661
2342 [Accessed March 19, 2020].

2343 Stillman, D.E. & Grimm, R.E., 2018. Two pulses of seasonal activity in martian southern mid-latitude
2344 recurring slope lineae (RSL). *Icarus*, 302(Supplement C), p.126–133.

2345 Stillman, D.E., Michaels, T.I. & Grimm, R.E., 2017. Characteristics of the numerous and widespread
2346 recurring slope lineae (RSL) in Valles Marineris, Mars. *Icarus*, 285, p.195–210.

2347 Stuurman, C.M. et al., 2016. SHARAD detection and characterization of subsurface water ice deposits in
2348 Utopia Planitia, Mars: SHARAD DETECTION OF ICE UTOPIA PLANITIA. *Geophysical Research*
2349 *Letters*, 43(18), p.9484–9491.

2350 Sullivan, R. et al., 2001. Mass movement slope streaks imaged by the Mars Orbiter Camera. *J. Geophys.*
2351 *Res.-Planets*, 106(E10), p.23607–23633.

2352 Sutter, B. et al., 2017. Measurements of Oxychlorine species on Mars. *International Journal of*
2353 *Astrobiology*, 16(3), p.203–217.

2354 Svitek, T. & Murray, B., 1990. Winter frost at Viking Lander 2 site. *Journal of Geophysical Research*,
2355 95(B2), p.1495.

2356 Tanaka, K.L., Skinner Jr, J.A. & Hare, T.M., 2005. Geologic map of the northern plains of Mars.

2357 Tebolt, M. et al., 2020. Slope, elevation, and thermal inertia trends of martian recurring slope lineae
2358 initiation and termination points: Multiple possible processes occurring on coarse, sandy slopes.
2359 *Icarus*, 338, p.113536.

2360 Teodoro, L. et al., 2018. Habitability and Biomarker Preservation in the Martian Near-Surface Radiation
2361 Environment. In *From Habitability to Life on Mars*. Elsevier, pp. 211–231. Available at:
2362 https://linkinghub.elsevier.com/retrieve/pii/B9780128099353000128 [Accessed March 23,
2363 2020].

2364 Thapa, P., Martin, Y.E. & Johnson, E.A., 2017. Quantification of controls on regional rockfall activity and
2365 talus deposition, Kananaskis, Canadian Rockies. *Geomorphology*, 299, p.107–123.

2366 Thomas, M.F., McEwen, A.S. & Dundas, C.M., 2020. Present-day mass wasting in sulfate-rich sediments
2367 in the equatorial regions of Mars. *Icarus*, 342, p.113566.

2368 Thomas, P.C. et al., 2009. Residual south polar cap of Mars: Stratigraphy, history, and implications of
2369 recent changes. *Icarus*, 203(2), p.352–375.

2370 Toner, J.D., Catling, D.C. & Light, B., 2014a. Soluble salts at the Phoenix Lander site, Mars: A reanalysis of
2371 the Wet Chemistry Laboratory data. *Geochimica et Cosmochimica Acta*, 136, p.142–168.

2372 Toner, J.D., Catling, D.C. & Light, B., 2014b. The formation of supercooled brines, viscous liquids, and
2373 low-temperature perchlorate glasses in aqueous solutions relevant to Mars. *Icarus*, 233(0), p.36–
2374 47.

Tornabene, L.L. et al., 2012. Widespread crater-related pitted materials on Mars: Further evidence for the role of target volatiles during the impact process. *Icarus*, 220(2), p.348–368.

Treiman, A.H., 2003. Geologic settings of Martian gullies: Implications for their origins. *Journal of Geophysical Research: Planets*, 108(E4), p.doi:10.1029/2002JE001900.

Turner, S.M.R. et al., 2016. Hydrothermal Activity Recorded in Post Noachian-aged Impact Craters on Mars: Post-Noachian Impact Craters. *Journal of Geophysical Research: Planets*. Available at: http://doi.wiley.com/10.1002/2015JE004989 [Accessed April 20, 2016].

Ulrich, M. et al., 2011. Polygon pattern geomorphometry on Svalbard (Norway) and western Utopia Planitia (Mars) using high-resolution stereo remote-sensing data. *Geomorphology*, 134(3–4), p.197–216.

Ulrich, M. et al., 2010. Thermokarst in Siberian ice-rich permafrost: Comparison to asymmetric scalloped depressions on Mars. *J. Geophys. Res.*, 115(E10), p.doi:10.1029/2010JE003640.

Vago, J.L. et al., 2017. Habitability on Early Mars and the Search for Biosignatures with the ExoMars Rover. *Astrobiology*, 17(6–7), p.471–510.

Vijayan, S. & Sinha, R.K., 2017. Amazonian fluvial outflow channels in Jovis Tholus region, Mars: FLUVIAL CHANNELS IN JOVIS THOLUS REGION. *Journal of Geophysical Research: Planets*, 122(5), p.927–949.

Vincendon, M., 2015. Identification of Mars gully activity types associated with ice composition. *Journal of Geophysical Research: Planets*, 120(11), p.1859–1879.

Vincendon, M. et al., 2015. Mars Express measurements of surface albedo changes over 2004–2010. *Icarus*, 251, p.145–163.

Vincendon, M. et al., 2010a. Near-tropical subsurface ice on Mars. *Geophysical Research Letters*, 37. Available at: http://dx.doi.org/10.1029/2009GL041426.

Vincendon, M. et al., 2019. Observational evidence for a dry dust-wind origin of Mars seasonal dark flows. *Icarus*, 325, p.115–127.

Vincendon, M., Forget, F. & Mustard, J., 2010b. Water ice at low to midlatitudes on Mars. *J. Geophys. Res.*, 115(E10), p.doi:10.1029/2010JE003584.

Viola, D. et al., 2015. Expanded secondary craters in the Arcadia Planitia region, Mars: Evidence for tens of Myr-old shallow subsurface ice. *Icarus*, 248, p.190–204.

Viola, D. & McEwen, A.S., 2018. Geomorphological Evidence for Shallow Ice in the Southern Hemisphere of Mars. *Journal of Geophysical Research: Planets*, 123(1), p.262–277.

Viviano, C.E., Moersch, J.E. & McSween, H.Y., 2013. Implications for early hydrothermal environments on Mars through the spectral evidence for carbonation and chloritization reactions in the Nili Fossae region: HYDROTHERMAL ENVIRONMENTS IN NILI FOSSAE. *Journal of Geophysical Research: Planets*, 118(9), p.1858–1872.

2410 Voelker, M. et al., 2017. Grid-mapping Hellas Planitia, Mars – Insights into distribution, evolution and
2411 geomorphology of (Peri)-glacial, fluvial and lacustrine landforms in Mars' deepest basin.
2412 *Planetary and Space Science*, 145, p.49–70.

2413 Wada, K. & Barnouin-Jha, O.S., 2006. The formation of fluidized ejecta on Mars by granular flows.
2414 *Meteoritics & Planetary Science*, 41(10), p.1551–1569.

2415 Wang, A. et al., 2019. Subsurface Cl-bearing salts as potential contributors to recurring slope lineae (RSL)
2416 on Mars. *Icarus*, 333, p.464–480.

2417 Ward, W.R., 1974. Climatic variations on Mars: 1. Astronomical theory of insolation. *Journal of*
2418 *Geophysical Research*, 79(24), p.3375–3386.

2419 Ward, W.R., 1992. Long-term orbital and spin dynamics of Mars. In *Mars*. University of Arizona Press,
2420 Tucson, AZ, United States, pp. 298–320.

2421 Ward, W.R., 1979. Present obliquity oscillations of Mars: Fourth-order accuracy in orbital *e* and *I*. *Journal*
2422 *of Geophysical Research: Solid Earth*, 84(B1), p.237–241.

2423 Webster, C.R. et al., 2018. Background levels of methane in Mars' atmosphere show strong seasonal
2424 variations. *Science*, 360(6393), p.1093–1096.

2425 Weiss, D.K. et al., 2017. Extensive Amazonian-aged fluvial channels on Mars: Evaluating the role of Lyot
2426 crater in their formation: Fluvial Channel Formation by Lyot Crater. *Geophysical Research Letters*,
2427 44(11), p.5336–5344.

2428 Weiss, D.K. & Head, J.W., 2015. Crater degradation in the Noachian highlands of Mars: Assessing the
2429 hypothesis of regional snow and ice deposits on a cold and icy early Mars. *Planetary and Space*
2430 *Science*, 117, p.401–420.

2431 Weiss, D.K. & Head, J.W., 2014. Ejecta mobility of layered ejecta craters on Mars: Assessing the influence
2432 of snow and ice deposits. *Icarus*, 233(0), p.131–146.

2433 Weiss, D.K. & Head, J.W., 2013. Formation of double-layered ejecta craters on Mars: A glacial substrate
2434 model. *Geophysical Research Letters*, 40(15), p.3819–3824.

2435 Weiss, D.K. & Head, J.W., 2016. Impact ejecta-induced melting of surface ice deposits on Mars. *Icarus*,
2436 280, p.205–233.

2437 Weitz, N. et al., 2018. Modeling concentric crater fill in Utopia Planitia, Mars, with an ice flow line model.
2438 *Icarus*, 308, p.209–220.

2439 Westbrook, O.W., 2009. *Crater ice deposits near the south pole of Mars*. Masters. Cambridge, MA:
2440 Massachusetts Institute of Technology.

2441 Whalley, W.B. & Azizi, F., 2003. Rock glaciers and protalus landforms: Analogous forms and ice sources
2442 on Earth and Mars. *J. Geophys. Res.-Planets*, 108(E4), p.doi:10.1029/2002JE001864.

Wheatley, D.F., Chan, M.A. & Okubo, C.H., 2019. Clastic pipes and mud volcanism across Mars: Terrestrial analog evidence of past martian groundwater and subsurface fluid mobilization. *Icarus*, 328, p.141–151.

Williams, K.E. et al., 2009. Ancient melting of mid-latitude snowpacks on Mars as a water source for gullies. *Icarus*, 200(2), p.418–425.

Williams, K.E. et al., 2008. Stability of mid-latitude snowpacks on Mars. *Icarus*, 196(2), p.565–577.

Williams, R.M.E. & Malin, M.C., 2008. Sub-kilometer fans in Mojave Crater, Mars. *Icarus*, 198, p.365–383.

Williams, R.M.E. & Phillips, R.J., 2001. Morphometric measurements of martian valley networks from Mars Orbiter Laser Altimeter (MOLA) data. *Journal of Geophysical Research: Planets*, 106(E10), p.23737–23751.

Willmes, M. et al., 2012. Surface age of the ice–dust mantle deposit in Malea Planum, Mars. *Planetary and Space Science*, 60(1), p.199–206.

Wilson, J.T. et al., 2018. Equatorial locations of water on Mars: Improved resolution maps based on Mars Odyssey Neutron Spectrometer data. *Icarus*, 299, p.148–160.

Wilson, L., 2004. Mars outflow channels: A reappraisal of the estimation of water flow velocities from water depths, regional slopes, and channel floor properties. *Journal of Geophysical Research*, 109(E9), p.E09003.

Wilson, L. & Head, J.W., 2002. Tharsis-radial graben systems as the surface manifestation of plume-related dike intrusion complexes: Models and implications. *Journal of Geophysical Research*, 107(E8). Available at: http://doi.wiley.com/10.1029/2001JE001593 [Accessed March 24, 2020].

Wilson, S.A. et al., 2016. A Cold-Wet Mid-Latitude Environment on Mars during the Hesperian-Amazonian Transition: Evidence from Northern Arabia Valleys and Paleolakes: A Late, Cold and Wet Climate on Mars. *Journal of Geophysical Research: Planets*. Available at: http://doi.wiley.com/10.1002/2016JE005052 [Accessed August 17, 2016].

Wordsworth, R. et al., 2013. Global modelling of the early martian climate under a denser CO2 atmosphere: Water cycle and ice evolution. *Icarus*, 222(1), p.1–19.

Wray, J.J. et al., 2009. Diverse aqueous environments on ancient Mars revealed in the southern highlands. *Geology*, 37(11), p.1043–1046.

Yoder, C.F. et al., 2003. Fluid Core Size of Mars from Detection of the Solar Tide. *Science*, 300(5617), p.299–303.

Yue, Z. et al., 2014. Quantitative analysis of the morphology of martian gullies and insights into their formation. *Icarus*, 243, p.208–221.

Zanetti, M. et al., 2010. Distribution and evolution of scalloped terrain in the southern hemisphere, Mars. *Icarus*, 206(2), p.691–706.

Zent, A.P. et al., 1986. Distribution and state of H2O in the high-latitude shallow subsurface of mars. *Icarus*, 67(1), p.19–36.